Theses and Dissertations--Civil Engineering

Civil Engineering

2012

AN INNOVATIVE APPROACH TO MECHANISTIC EMPIRICAL PAVEMENT DESIGN

Ronnie Clark Graves II
University of Kentucky, clark.graves@uky.edu

STUDENT AGREEMENT:

I represent that my thesis or dissertation and abstract are my original work. Proper attribution has been given to all outside sources. I understand that I am solely responsible for obtaining any needed copyright permissions. I have obtained and attached hereto needed written permission statements(s) from the owner(s) of each third-party copyrighted matter to be included in my work, allowing electronic distribution (if such use is not permitted by the fair use doctrine).

I hereby grant to The University of Kentucky and its agents the non-exclusive license to archive and make accessible my work in whole or in part in all forms of media, now or hereafter known. I agree that the document mentioned above may be made available immediately for worldwide access unless a preapproved embargo applies.

I retain all other ownership rights to the copyright of my work. I also retain the right to use in future works (such as articles or books) all or part of my work. I understand that I am free to register the copyright to my work.

REVIEW, APPROVAL AND ACCEPTANCE

The document mentioned above has been reviewed and accepted by the student's advisor, on behalf of the advisory committee, and by the Director of Graduate Studies (DGS), on behalf of the program; we verify that this is the final, approved version of the student's dissertation including all changes required by the advisory committee. The undersigned agree to abide by the statements above.

<div align="right">

Ronnie Clark Graves II, Student

Dr. Kamyar Mahboub, Major Professor

Dr. Kamyar Mahboub, Director of Graduate Studies

</div>

AN INNOVATIVE APPROACH TO MECHANISTIC EMPIRICAL
PAVEMENT DESIGN

DISSERTATION

A dissertation submitted in partial fulfillment of the requirements
for the degree of Doctor of Philosophy in
Civil Engineering in the College of Engineering
at the University of Kentucky

By
Ronnie Clark Graves II

Lexington, Kentucky

Director: Dr. Kamyar Mahboub Professor of Civil Engineering

Lexington, Kentucky

2012

ABSTRACT OF DISSERTATION

AN INNOVATIVE APPROACH TO MECHANISTIC EMPIRICAL
PAVEMENT DESIGN

The Mechanistic Empirical Pavement Design Guide (MEPDG) developed by the National Cooperative Highway Research Program (NCHRP) project 1-37A, is a very powerful tool for the design and analysis of pavements. The designer utilizes an iterative process to select design parameters and predict performance, if the performance is not acceptable they must change design parameters until an acceptable design is achieved. The design process has more than 100 input parameters across many areas, including, climatic conditions, material properties for each layer of the pavement, and information about the truck traffic anticipated. Many of these parameters are known to have insignificant influence on the predicted performance

During the development of this procedure, input parameter sensitivity analysis varied a single input parameter while holding other parameters constant, which does not allow for the interaction between specific variables across the entire parameter space. A portion of this research identified a methodology of global sensitivity analysis of the procedure using random sampling techniques across the entire input parameter space. This analysis was used to select the most influential input parameters which could be used in a streamlined design process.

This streamlined method has been developed using Multiple Adaptive Regression Splines (MARS) to develop predictive models derived from a series of actual pavement design solutions from the design software provided by NCHRP. Two different model structures have been developed, one being a series of models which predict pavement distress (rutting, fatigue cracking, faulting and IRI), the second being a forward solution to predict a pavement thickness given a desired level of distress. These thickness prediction models could be developed for any subset of MEPDG solutions desired, such as typical designs within a given state or climatic zone. These solutions could then be modeled with the MARS process to produce am "Efficient Design Solution" of pavement thickness and performance predictions. The procedure developed has the potential to significantly improve the efficiency of pavement designers by allowing them to look at many different design scenarios prior to selecting a design for final analysis.

KEYWORDS: Mechanistic-Empirical Pavement Design, Sensitivity, Pavement
Performance, Pavement Design Reliability, Thickness Design

Ronnie Clark Graves II
Student's Signature

December 13, 2012
Date

AN INNOVATIVE APPROACH TO MECHANISTIC EMPIRICAL
PAVEMENT DESIGN

By

Ronnie Clark Graves II

Dr. <u>Kamyar Mahboub</u>
Director of Dissertation

Dr. <u>Kamyar Mahboub</u>
Director of Graduate Studies

<u>December 13, 2012</u>
Date

TABLE OF CONTENTS

List of Tables

List of Figures

1.0 Background

1.1 Introduction

A pavement is an engineered structure designed to transmit vehicle loads to the soil or rock subgrade below. Pavements are typically a multilayer system with the relatively weaker materials below and progressively stronger materials above. This type of structure leads to an economical use of available materials. Flexible pavements typically consist of several layers starting with an unbound base such as DGA (dense-graded-aggregate), one or more courses of asphalt bound base (Hot Mix Asphalt – HMA) following by an asphalt riding surface. Rigid pavements consist of two layers, the concrete slab and the bound or unbound base layer (Huang, 2004). An idealized pavement structure is given in Figure 1.

Bound Material (3" – 15" thick) **Hot Mix Asphalt or Portland Cement Concrete**
Unbound Material (4" – 20" thick) **Crushed Aggregates**
Subgrade Material **Compacted Native Soil or** **Modified Materials**
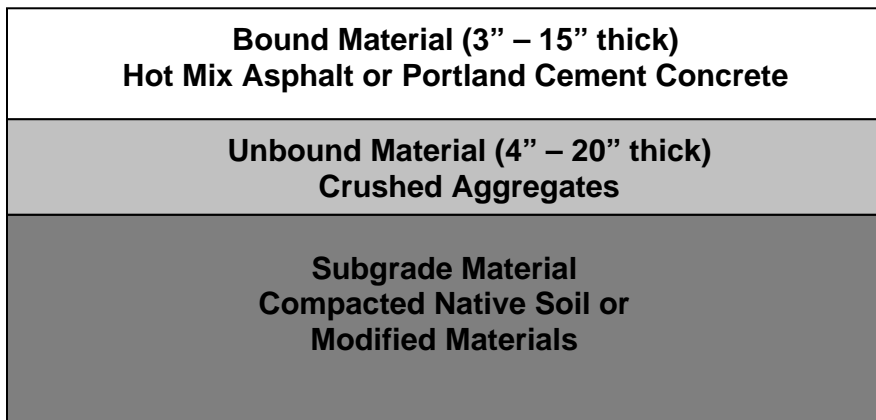
Figure 1. Idealized pavement structure

Each of these layers in a pavement structure has different properties which define its strength and it response to changes in the environment and the passage of vehicle loads along the roadway. For instance, Hot Mix Asphalt (HMA) is very sensitive to changes in temperature. This change may reduce the strength of the asphalt by as much as 60 – 70 percent during the summer months. While the subgrade materials may be influenced by the amount of moisture which may be present. Again fluctuations of more than 50 percent would not be uncommon as the rainfall changes throughout the year (Ovik, Birgisson, & Newcomb, 2000).

In its simplest form the design of a pavement deals with determining the thickness of each of the pavement layers given in Figure 1, taking into consideration their materials and their corresponding strength, along with the amount of traffic which the roadway will carry. Design procedures typically fall into three categories:

- Mechanistic – analysis of the engineering response to the pavement based on the load applied, or essentially a theoretical analysis of the pavement.

- Empirical – an analysis based on experience or a detailed experiment

- Mechanistic/Empirical – a procedure which is based on theory, then has been calibrated based on observed conditions or experimental testing.

1.2 Historical Pavement Design

Pavement design in the United States has been an evolutionary process beginning early in the 20th century. There have been many evolutions of mechanistic, empirical and mechanistic-empirical procedures developed using a variety of road tests and in-service pavements. The first national effort in development of a pavement design procedure was the road test conducted by the American Association of State Highway

Officials (AASHO) (AASHO, 1961). This organization is now called the American

Association of State Highway and Transportation Officials (AASHTO).

This road test was conducted in Ottawa, Illinois beginning in 1958 and continuing

into 1960. The test consisted of test tracks which were built to a variety of designs,

varying the thickness of the pavement layers and the traffic loads which were applied.

Loaded military vehicles were used to apply the traffic loads; periodic inspections of the

pavement structure were conducted to measure the condition of the roadway. These

inspections included measurements of roughness, visual observations of the roadway

condition, deflection of the pavement under loadings and determination of the Pavement

Serviceability Rating (PSR) (AASHO, 1961). PSR was a measure of the overall

condition of the pavement structure as determined by a group of individuals.

There were several drawbacks to this experiment. The experiment used limited

types of construction materials. Therefore only limited information is available regarding

how material strength would affect performance of the roadway. In addition, the test

took place in a single climatic location, while it is very similar in climate to Kentucky; it

is quite different than other geographic locations across the country. Also traffic loadings

were relatively modest compared to what is seen on today highways.

The results of this road test were utilized to develop a strictly empirical design

procedure based on the observed roadway conditions and selected design parameters. It

was first published in 1972. Subsequent revisions of the design procedure were adopted

by AASHTO in 1986, 1993 and 1998 (AASHTO, 1993).

1.3 Kentucky Procedure

The pavement design procedure currently used by Kentucky is a mechanistic/empirical procedure which has been developed within the state beginning in the early 1940's (Baker & Drake, 1949). The initial work was empirically based and was refined though many years of evolution by monitoring the condition of in-situ pavements. Based on these observations, modifications were made to the design procedure through the early 1960's. In the 1960's work began to develop a mechanistic design procedure based on the "limiting strain" concepts (Southgate, Deen, & Havens, 1968). These concepts limited the amount of vertical compressive strain which was present at the top of the subgrade layer and the amount of tensile strain at the bottom of the asphalt layer. This procedure was calibrated with the empirical data which had been previously observed in Kentucky. The current design procedure was developed through the late 1970's and early 1980's (Havens, Deen, & Southgate, 1981). It too has drawbacks similar to the AASHTO procedure, in that it did not use different materials or provide a means to change the design based on the availability of premium or higher strength materials.

1.4 AASHTO 1993 Design Procedure

The predominant procedure currently in use for pavement design in the United States today is the AASHTO 1993 guide. As previously mentioned, the AASHTO 1993 guide was developed in the late 1950's and early 1960's, with only minimal changes to the procedure which is utilized today.

The design procedure was based on the accelerated AASHO road test conducted in Ottawa Illinois. This test consisted of several different test tracks of varying

construction types and material type at various thicknesses of constructed layers

(Portland Cement Concrete, Hot-Mix Asphalt, and Granular Materials). Loaded military

trucks were driven across these sections to simulate the traffic which is observed on

normal roadways. At periodic intervals these pavement structures were evaluated by the

research team to monitor their condition. The pavement condition was rated on a

subjective scale from 0 to 5. This scale was a measure of the "Serviceability" of the

pavement structure. The design procedure was developed based on relating this

"Serviceability" to the, basic material properties, and the accumulated traffic into an

empirical design procedure.

The design procedure introduced the concept of "Structural Number" concept for

flexible pavements which was a means to relate the overall strength of the pavement

structure. This strength could be obtained by increasing thickness of either the hot-mix

asphalt or granular base materials. Each of these materials was assigned a strength

coefficient or "Layer Coefficient" based on laboratory testing of the material strength.

The original intent was that agencies utilizing the design guide would calibrate the

material strengths to those typical to their construction practices and materials. However,

default values have traditionally been utilized routinely by many agencies. The lack of

calibration, the fact that the test occurred at a single climatic location with limited

materials all of led to the need to develop a more robust design method.

1.5 National Cooperative Highway Research Program (NCHRP) 1-37A

The AASHTO Joint Task Force on Pavements recommended in the mid 1990's

that the existing pavement design procedure needed to be revised (NCHRP, 2004). They

recommended that the design guide should be a mechanistic-empirical procedure which utilized pavement design theory with real world pavement performance.   In addition a report by the United States General Accounting Office also indicated that the design process was outdated and should be updated (GAO, 1997). The AASHTO Joint Task Force initiated a research project through the National Cooperative Highway Research Program (NCHRP) which functions under the Transportation Research Board (TRB) of the National Academy of Sciences. This project, 1-37A was initiated in 2007 with a total cost in excess of $6,000,000; it was completed and released to the research community in July 2004 (NCHRP, 2004). The goal of this research effort was to utilize existing methodologies to address some of the shortcomings of the previous pavement design guide.

The new mechanistic-empirical design procedure implements an integrated analysis procedure for predicting pavement performance over time, accounting for the interaction of traffic loadings, environmental factors and structural materials. In addition, it provides a means to evaluate design input variability and reliability.

This design guide represents a major change in the way pavement structures are designed. A general overview of both the AASHTO 1993 procedure and the NCHRP procedure is given in Figure 2. The designer must first consider the site conditions such as; traffic, climate, subgrade, and existing pavement condition for rehabilitation and construction conditions.
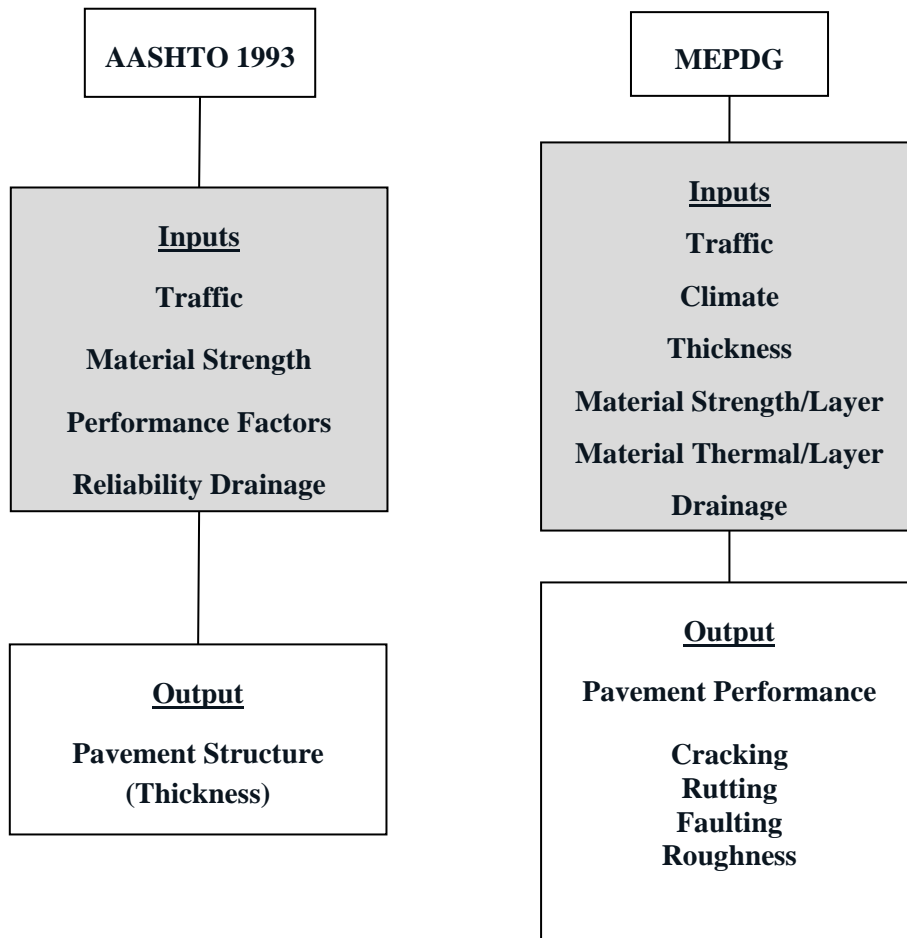
Figure 2. Comparison of existing and MEPDG design process

The designer then proposes a trial design which is evaluated by the mechanistic empirical

process to determine key performance indicators such as cracking and smoothness. If the

design does not meet the desired performance criteria, it is revised and the process is

repeated as necessary. The designer has the ability to be involved in the design process

and to consider different design features and materials for the site conditions which exist.

A general schematic of the process is given in Figure 3. A more detailed flowchart is

provided in Figure 4.
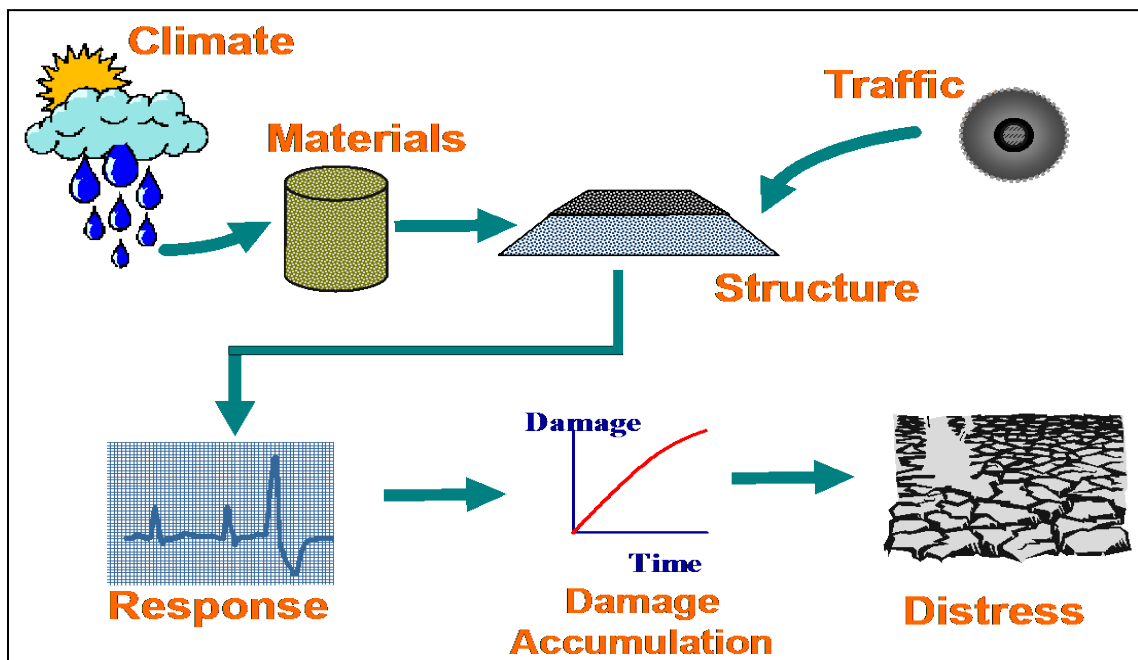
Figure 3. Overview of NCHRP design process (NCHRP, 2004)
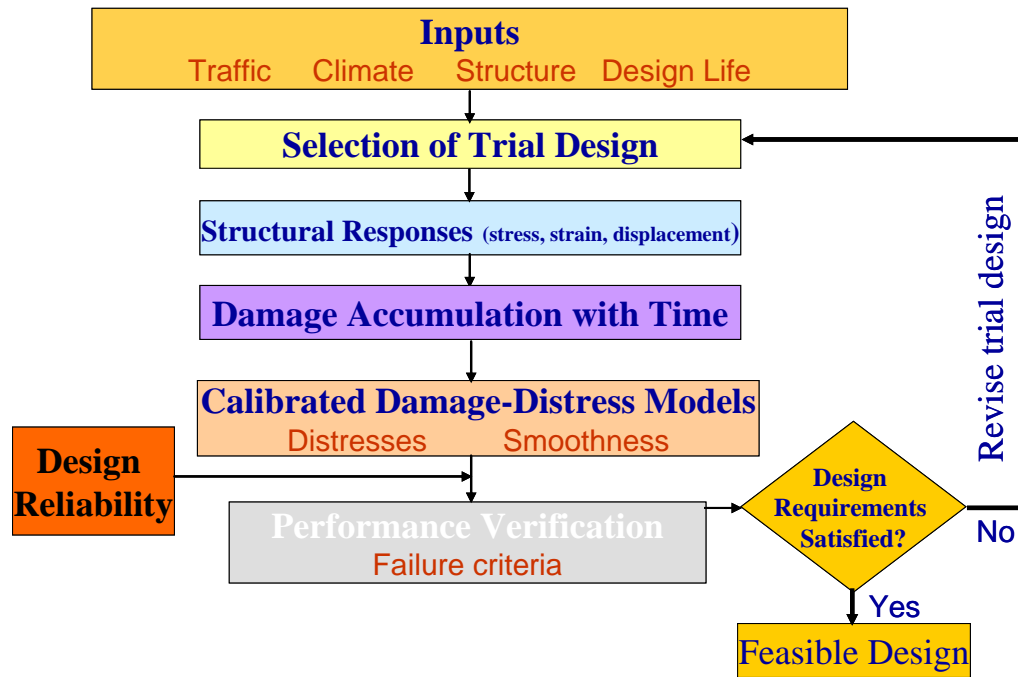
Figure 4. Flowchart of NCHRP design process

The design guide is structured in a hierarchical manner, in that the design inputs

may be established at one of three input levels. These levels essentially define the

amount of confidence the user has for a given input, or how this input was determined.

As an example for traffic, a Level I input might be to have detailed analysis of the

number and weight of trucks which would be specific to a particular project.   Level II

might utilize very detailed analysis of the number of trucks and regional averages for

truck weights. Level III would utilize average daily traffic, an assumption for the number

of trucks based on the type of roadway, and national averages for truck weights. These

types of scenarios would be carried out for each input required. It is anticipated that the

majority of the designs will be conducted using Level II input parameters. These designs

9

are carried out using an integrated software program developed during the I-37A research project.

The design process calculates stresses and strains in various locations through the pavement structure based on the input parameters utilizing a linear elastic analysis for flexible pavements and a finite element analysis for rigid pavements. These resulting stresses and strains are then used to calculate the damage to the pavement structure based on a variety of transfer functions or distress models which have been developed through other research efforts. These transfer functions have been calibrated using more than 800 long-term pavement performance sites across the country, which has been monitored for more than 15 years, initially through the Strategic Highway Research Program (SHRP) and currently by the Long-Term Pavement Performance Group within the Federal Highway Administration (FHWA). These sites were selected to provide long-term information regarding the performance of a variety of pavement structures across the country. A wide range of variables have been monitored through the project including, material characterization, traffic, and observed distresses. As was previously mentioned, these sites were utilized to calibrate the models used in the I-37A design process. It should be noted that these models should be considered national calibration models and were not intended to be utilized in place of local agency calibration.

This design process may be utilized to design either Hot Mix Asphalt (HMA) or Portland Cement Concrete (PCC) pavement structures. The input variables for traffic and climate are identical for either pavement type, while the materials and construction related inputs may be different depending on the type of pavement being designed. Table

1 summarizes the traffic and climate inputs which are required. Table 2 and Table 3

provide summaries of the inputs which are required for AC and PCC pavements. Table 4

provides an overview of the required input parameters for granular base and subgrade

materials and Table 5. provides information regarding additional input parameters. The

model utilizes these design inputs to calculate the damage or distress of the pavement

structure incrementally through time on a monthly basis.

Table 1. Traffic and Climate Parameters

Parameter	Typical Range
AADTT (veh/day)	0 – 30,000
Number of Lanes in Design Direction	1 - 10
% Truck in Design Direction	30 - 70
% Trucks in Design Lane	50 - 100
Operational Speed (mph)	15 – 70
Monthly Adjustment Factor	0 – 1 vary by month and vehicle classification
Vehicle Classification Distribution	17 different types of traffic distribution
Hourly Traffic Distribution	Infinite Number of Combinations will select 5 – 10 typical distributions
Traffic Growth (%)	None, Linear, Compound 0 – 5 %
Axle Load Distribution Factor (%)	Distribution of Weights for Single, Tandem, Tridem, Quad Axle Groups. Potentially 4 – 5 different distributions for each axle based on type of road
Mean Wheel Location Inches from Lane edge (in)	12 – 24 inches
Traffic Wander Standard Deviation (in)	5 – 15 inches
Design Lane Width (ft.)	8 – 14 ft.
Number of Axles Per Truck	Number of axles by Vehicle Classification and Axle Group, 4 -5 different distributions based on type of road
Axle Width (ft.)	7.5 – 9.5 ft.
Dual Tire Spacing (in)	10 – 14 in
Tire Pressure (psi) Single and Dual	80 – 120 psi

Axle Spacing (in)
    Tandem
    Tridem
    Quad
	
	45 – 57 in
	43 – 55 in
	43 – 55 in

Wheelbase (used only for Plain PCC pavement Short (length / percent trucks) Medium (length / percent trucks) Long (length / percent trucks)	 11 – 13 ft. / 0 – 100 percent 14 – 16 ft. / 0 – 100 percent 17 – 19 ft. / 0 – 100 percent
Climate Data Weather Station Select one of 800 weather stations Or interpolate based on lat/long and elevation Depth to Water Table Single Depth (ft.) Seasonal Depth (ft.)	 Will Select stations from four climate zones (wet/freeze, wet/no-freeze, dry/freeze, dry/no-freeze) across the country 2 – 25 ft. 2 – 25 ft.

Table 2. Asphalt Pavement Layer Parameters

Parameter	Typical Values
Asphalt Layers (Separate data for each Layer)	
Asphalt Mix	
Thickness (in)	4.5 – 18
Cumulative Percent Retained on 3/4	0 – 100
Cumulative Percent Retained on 3/8	0 – 100
Cumulative Percent Retained on #4	0 – 100
% Passing #200	0 – 100
AC Binder Grade/Strength	PG 76-22 PG 64-22
Reference Temperature	60 – 80
Poisson's Ratio	0.25 - 0.45
Effective Binder Content %	8 – 15
Air Voids %	2 – 8
Total Unit Weight (lb./ft^3)	140 - 160
Thermal Conductivity of Asphalt	0.57 - 0.77
Heat Capacity of Asphalt	0.27 – 0.47
Other Parameters	
Surface Shortwave absorptivity	0.75 – 0.95
Thermal Cracking	
Average Tensile Strength	200 – 500
Creep Test Results	Creep Compliance Test Results
Mix Coefficient of Thermal Contraction	
Mixture VMA (%)	12 – 24
Aggregate Coefficient of Thermal Contraction	$4 \times 10^{-6} – 6 \times 10^{-6}$
Distress Potential (% lane area)	Mean and Standard Deviation

Table 3. Rigid Pavement Layer Parameters

Parameter	Typical Values
Unit Weight	135 – 145 pcf
Poisson's Ratio	0.10 – 0.25
Coefficient of Thermal Expansion	$5.5 \times 10^{-6} – 7.5 \times 10^{-6}$
Thermal Conductivity	1.0 – 1.5
Heat Capacity	0.15 – 0.40
Cementation Material Factor (lbs. /yd.)	500 - 700
Water/Cement Ratio	0.3 – 0.5
Aggregate Type	Dolomite, Limestone, Granite, Quartzite, Basalt, Synetite, Rhyolite, Chert, Gabbro
Reversible Shrinkage	40 – 60%
Time to Develop 50% of ultimate Shrinkage	20 – 40 days
Curing Method	Curing Compound, Wet Curing
Compressive Strength	3000 – 6000 psi

Table 4. Granular Base and Subgrade Parameters

Parameter	Typical Range
Granular Materials	
Thickness (in)	4 – 24
Modulus (psi) (single or seasonal)	10,000 – 100,000
Coefficient of Lateral Pressure	0.4 – 0.6
Poisson's Ratio	0.25 – 0.45
Plasticity Index	1 – 20
Percent Passing #200	0 – 20
Percent Passing #4	0 – 100
D60 (mm)	0 – 10
Compacted Unbound Material or Uncompacted Natural Stone	Select One
Subgrade Materials	
Modulus (psi) (single or seasonal)	10,000 – 100,000
Coefficient of Lateral Pressure	0.4 – 0.6
Poisson's Ratio	0.25 – 0.45
Plasticity Index	1 – 20
Percent Passing #200	0 – 20
Percent Passing #4	0 – 100
D60 (mm)	0 – 10
Compacted Unbound Material or Uncompacted Natural Stone	Select One

Table 5. General Project Parameters

Parameter	Typical Value
Initial IRI in/mi	40 – 60 for AC 50 – 70 for PCC
Base/Subgrade Construction Month and Yr.	Variable Through all Months and Multiple Years
Pavement Construction Month and Year	Variable Through all Months and Multiple Years
Traffic Open Month and year	Variable Through all Months and Multiple Years
Design Life (years)	10, 20, 30

The NCHRP process predicts the following individual distresses for HMA pavements; Permanent deformation (rutting), fatigue cracking (both from the bottom of the asphalt to the surface and from the top of the asphalt surface down), thermal cracking, and roughness. Examples of rutting, fatigue cracking, and thermal cracking are presented in Figure 5 through Figure 7.

Figure 5. Typical HMA rutting

Figure 6. Typical HMA fatigue cracking

Figure 7. Typical HMA thermal (block) cracking

For Rigid pavements (PCC Pavements), the NCHRP model predicts the following

individual distresses, faulting between the joints, top-down and bottom-up cracking, and

roughness. Examples of joint faulting and slab cracking are given in Figure 8 and

Figure 9.

Figure 8. Typical PCC transverse cracking

Figure 9. Typical PCC joint faulting

The roughness that is predicted for both flexible and rigid pavements is a model that has been developed as a function of all of the other predicted distresses.

The designer must determine what level of distress is acceptable for his given application and conduct a series of model runs to determine a combination of materials and construction techniques which will meet his criteria for the given traffic level. This predicted distress is predicted on a monthly basis for the life of the pavement design. An example of the model results for asphalt pavement rutting for a 20-year design is given in Figure 10
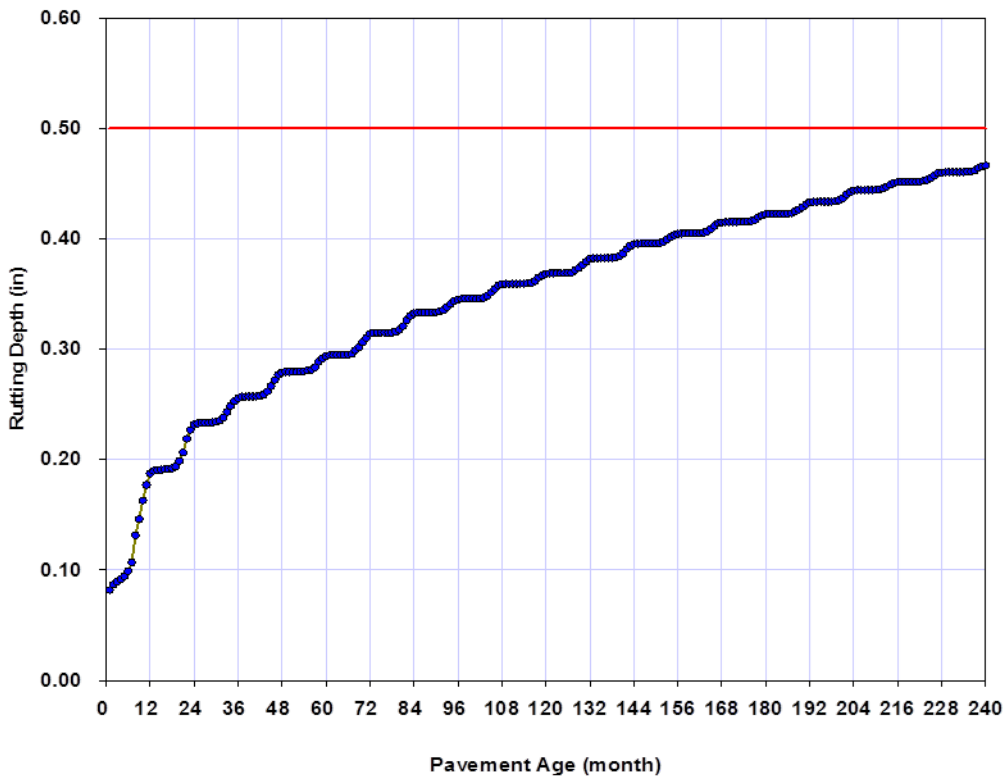
Figure 10. Typical MEPDG design result

1.6 Problem Statement

As was seen in the previous sections the new design process is quite complex requiring numerous input factors dealing with traffic, climate, materials and construction. The guide does not provide any information as to how sensitive the design models may be to any of the required inputs. The developers of the model have only provided very minimal evaluations as to how the model would react to changes in any input parameters, such as thicker asphalt thicknesses have less distress for a given traffic level than do thinner asphalt thicknesses.

In the recently completed FHWA workshop (Darter, Khazanovich, Yu, & Mallela, 2005) on the new design process, it was stated that a sensitivity analysis is key to the implementation of the design process. Other individuals have indicated that evaluation of the sensitivity was a component of the guide which had not been addressed. A full understanding of the complete sensitivity of the model to its inputs is a necessity since some of the design inputs may require considerable expenditure of resources to obtain values for local conditions. If it can be demonstrated that the default values of some input variables can be utilized, then available resources can be focused on the inputs which are most important.

The product produced during NCHRP 1-37A is a pavement analysis process, pavement designers must use this process and them make the appropriate decisions regarding what type of pavement should be built and the materials with which it should be built. Existing design methodologies only allow for minimal changes in material characteristics and once these decisions are made, the overall thickness of the pavement structure can be determined directly. The new process is a major shift in how a pavement

is currently designed. In the new methodology, the designer may have the opportunity to change many material properties which will change the overall performance of the pavement structure; however this leads to a process which is iterative in nature instead of a direct solution to a pavement design problem. As was mentioned in previous sections, the designer must make assumptions regarding a potential design and available materials and then execute the model to determine the performance of the designed pavement, if the performance is not acceptable, additional trials must be conducted until acceptable predicted conditions have been achieved. This could be a very cumbersome and tedious process since there are a wide variety of input variables and it is unknown at this time which input variable would have the largest impact on the resulting performance prediction. The methodology is structured around an analysis tool which executed repeatedly in search of a suitable design.

The procedure in its current form could be difficult for a highway agency to implement and utilize on a regular basis. A streamlined, more direct utilization of the developed model would be an invaluable tool to the pavement community. Work completed in this research effort produces a starting point that can be then be refined by utilizing the NCHRP procedure.

Another issue, which has not been addressed, is the calibration of the model to local conditions. As was previously mentioned, the models which utilize the calculated stresses and strains to determine the observed distress of the pavement structure have been developed on a national basis. These models must be calibrated to predict the distresses which are actually observed on a local (statewide) level. The guide does

provide some information as to how this would be accomplished. Guidance regarding the

local calibration of the guide is addressed in NCHRP project, NCHRP 1-40B "Local

Calibration Guidance for the Recommended Guide for Mechanistic-Empirical Design of

New and Rehabilitated Pavement Structures" (AASHTO, 2010)

1.7 Significance of Research

It is anticipated that this project will identify the key input parameters which have

the most significant impact on the pavement performance predicted by the 1-37A model.

In addition, the development of a streamlined model will expand the potential user base

of the model, by allowing those who may not have the expertise to interpret the large

array of input parameters, a more streamlined means to analyze and design pavements.

The streamlined model with its reduced set of input values will provide a starting point or

initial trial design, which can be further refined by using the full NCHRP design model.

It is intended to be a complement to the NCHRP procedure rather than a complete

replacement.

2.0 Design Guide Sensitivity Analysis

2.1 Introduction

Sensitivity analysis is the evaluation of how the variation in the output of a model (numerical or otherwise) can be attributed to the input parameters of the model. The goal of sensitivity analysis is to determine how these changes in output may affect the decision that is made using the model results.

There are a number of techniques which can be used for evaluation of elaborate computer models; each has its own advantages and disadvantages. Many factors are involved in determining which method would provide the best evaluation of the model in questions. As a whole, sensitivity analysis is used to increase the confidence in the model and its predictions, by providing an understanding of how the model response variables respond to changes in the inputs. Sensitivity analysis is closely linked to uncertainty analysis which aims to quantify the overall uncertainty associated with the response as a result of uncertainties in the model input.

Sensitivity analysis methods may be grouped into three general classes: screening methods, local sensitivity analysis, and global sensitivity analysis (Saltelli, Chan, & Scott, 2000). Screening methods typically are used to rank a series of input factors in order of importance; they generally do not provide quantifiable information regarding how much more important a given factor is than other factor. Local sensitivity analysis concentrates on the local impact of the factors on the model; it is essentially a one-factor-at-a-time analysis, which means one factor is varied while all others are held constant.

A global sensitivity analysis typically varies the input parameters across the entire input space.   Sampling based methods of uncertainty and sensitivity analysis which may utilize Monte Carlo sampling and Latin Hyper Cube Sampling of the input parameters have also been shown to be effective in the evaluation of complex model sensitivity and have been utilized in a variety of applications (Helton & Davis, 2000), (Saltelli, Chan, & Scott, 2000), (Mrawira, 1996). In this type of analysis, a sample is taken from the distribution of each input variable and run through the model to be evaluated. The resulting outputs of each model run are then compared to the input parameter space to evaluate input sensitivity. A schematic of this process is given in Figure 11.
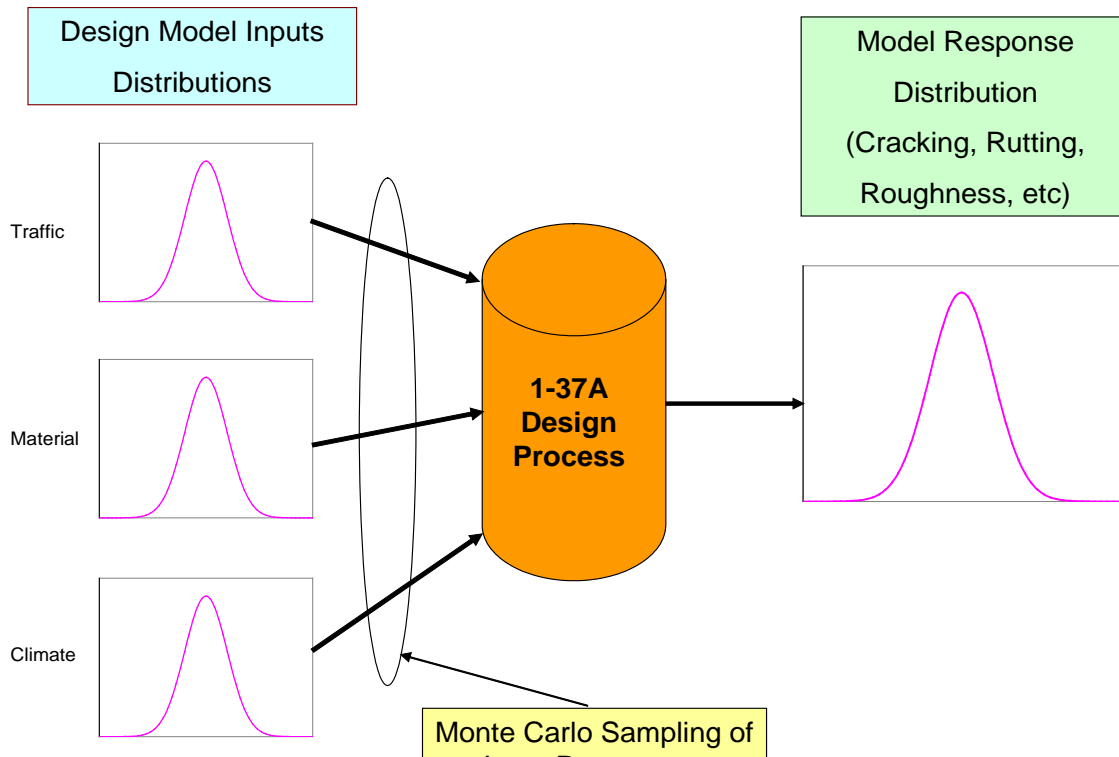
Figure 11. Global sensitivity analysis example

This process is repeated through numerous simulations using defined distributions of the input parameters, creating a matrix of different models runs, across the full range of input values with each run having a model result as the output. This results in a distribution of the model output parameters. The matrix of model inputs and resulting outputs may then be evaluated by various techniques to address the uncertainty and sensitivity of the model to its input parameters.

A variety of methods to evaluate input sensitivity using the sampling based process outlined above are available (Iman & Helton, 1995). These methods include

graphical measures such as scatter plots, correlation techniques such as Pearson's and Spearman's correlation coefficients, regression analysis, partial correlation, and rank transformations.

Iman and Helton, along with others have utilized the techniques of Pearson's and Spearman's correlation coefficients to evaluate the global sensitivity analysis results. These correlation coefficients provide a means to evaluate the relative sensitivity of a given input to the output of interest. In general, a negative correlation coefficient indicates that as the input parameters increased the output would decrease, while a positive coefficient indicates that at the input parameter increases the output increases. Pearson's correlation coefficient makes the assumption that the relationship between the input and output is linear, while Spearman's rank correlation converts the actual raw values to ranks and does not require the assumption of linearity (Saltelli, Tarantola, & Ratto, 2004). Since the design guide is a complex system and all the relationships may not be linear, both correlation techniques were utilized to evaluate the sensitivity of the input variables.

A sampling based methodology has been developed to evaluate various inputs of the design guide (Graves & Mahboub, 2006). This analysis utilized a sampling based technique where the entire input parameter space of selected input variables is sampled. The resulting samples are then used to create a matrix of design scenarios which may then be run through the NCHRP MEPDG software. The NCHRP MEPDG software will then predict the various performance parameters (cracking, rutting, faulting and rideability) of each design scenario. These performance outputs and the corresponding

input parameters may then be analyzed to evaluate the sensitivity of each input parameter with respect to each predicted distress.

Once the significant parameters have been determined, appropriate default values may be assigned to the remaining input variables, thus streamlining the design process. In addition, a better understanding of the sensitivity of the input parameters will allow designers to focus attention on the collection of appropriate data during the local calibration process. This understanding will permit the best use of available resources in the collection of the historical data on given projects which are used for calibration. Attention may be focused only on the parameters which have the most significant effect on the predicted performance. Information relating to these sensitivity analysis results will be included in later chapters.

2.2 Summary of Existing Sensitivity Analysis conducted by others

A variety of sensitivity analyses have been completed by others to try and better understand the influential input parameters of the process. All of these sensitivity analyses have utilized the one-factor-at-a-time method; where a single parameter of interest is changed while all others remain constant. This is generally referred to as local sensitivity analysis (Helton, 2004).

A number of studies have been completed in recent years to address the local sensitivity of the MEPDG process. These studies have evaluated various aspects of granular base material properties and thickness, HMA materials and thickness, PCC thickness and materials, and traffic parameters.

Two studies examined sensitivity of the predicted flexible pavement distresses based on the variation of input parameters. In each case, a base pavement structure has been selected and then a variety of parameters have then been varied one-at-a-time to evaluate sensitivity. Predicted performance of each range of variables compared to the base-case scenario. The first study by Lee and Hall (2004) looked at the following parameters: Poisson's ratio, surface shortwave absorptive, heat capacity, thermal conductivity, air voids, binder grade, total unit weight, effective binder content. Two different asphalt mixture sizes were evaluated; 0.5-inch and 1.0-inch size maximum aggregate. In addition, four typical HMA gradations obtained from sources within Arkansas were utilized. Their results indicated that for surface-down cracking, only air voids and effective binder content for 0.5-inch mixes had a significant impact on performance. For bottom-up damage, air voids and effective binder content for both mix sizes were found to be significant, no significant input variable was found for rutting and only air voids and effective binder content for 0.5-inch mixes was found to be significant for IRI. It should be noted that these studies were for a single traffic level, subgrade strength and climatic location.

The second study was conducted as part of the development of the MEPDG design process at the University of Arizona, by El-Basyouny and Witczak (2004). This study focused on the sensitivity of the following: bottom-up fatigue cracking, top-down fatigue cracking and permanent deformation. This study was again a one-factor-at-a-time analysis where all parameters remained constant with the exception of the parameters of interest.

This study in general evaluated the influence of the following factors on the resulting prediction of fatigue cracking and longitudinal cracking:

AC Stiffness – Thin Pavements	AC Stiffness – Thick Pavements
AC Thickness	Subgrade Modulus
AC Mix Air Voids	Asphalt Content
Depth to GWT	Traffic Volume
Traffic Speed	Traffic Analysis Level (Level 1, 2, 3)
MAAT (Mean Annual Air Temp.)	Depth to Bedrock

This study identified the general relationship between each of these inputs and the resulting outputs, while generally all other input parameters remained constant. It was found that subgrade stiffness and traffic generally are influential in the prediction of performance, while some of the other parameters have varying degrees of significance.

A study by Bracher and Papagiannakis (2004), evaluated the potential sensitivity of the various hierarchal levels and sampling schemes for the design guide traffic inputs. These hierarchal levels deal with the source of traffic data which is utilized in the design, site specific WIM, classification, volume, etc. or, regional and national average values. As would be expected, it was illustrated that the variability of traffic data may have a significant impact on the predicted performance of the pavement system. It illustrated that regional WIM data will generally provide designs which would overestimate the base case (continuous site specific data) by less than 20 percent.

A recent study by Masad and Little (2004) indicated that base modulus and thickness have significant influence on the IRI and longitudinal cracking. The influence of these properties on fatigue cracking is approximately half of the influence of the

properties on longitudinal cracking. It also stated that the granular base material properties did not seem to have an influence on permanent deformation of the pavement.

It should be noted that these studies did not find sensitivity too many of the minor variables and variables which are not normally associated with pavement design. It may be seen from each of these studies that the inferences which may be made regarding the significance of an input variable are made while the majority of the other factors remain constant. This type of analysis does not reflect the influence of the variation of the other parameters in the model. It should also be noted that any analysis of the significance of a given input variable should be evaluated in terms of how the magnitude of the change in this variable would affect design. For example, if predicted fatigue cracking changes from 2 to 3 percent due to the change in a given input variable, it could be indicated as being significant since it changes by 50 percent. However, in terms of evaluating a particular design neither 2 nor 3 percent is significant in selecting a pavement structure.

2.3 Sampling Based Sensitivity

Based on the review of the available local sensitivity analysis, a study of sampling based sensitivity analysis (Graves & Mahboub, 2006) has been conducted on a subset of the input variables for both flexible and rigid pavements. This subset of variables has been determined based on the results of the other local sensitivity analysis previously outlined and the experience of using Kentucky's mechanistic-empirical pavement design process. In addition, these input parameters were chosen due to their ability to be controlled in the construction process or a parameter that is routinely determined about a project site during the design phase. Many of the factors listed in Table 1 through Table

5 are not routinely measured as part of a pavement construction process. Some of these

parameters do not have standardized testing procedures developed and were included to

allow for future enhancements of the design methodology. The results of the design

process may be sensitive to some of these input parameters, however, since they are not

readily available at the time of design; they were not included in this analysis.

Flexible Pavement Sensitivity
    This initial study for flexible pavement structure focused on the eight individual input

parameters outlined below:

- Average Annual Daily Truck Traffic (AADTT)
- Truck Traffic Classification (TTC)
- Hot Mix Asphalt (HMA) Thickness
- Subgrade Strength (characterized by CBR)
- Nominal HMA Base Size
- Asphalt Content (AC) Binder Grade (standard grade and "bumped" grade for improved performance)
- Climate Zone
- Construction Month

The individual values which were varied and utilized in the study are given in Table 6.

Table 7 provides information on the default values utilized from the design guide for

other input parameters.

Table 6. Design Guide HMA Input Parameters

AADTT	Truck Traffic Classification	Nominal HMA Thickness (in)	Subgrade CBR	Nominal HMA Base Aggregate Size (in)	Climate Zone	Construction Month
100	1	5	2	0.75	Cheyenne	Jan.
500	4	6	4	1.0	Phoenix	April
1,000	6	7	6	1.5	Lexington	July
2,000	12	8	8		Birmingham	Oct.
4,000		9	10			
6,000		10				
8,000		11				
10,000		12				
15,000		13				
25,000		14				

Table 7. Other Default Input Parameters

Traffic Inputs	Software Defaults were utilized with the exception of AADTT and TTC
Climate Inputs	Water Table depth was assumed to be 20 feet for all design sections. Individual weather stations in the cities provided in Table 3 were used for generation of the climate files
Structure Inputs Drainage and Surface Properties	Software Defaults were utilized
HMA Layers	Software Defaults were utilized with the exception of the items given in Table 4
Granular Layer	Thickness = 8.0 inches, Modulus = 40,000 psi All other parameters were software defaults based on base type
Subgrade	Subgrade CBR varied as stated in Table 3, all other parameters defined by software based on CL Soil Classification

A brief discussion of each parameter is given below. AADTT were selected across a

range from 100 to 25,000 trucks per day. This range would represent typical traffic

levels what would be expected on most highways. The TTC categories were selected

from the default vehicle classification distributions provided in the design guide software.

These distributions would represent the typical ranges which would be expected for

roadways which have a predominance of single-trailer trucks. A summary of the types of

vehicles which are classified in each vehicle type are given in Figure 12.   The

distributions used in this analysis are illustrated graphically in Figure 13.

FHWA VEHICLE CLASSIFICATION
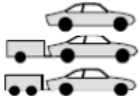
CLASS GROUP		DESCRIPTION	NO. OF AXLES
1		MOTORCYCLES	2
2		ALL CARS CARS	2
		CARS W/ 1-AXLE TRAILER	3
		CARS W/ 2-AXLE TRAILER	4
3		PICK-UPS & VANS 1 & 2 AXLE TRAILERS	2, 3, & 4
4		BUSES	2 & 3
5		2-AXLE, SINGLE UNIT	2
6		3-AXLE, SINGLE UNIT	3
7		4-AXLE, SINGLE UNIT	4
8		2-AXLE, TRACTOR, 1-AXLE TRAILER (2&1)	3
		2-AXLE, TRACTOR, 2-AXLE TRAILER (2&2)	4
		3-AXLE, TRACTOR, 1 AXLE TRAILER (3&1)	4
9		3-AXLE, TRACTOR, 2-AXLE TRAILER (3&2)	5
		3-AXLE, TRUCK W/ 2-AXLE TRAILER	5
10		TRACTOR W/ SINGLE TRAILER	6 & 7
11		5-AXLE MULTI-TRAILER	5
12		6-AXLE MULTI-TRAILER	6
13	ANY 7 OR MORE AXLE		7 or more
14	NOT USED		
15	UNKNOWN VEHICLE TYPE		

HEAVY TRUCKS (spanning classes 8–13)

Figure 12. FHWA Vehicle classification (TMG Update 2012)
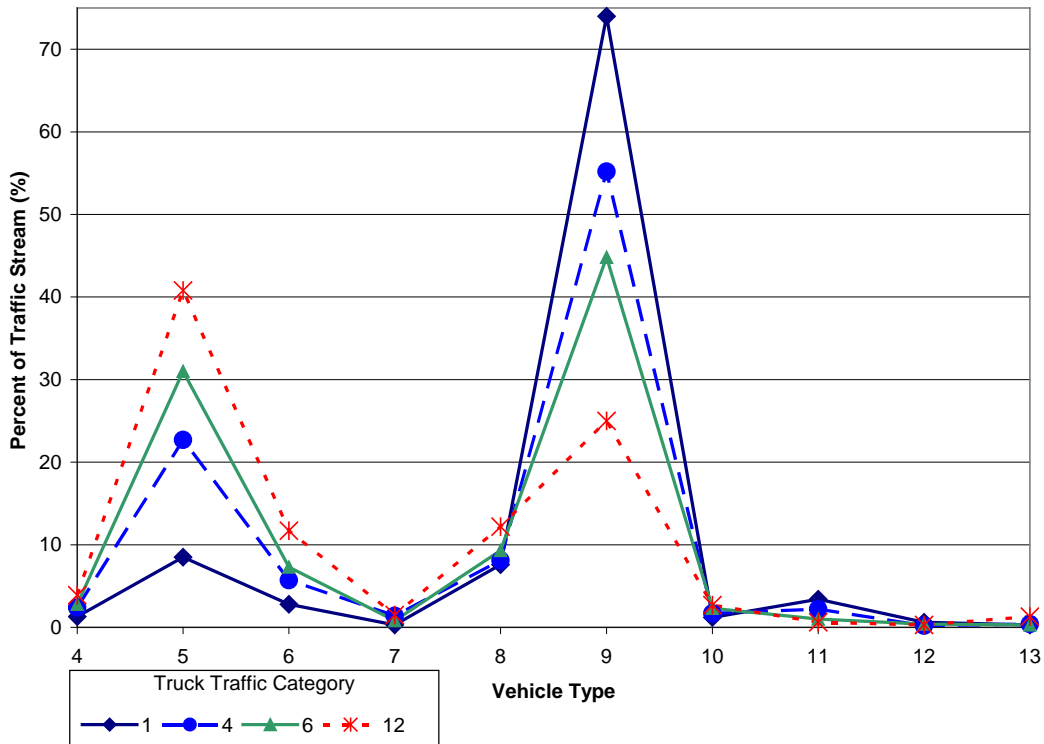
Figure 13. Typical truck traffic classifications

For the HMA layers, a thickness of 1.5-iinches was selected for all surface mixtures. For Thicknesses greater than 6.5 inches the HMA base layers were separated into two layers (NCHRP, 2011) , due to anomalies which have been discovered in the design software for thickness greater than 9 inches, these anomalies produced inconsistent results if the total thickness remained in a single layer.

The subgrade strength was varied across a range from California Bearing Ratio (CBR) of, 2 to 10 for a CL soil type. The California Bearing Ratio is a laboratory test method used to measure the load carrying capacity of subgrade soils and granular bases. All other soil parameters were set to the defaults provided by the design software based on the type of soil selected.

Three HMA base nominal aggregate sizes were selected for trials in this study as follows: 0.75, 1.0, and 1.5-inch these represent the typical designs utilized throughout the asphalt industry. The gradations and volumetric parameters (density, air voids, asphalt content, etc.) for these mixtures are given in Table 8. They were selected from typical mixtures currently utilized in Kentucky. A 0.5-inch top size aggregate surface course was utilized for each design section, the material properties for this mix are also provided in Table 8.

Table 8. Average HMA Gradations from the Kentucky Transportation Cabinet

Mix Size (in)	VMA (%)	Unit Weight lb./ft^3	Air Voids (%)	Effective Binder (%)	% Retained 3/4-in Sieve	% Retained 3/8-in Sieve	% Retained No. 4 Sieve	% Passing # 200
0.75	13.4	150.7	6.3	7.3	4.7	29.7	59.4	5.0
1.0	12.9	151.3	6.7	6.3	13.7	36.9	64.9	4.7
1.5	12.3	152.3	6.5	5.9	23.8	49.4	70.1	4.2
0.5 surface	15.4	149.0	7.0	8.4	0.0	13.1	40.6	5.2

A performance graded (PG) binder of PG 64-22 indicates that the average seven-day maximum pavement temperature would be 64° C and the minimum pavement design temperature likely to be experienced would be -22° C. When using performance graded binders, the practice of "bumping" the binder grade refers to increasing the high temperature component of the grading to a higher level to compensate for slower traffic speeds or higher traffic volumes. The practice of "bumping" the Superpave binder (KYTC, 2009) grade for the upper layers of the pavement structure was also evaluated.

For this analysis, the "bumped" grade was selected as two high temperature grades above the default determined for the climatic location discussed below.

Four different climatic locations were selected across the country, which generally represent the four climatic zones (wet - no freeze, wet - freeze, dry – no freeze, and dry - freeze) outlined during the Strategic Highway Research Program (SHRP), (Smith, 1993), PG binder grades for these locations were determined using the LTTP Bind software version 2.1 (FHWA, 1999). These locations along with their default PG grade and "bumped" grade are as follows:

- Lexington, KY (PG 64-22, PG 76-22)

- Birmingham, AL (PG 64-16, PG 76-16)

- Cheyenne, WY (PG 58-28, PG 70-28)

- Phoenix, AZ (PG 70-22, PG 82-10)

The month of construction was also varied across each of the seasons of the year, January, April, July, and October. Each of these inputs was assigned a discrete uniform distribution across the range of values indicated in Table 6..

These distributions were then sampled using a Monte Carlo sampling routine using SIMLAB (SIMLAB 2006) to produce different design scenarios covering the complete range of the input parameter space. The number of samples required for this type of analysis is generally in the range from 8 to 10 times the number of input variables (Saltelli, Tarantola, & Ratto, 2004). The remaining variables necessary to evaluate the design were assigned default values based on the MEPDG software. These scenarios were then processed through the MEPDG software to produce a matrix of outputs for the

37

following distresses: longitudinal cracking, fatigue cracking, HMA rutting, total rutting, and IRI.

These distresses were summarized at the 20-year level for use in the sensitivity analysis. The matrix of outputs and their corresponding matrix of input variables are then used to evaluate the sensitivity of the design guide to the input parameters varied in the sampling process.

2.4 Evaluation of Sensitivity

The analysis of input sensitivity was accomplished by determining the Pearson's Correlation Coefficient and the Spearman's Rank Correlation Coefficient for the relationship between the input parameters and the resulting output. To aid in evaluating the sensitivity of each output with respect to the input parameters, "Tornado" charts were produced for each output parameter. These charts illustrate the Pearson's and Spearman's coefficients for each input parameter being studied. These results are given in Figure 14 through Figure 16. The figures show that input parameters may have higher or lower correlation coefficients depending on the output which is being analyzed. Correlations marked with an "★" are significant at the 95% confidence level. This statistic along with the relative ranking of the individual input parameters was used to evaluate the input parameters which have the least significance.

Figure 14 illustrates that fatigue cracking is significantly related to HMA thickness, subgrade strength and AADTT, while the other parameters are somewhat less significant. It should be noted that AADTT and HMA thickness indicate a much stronger relationship than the other variables. For total rutting; AADTT, HMA thickness,

38

subgrade, and binder grade "bump" appear to be the most significant factors, with AADTT again being the predominant factor. For IRI several factors appear to exhibit influence and thus may be deemed significant; however, it should be noted that in the MEPDG design guide, the IRI determined as a function of all the other accumulated distresses. This fact would tend to lead to the results which are shown in Figure 16, which indicates that several of the factors which have been discussed have significant influence, with the exception of nominal base size and binder grade "bump"? In general AADTT, AC thickness, climate zone and subgrade strength have large influences across all output parameters, while the remaining variables exhibit varying degrees of influence.

Alligator Cracking
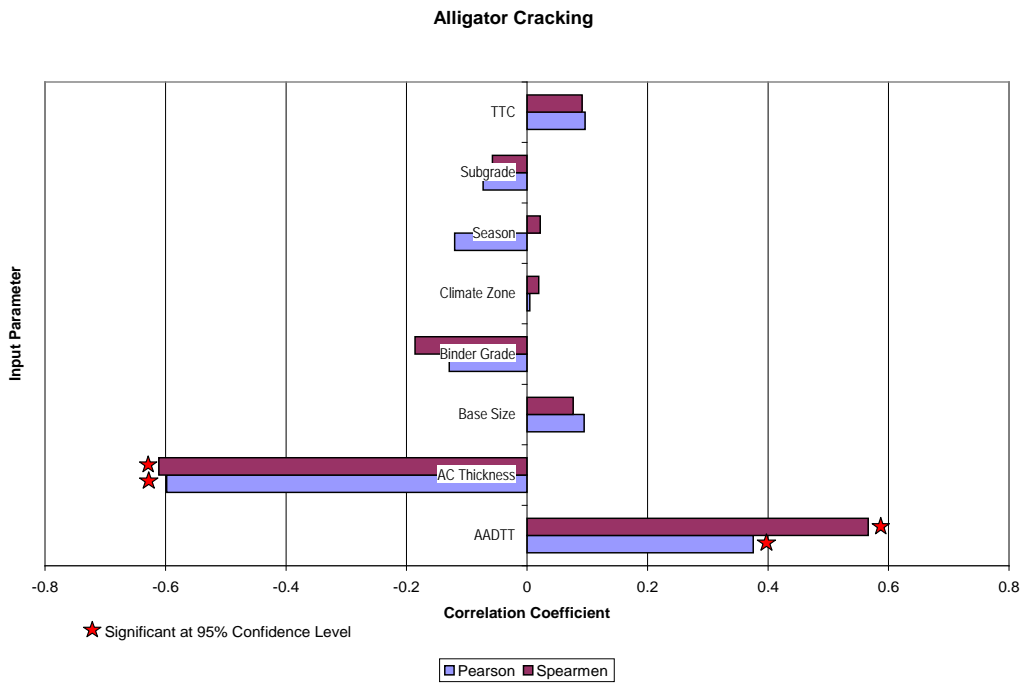
Figure 14. Correlation Coefficients Fatigue Cracking
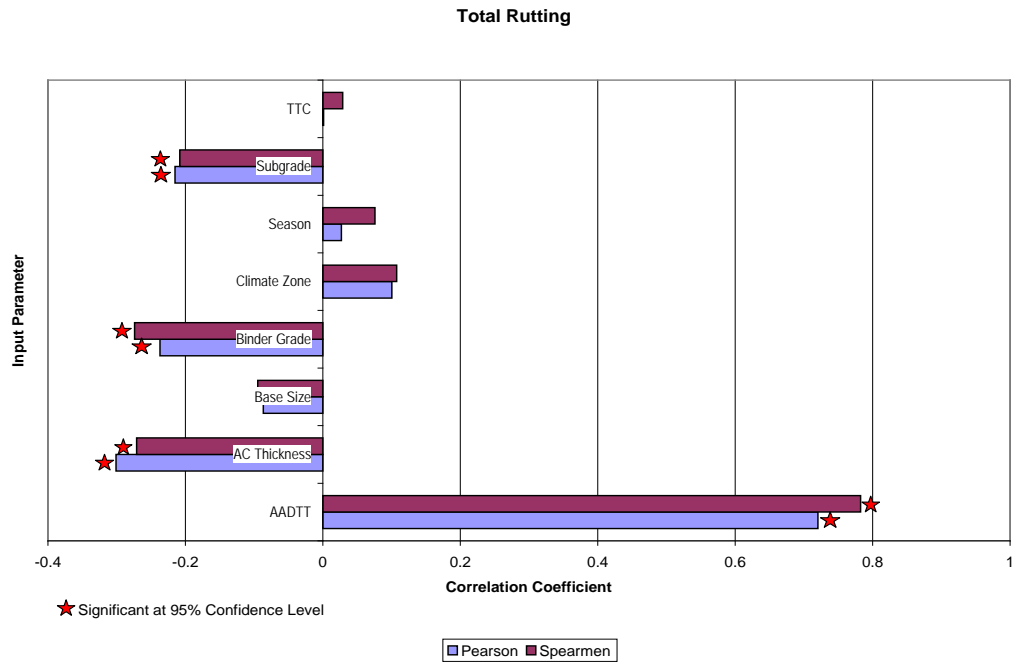
Figure 15. Correlation Coefficients Total Rutting
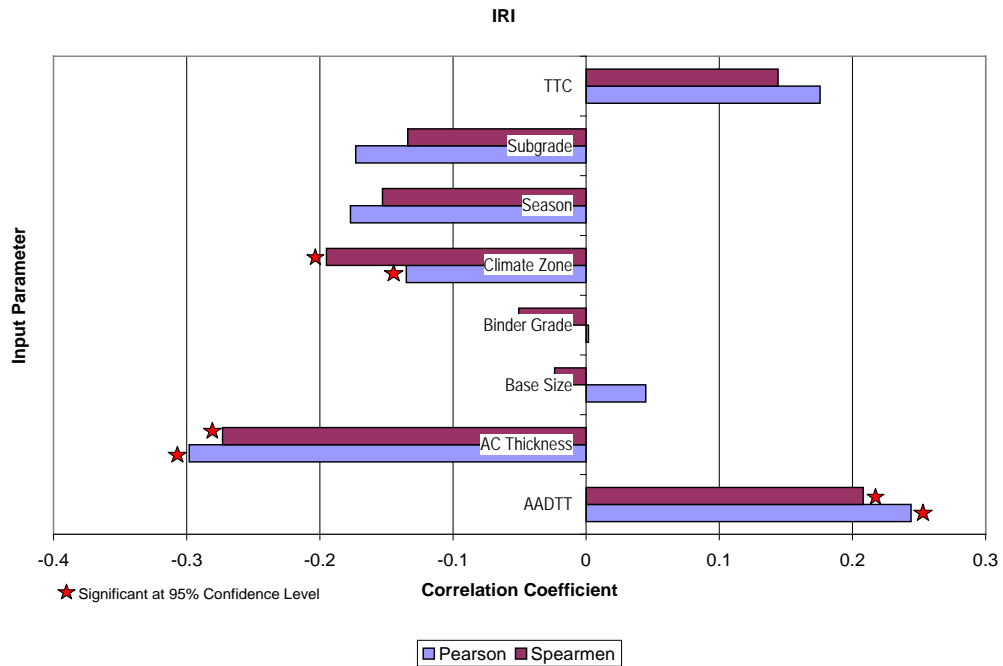
Figure 16. Correlation Coefficients for IRI

40

It would appear that the resulting outputs are least sensitive to construction month, binder grade "bump", TTC, climate zone, and nominal base size. Utilizing some type of default value for these inputs may provide satisfactory results in prediction of the output performance. Based on this analysis, default values for binder grade (no binder grade "bump"), TTC, nominal base size and construction month were selected as follows:

- Binder Grade (default based on climate zone, no "bump" in grade)

  Lexington, KY PG 64-22

- Construction Month: June

- Truck Traffic Classification (TTC): 6

- Nominal Base Size 1.0-inch (25 mm)

To address the feasibility of using these default input parameters, a sample of design scenarios were obtained from the original group of used in the sensitivity analysis. These design scenarios were selected so that they contained none of the default input values outlined above (binder grade bump, construction month, TTC, or nominal base size). Therefore in each case the original values for these parameters were replaced by the default values. The MEPDG was then run using this reduced set of parameters and then run again using the original parameters. The results from these two different software runs were then compared. A summary of these results is shown in Figure 17 through Figure 19. These figures that the predicted distresses using the reduced set of parameters (default values) correlates very well with the original model which included specific inputs for each input.

The MEPDG models that predict the distress have standard errors associated with their prediction models. A summary of the regression statistics of the prediction models in the MEPDG are given in Table 9.

Table 9. Statistical Results of MEPDG Performance Models (NCHRP, March 2004)

Model	R^2	Number of Observations	S_e
Longitudinal Cracking	Not Reported	414	1,242 ft./mile
Fatigue Cracking	Not Reported	461	6.2%
HMA Rutting	0.648	387	0.063 in
Subgrade Rutting	0.136	387	0.045 in
IRI (Unbound Agg. Base)	0.620	353	24.5 in/mile
PCC Faulting	0.60	161	0.022 in
PCC Cracking	0.75	516	6.9 %
PCC IRI	0.60	183	27.2 in/mile

The data contained in the table indicates the standard error (S_e) may be quite large relative to the predicted values of a given distress. In many cases this standard error is greater than the differences which were observed between the data sets compared in the following figures.
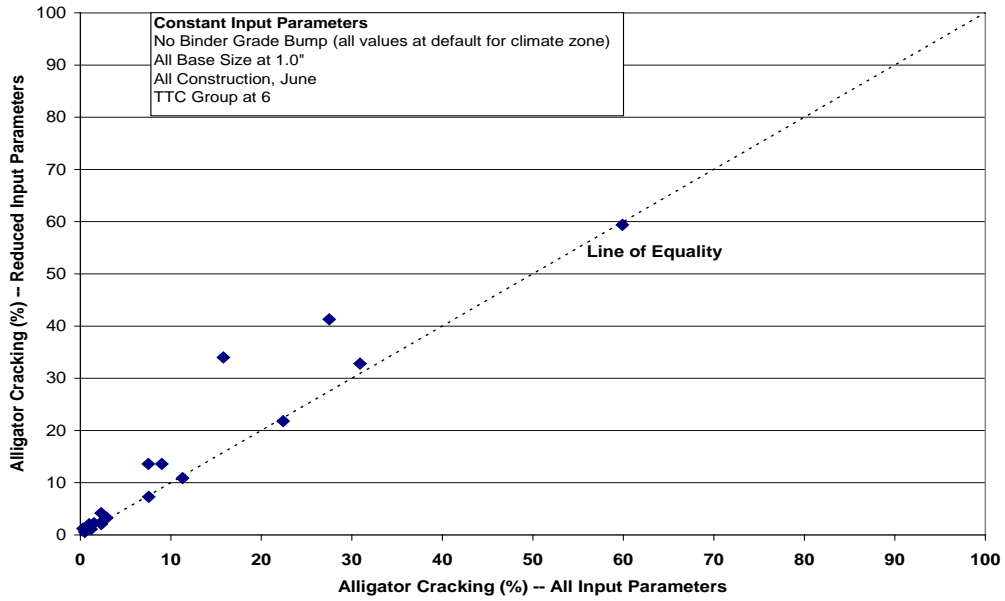
Figure 17. Comparison of reduced model and original model, fatigue cracking
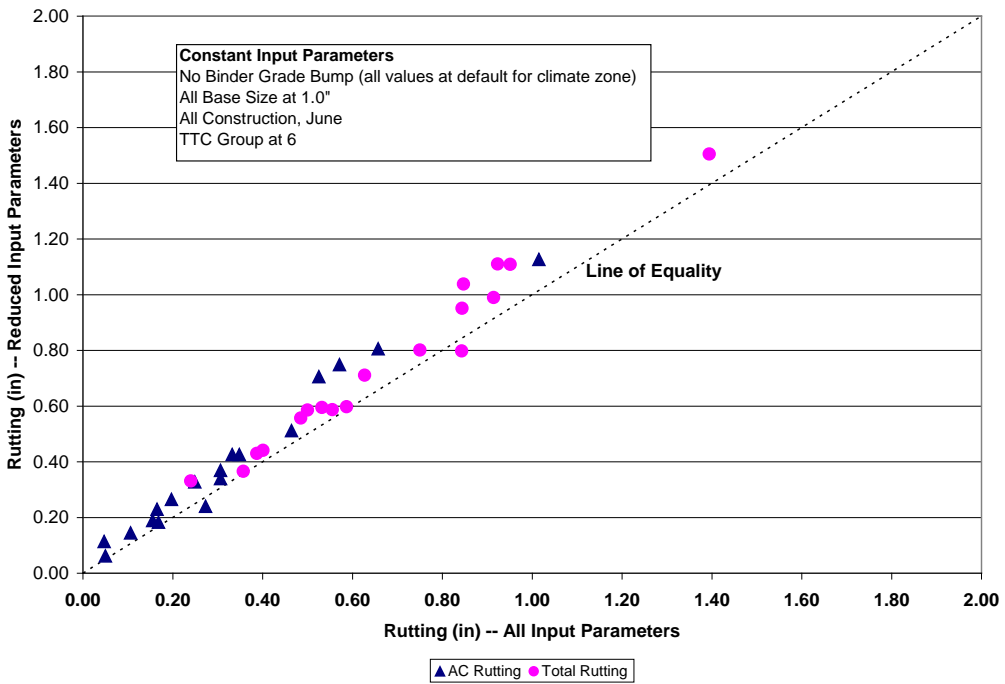
Figure 18. Comparison of reduced model and original model, rutting
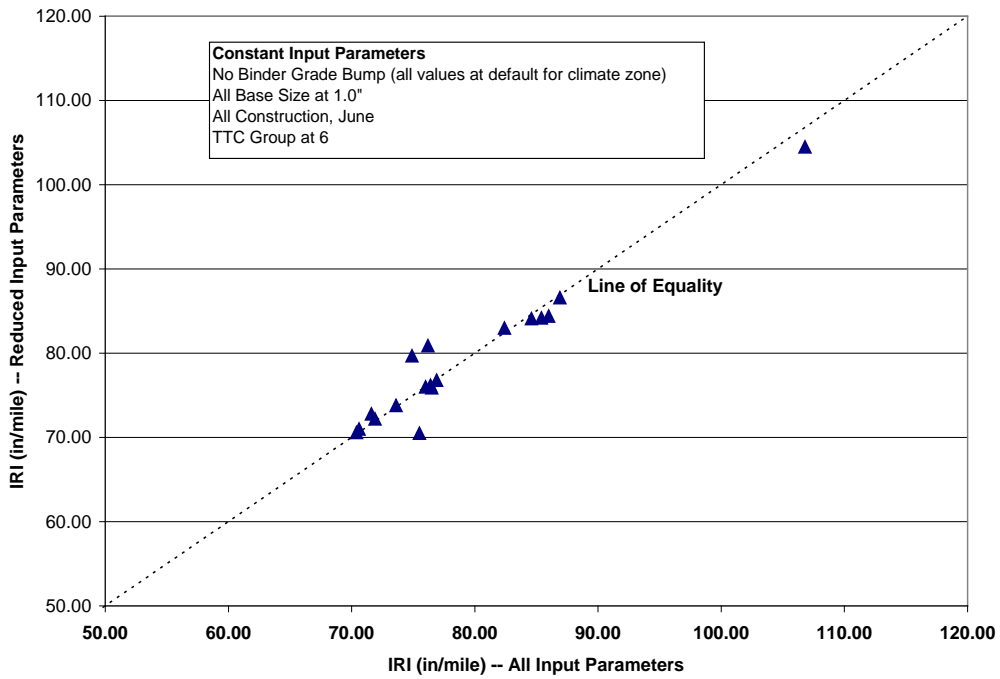
Figure 19. Comparison of reduced model and original model -- IRI

It is also interesting to note that in Figure 18 there is not a significant change in the predicted rutting when the "bumped" binder grade is not utilized.

As a means to evaluate these comparisons a single factor ANOVA was conducted between the results of the reduced parameter set and the complete input parameter set. The ANOVA results indicated that at the 95% confidence level there is no significant difference between the results. The ANOVA results are contained in Table 10.

44

Table 10. ANOVA Results for Actual vs. Predicted Distresses

Comparison	$F_{Calculated}$	$F_{Critical}$ (95%)
Longitudinal Cracking	0.257	4.130
Fatigue Cracking	0.241	4.130
AC Rutting	0.656	4.130
Total Rutting	0.581	4.130
IRI	0.000	4.130

Asphalt Mixture Sensitivity

In the previous section the overall sensitivity of the predicted performance was

evaluated over a wide range of different parameters. To further refine the influence

HMA mix parameters, used for quality control of pavement construction have on

predicted performance, additional variables were introduced into the sensitivity analysis

as follows:

- HMA base and surface air voids

- HMA base and surface effective binder content

- HMA base and surface gradation

- Surface layer Superpave binder grade.

Aggregate specific gravities were selected for a given aggregate source typical for

Kentucky. It was assumed that this would remain constant for a specific construction

project, it was therefore assumed that constant values of maximum specific gravity (G_{mm})

and bulk specific gravity of the aggregate (G_{sb}) could be utilized. Based on these

assumptions, in conjunction with the parameters listed in Table 2., the bulk specific

gravity of the mix (G_{mb}) and resulting unit weight at various void contents may be

determined. In addition, once the G_{mb} is known, the mixture voids in the mineral

aggregate (VMA) may then be calculated for each G_{mb} and asphalt content. Once the

VMA is known, it may be used in conjunction with air voids to determine the effective

binder content (by volume) used in Level 3 of the MEPDG software. Therefore, the

properties are linked together to provide realistic information regarding the mix instead of

just varying each parameter across a range independently. These linked properties

provide effective binder contents that range from 9.8 to 11 percent, and unit weights

ranging from 137 to148 lbs. /ft^3, depending upon it being a surface mix or base mix.

The analysis of the HMA mixture inputs sensitivity was accomplished by

determining the Pearson's Correlation Coefficient and the Spearman's Rank Correlation

Coefficient for the relationship between the input parameters and the resulting output. To

aid in evaluating the sensitivity of each output with respect to the input parameters,

"Tornado" charts were produced for each output parameter. These charts illustrate the

Pearson's and Spearman's coefficients for each input parameter being studied. These

results are given in Figure 20 through Figure 22. These figures show that input

parameters may have higher or lower correlation coefficients depending on the output

which is being analyzed.
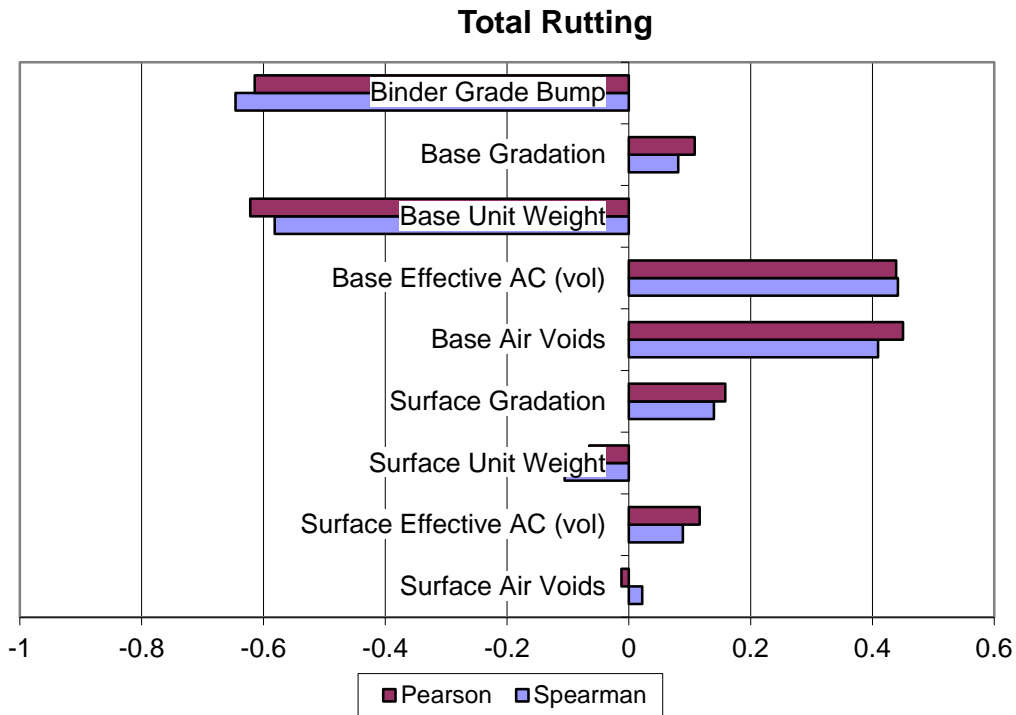
Total Rutting

Figure 20. Correlation coefficient total rutting

Alligator Cracking
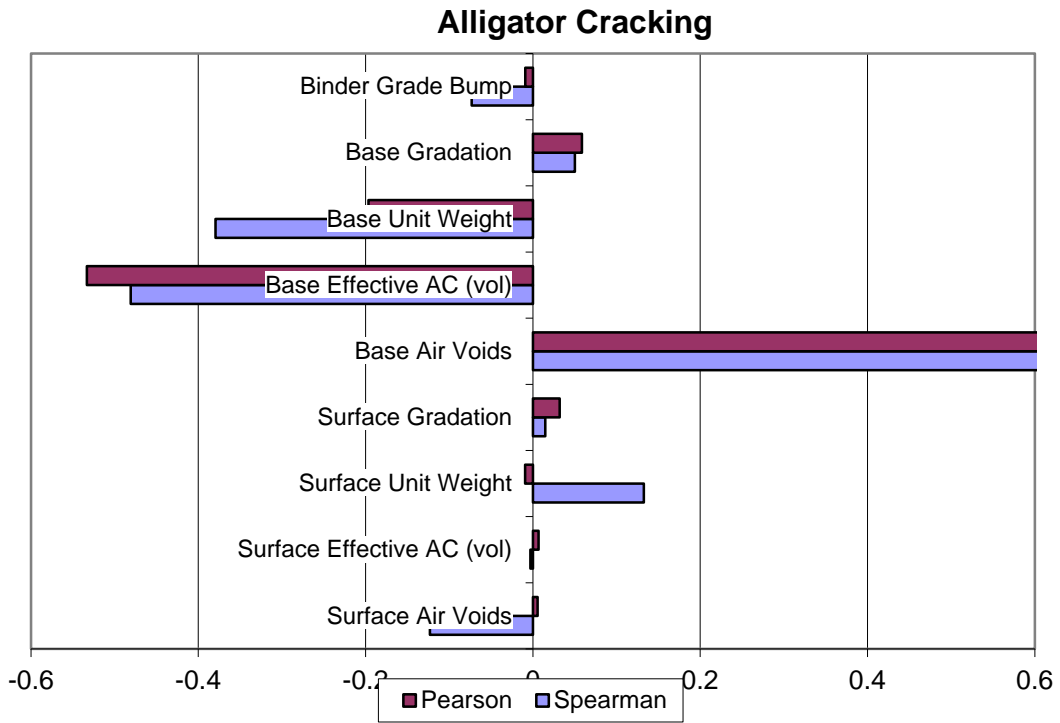
Figure 21. Correlation coefficient fatigue cracking

IRI
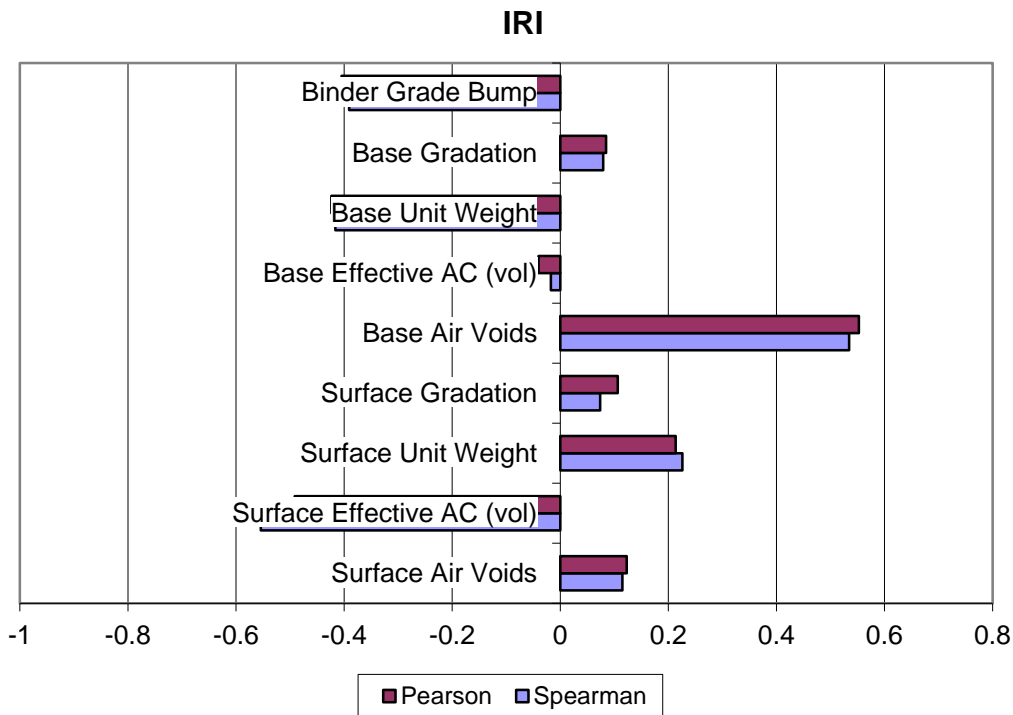
Figure 22. Correlation coefficient IRI

Based on the results of these sensitivity analysis and experience in Kentucky's mechanistic-empirical pavement design procedure, a subset of variables have been selected which represent typical pavement design parameters. It has been seen from this analysis that various hot-mix-asphalt (HMA) mixture parameters (void content, asphalt content, and etc.) do have some impact on performance. However, these are parameters which are used as part of typical construction quality control, to insure minimum standards are met. The final mixture parameters utilized through the remainder of this study are based on specific minimum standards, which lead to more conservative designs.

Rigid Pavement Sensitivity

The sensitivity analysis of for rigid pavements (PCC Pavements) has focused on the following seven parameters; Average Annual Daily Truck Traffic (AADTT), PCC Thickness, PCC Strength, subgrade strength, granular base thickness, and granular base strength.

The individual values which were varied and used in the study are given in Table 11. Table 12 provides information on the default values chosen from the design guide for other input parameters.

Table 11. Rigid Pavement Design Parameters

AADTT	Portland Cement Concrete Thickness (in)	Portland Cement Concrete Strength – Modulus of Rupture (psi)	Subgrade Strength (psi)	Granular Base Thickness (in.)	Granular Base Strength (psi)
100	6	500	8,000	6	20,000
500	7	600	10,000	8	30,000
1,000	8	700	13,000	10	40,000
2,000	9	800	16,000	12	
4,000	10				
6,000	11				
8,000	12				
10,000	13				
15,000	14				
25,000					

Table 12. Other Rigid Pavement Default Parameters

Traffic Inputs	Software Defaults were utilized with the exception of AADTT and TTC
Climate Inputs	Water Table depth was assumed to be 20 feet for all design sections. Individual weather stations in the cities provided in Table 3. were used for generation of the climate files
Structure Inputs Drainage and Surface Properties	Software Defaults were utilized
Portland Cement Concrete Layers	Software Defaults were utilized with the exception of the items given in Table 1.
Granular Layer	Software Defaults with the exception of values given in Table 11. All other parameters were software defaults based on base type
Subgrade	Subgrade CBR varied as stated in Table 3., all other parameters defined by software based on CL Soil Classification

The analysis of the PCC pavement structures was accomplished by determining

the Pearson's Correlation Coefficient and the Spearman's Rank Correlation Coefficient

for the relationship between the input parameters and the resulting output for a random

sampling of the input space identified in Table 11. To aid in evaluating the sensitivity of

each output with respect to the input parameters, "Tornado" charts were produced for

each output parameter. These charts illustrate the Pearson's and Spearman's coefficients

for each input parameter being studied. These results are given in Figure 23 through

Figure 25.
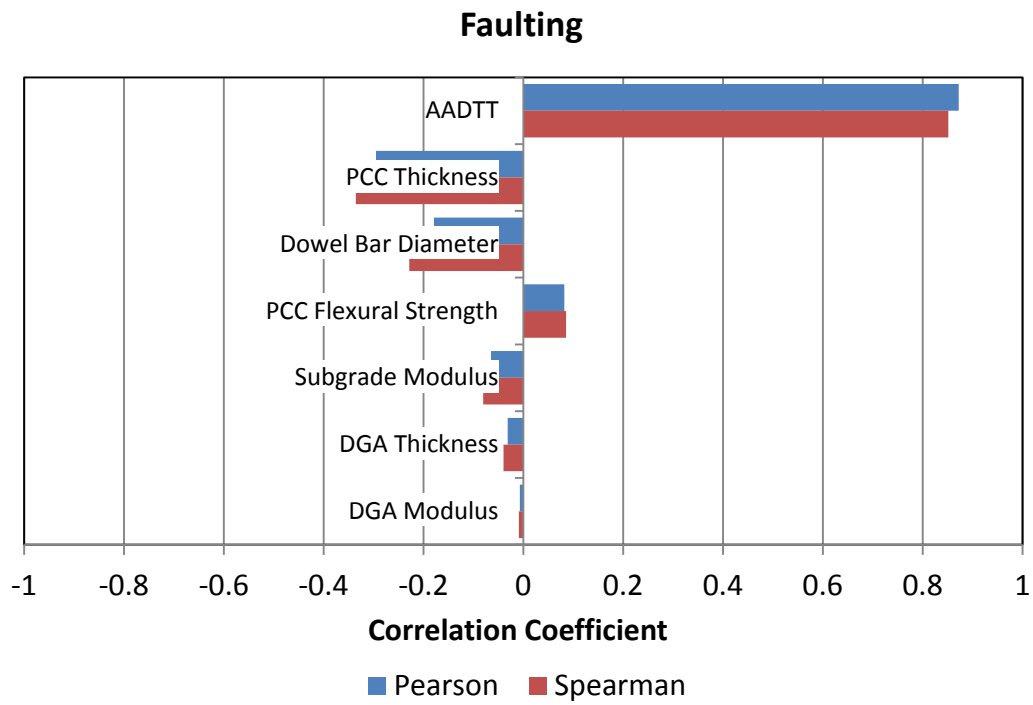
Faulting

Figure 23. Correlation coefficient for PCC faulting
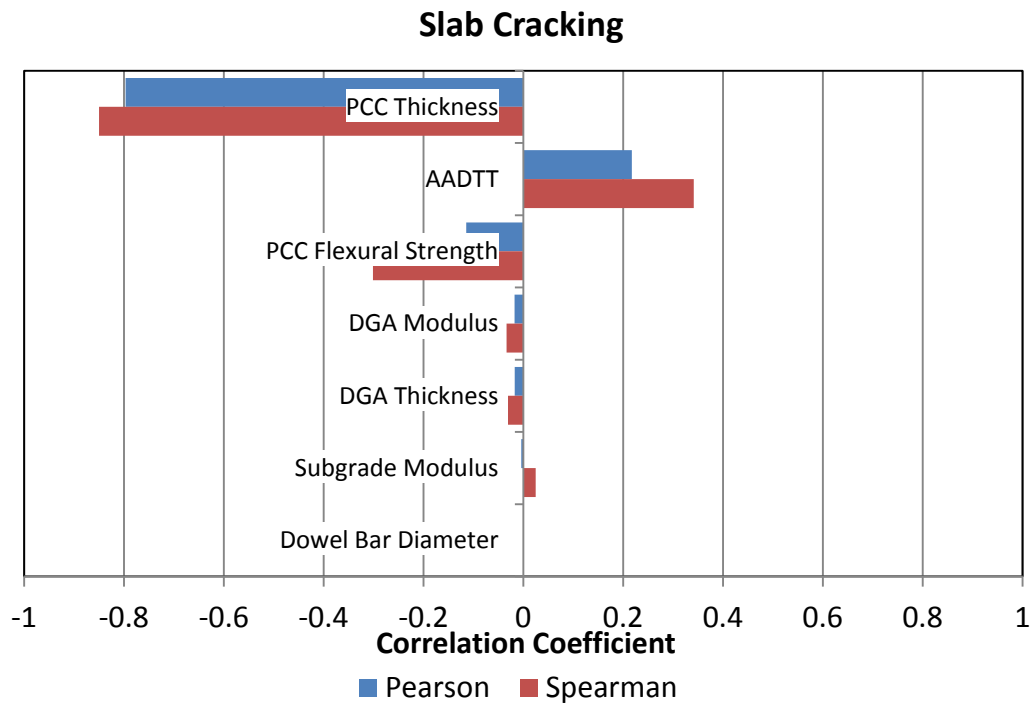
Slab Cracking

Figure 24. Correlation coefficient for PCC slab cracking
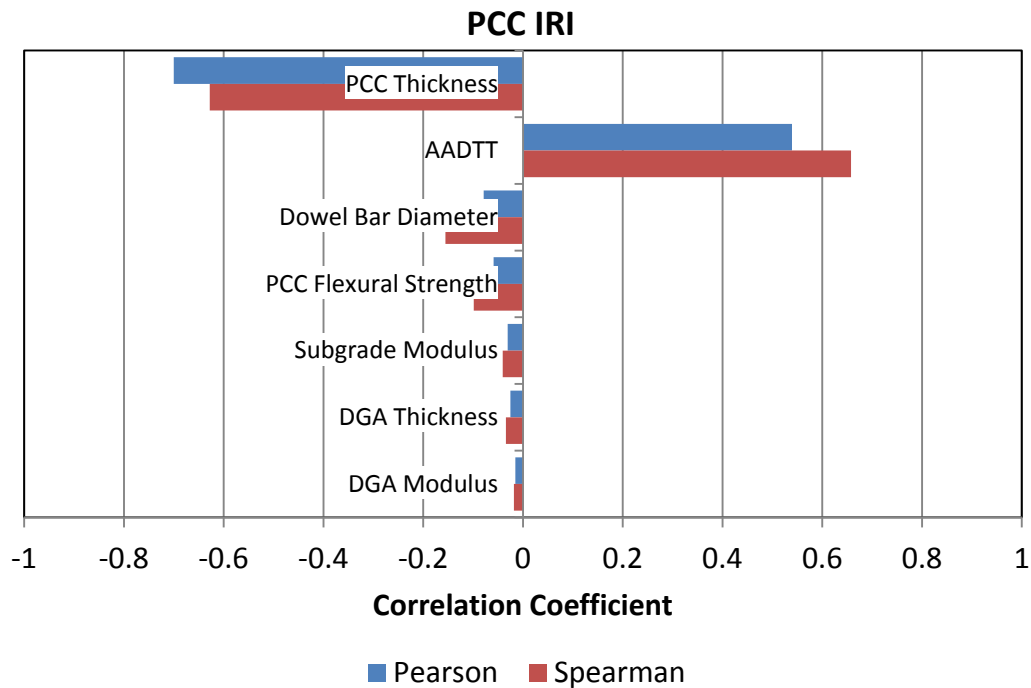
PCC IRI

Figure 25. Correlation coefficient for PCC IRI

It may be seen from these graphs that pavement thickness and traffic (AADTT) are the most highly correlated variables in the analysis. These results are very similar to the results for flexible pavements which were discussed earlier, in that thickness of HMA and traffic had the highest correlation in that analysis as well. It is interesting to note that subgrade strength, and DGA strength and thickness have very little correlation to any of the distresses. Flexural strength does appear to have some correlation with the predicted distress. In most agencies a minimum strength is specified for PCC pavements, the remainder of this study will utilize a typical minimum value which will lead to more conservative designs. The final input parameters used for the remainder of this study will be outlined in subsequent chapters

3.0 Design Reliability

3.1 Introduction

The Mechanistic-Empirical Pavement Design Guide (MEPDG) Version 1.1 developed under NCHRP 1-40 is a very complex tool for the evaluation of pavement structures, with many input factors which characterize materials, climate, traffic and construction. A key component of the design tool is the concept of design reliability. The reliability is the probability that any particular type of distress (or combination of distress manifestations) will remain below or within the permissible level during the design life of the roadway (AASHTO, 1993). In the NCHRP MEPDG (NCHRP, 2004) reliability is defined as the probability that each of the key distress types and smoothness will be less than a selected critical level over the design period. In the previous AASHTO 1993 Design Guide reliability was defined in terms of the number of equivalent single axle loads to terminal serviceability being less that the number of equivalent single axle loads actually applied (NCHRP, 2004).

The distresses predicted by the MEPDG represent mean values based on the results of the design inputs being processed through the mechanistic model and then applying transfer functions to determine predicted distresses. A reliability factor is then applied to this mean value based on the accuracy of the prediction model. Therefore, the basic results of the design guide are at a 50 percent reliability level, which means there is a 50 percent chance that the predicted distress will be higher or lower than this value.

In the development of the NCHRP design guide, the original intent was to have a full probabilistic analysis where designers would provide mean (average) input values for

various input parameters along with some measure of variability. These inputs were then

to be sampled using a Monte Carlo type of sampling to produce a true probabilistic

performance prediction. Due to the intensive computational time necessary to run a

single design (in excess of 20 minutes) this was not feasible.

3.2 MEPDG Reliability Concept

Several methodologies are available to conduct reliability based design, including

simulation methods (Monte Carlo Simulation) and other closed form analytical methods.

The reliability process in the new MEPDG is based on the ability of the performance

models to predict actual distresses of the sites used for calibration. The major

components of the errors associated with these predictions for rigid pavements were

defined by Darter (Darter, Khazanovich, Yu, & Mallela, 2005) as follows:

- *Input Error* -- error associated with the estimating each design input.

- *Measurement Error of Distress* – variation of measuring a given distress quantity.

- Pure Error – random or normal variability between distresses exhibited by exact
  replicate sections.

- *Model or Fitting Error* – inability of the model to predict actual pavement
  performance.

The reliability included in the new MEPDG was developed during the calibration

of the prediction models within the design guide. These prediction models consist of

"transfer functions" which predict a given distress based on measured pavement

responses. These transfer functions were calibrated utilizing data from national Long

Term Pavement Performance (LTPP) and another field pavement studies across the

country. The LTPP project was a national study on which contained over 800 pavement

sections across the country (Stubstad, Tayabji, & Lukanen, 2002). These pavement sections were periodically reviewed for performance. In addition, extensive testing was conducted to determine the various engineering properties of the pavement structure.

The general concept for reliability uses the standard deviation of the prediction model (standard error of the estimate) to determine the appropriate design reliability.

An example of the process utilized to determine this reliability is given below. Figure 26 provides an example plot of the predicted versus measured slab cracking for jointed plane concrete pavements, the results are broken up into four regions. These regions will be used to segment the variability in the predicted performance.
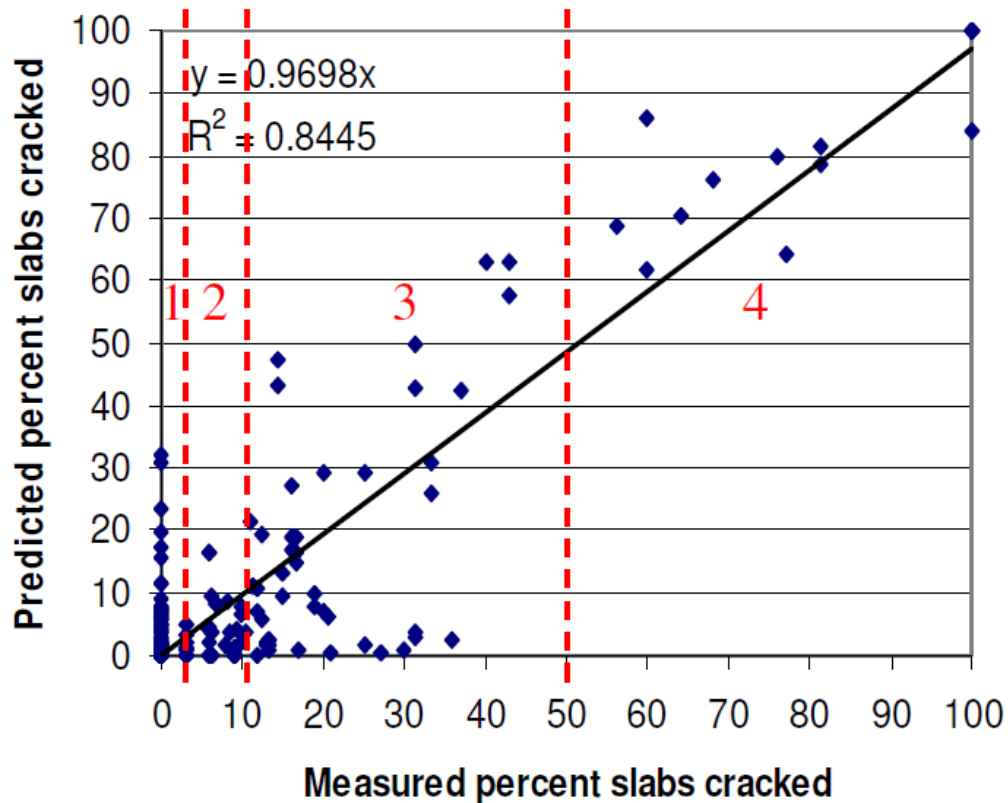
Figure 26. Example of accuracy of MEPDG prediction model (Darter M. , 2007)

It may be seen from the scatter in the data in Figure 27 that the difference between the measured and predicted data is quite significant in many areas. These residuals (measured – predicted distress) are used to determine the variability of the prediction model at various levels of distress.

The distress data utilized for calibration were then analyzed further by determining the mean and standard deviation of the predicted and measured data within each group (NCHRP, 2003). It was assumed that the data within each group is normally distributed and therefore techniques relating to standard normal distributions may be used. Relationships were then developed to relate the grouped information for the measured and predicted distress

In Figure 26, four areas are identified at various measured distress levels. Within each of these areas, the standard deviation of the residual is determined and utilized as the measure of model variability within that ranges. These discrete values are then used to develop a relationship relating the standard deviation versus predicted distress for the full range of anticipated results. An example of this method is given in Figure 27 below.
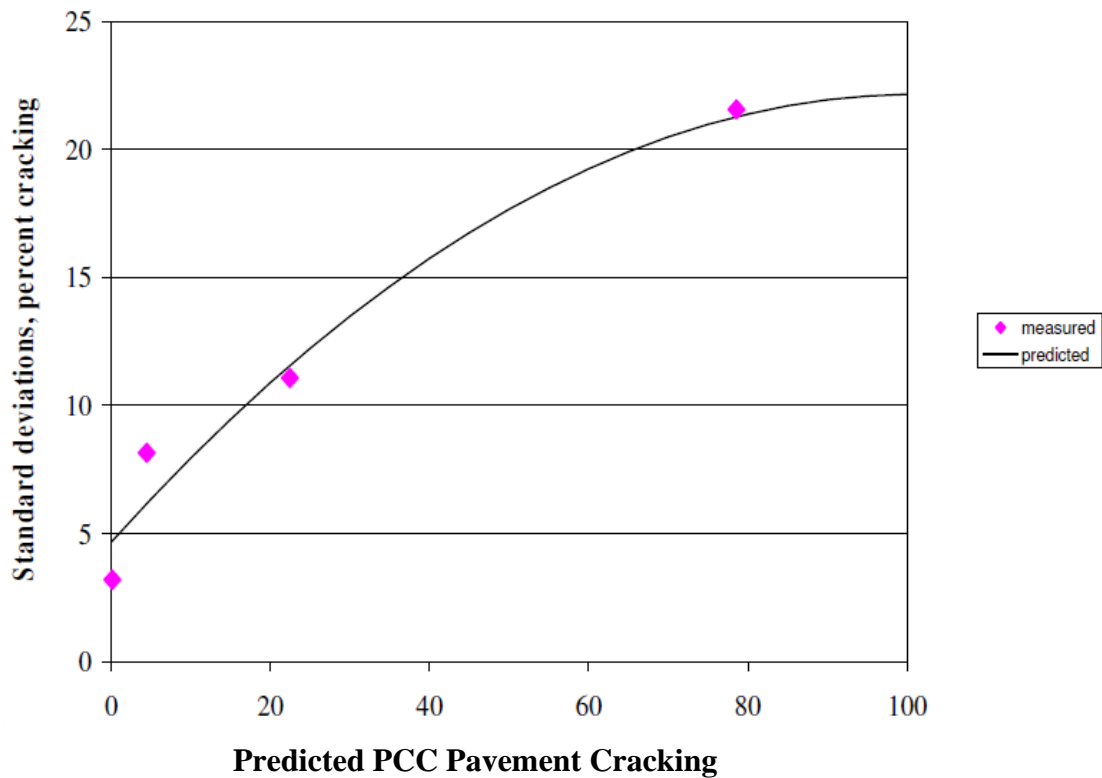
Figure 27. Variable standard deviation used for reliability analysis (Darter M. , 2007)

The final step to evaluate the reliability utilized in the MEPDG involved relating the predicted distress to the standard deviation of the measured distress for each group. This standard deviation may then be used to calculate the reliability of the predicted distress at any level.

This standard deviation relationship or residual error contains all the available information regarding the ways in which the prediction model fails to properly explain the observed distress (scatter in predicted results). The relationship in Figure 27 is defined as follows:

$$STD_c = -0.00172 * CRACK_{50}^2 + 0.3447 * CRACK_{50} + 4.6772$$

where:

STD_C = *standard deviation for cracking*

$CRACK_{50}$ = *predicted cracking (50% reliability)*

The resulting standard deviation and the cracking at 50% reliability may be used to determine the cracking at any given reliability level based on the assumption that these standard deviations are normally distributed. This method is illustrated as follows:

$$CRACK_R = CRACK_{50} + STD_C \cdot Z_R$$

where:

$CRACK_R$ = *predicted cracking at reliability level R, percent slabs*

$CRACK_{50}$ = *predicted cracking based on mean inputs (50% reliability), percent slabs*

STD_C = *standard deviation of cracking at predicted level of mean cracking*

Z_R = *standard normal deviate (one-tailed)*

This concept is graphically illustrated in Figure 28.
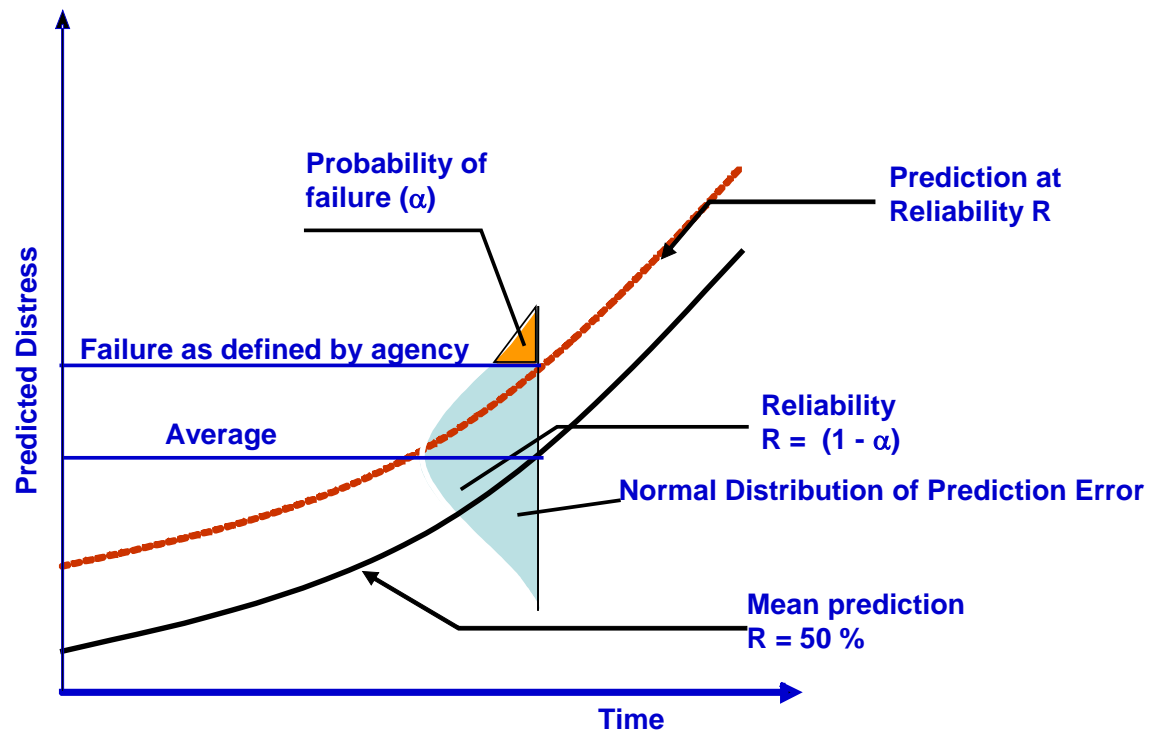
Figure 28. Example of design reliability for given distress, (NCHRP, 2004)

There are a number of drawbacks to utilizing this type of concept for reliability-based design. (Pierce, 2007). The original calibration of the design guide was undertaken on a national basis, therefore, for some deterioration modes there may be more calibration data at lower distress levels, this could lead to the reliability being less reliable at higher distress levels due to less data points being available.

This same methodology is used regardless of the input level utilized; therefore, better reliability cannot be achieved by providing more accurate input parameter information. In addition, this concept also assumes that the predicted results are always normally distributed, which may not necessarily be the case.

A study has been undertaken to evaluate the impact of input parameter

distributions on the predicted performance and its reliability (Graves & Mahboub, 2011).

This study outlines a potential means to utilize simulation-based techniques (Monte

Carlo) to evaluate the variation in predicted performance based on the variability of a set

of input parameters for a specific pavement design section. Other work has illustrated the

use of simulation techniques to conduct sensitivity analysis for the MEPDG Design

Guide (Graves & Mahboub, 2006). This study will utilize similar techniques, but will

include input distributions which represent the anticipated variability for a given

pavement design project.

3.3 Input Parameter Variability

Many factors are involved in establishing the appropriate input variability for a pavement

design. Considerable work has been done in recent years evaluating the variability of

pavement construction parameter (NCHRP Project 20-50), (Stubstad, Tayabji, &

Lukanen, 2002). The results of this work provide insight into the variability of in-situ

pavement materials, both their strength and the thickness at which they were constructed.

This information provides a measure of the potential variability which may occur in the

construction of roadways. A brief summary of coefficients of variation from

backcalculated layer moduli for selected pavement materials obtained from this study are

given in Table 13.

Table 13. Coefficient of Variation of Backcalculated Moduli

Layer	CV's Recommended for Pavement Design		
	Average (%)	Lower (%)	Upper (%)
Asphalt Concrete	39	17	72
Granular Base	50	17	92
Granular Subbase	74	16	150
Subgrade	35	6	92

Table 13 illustrates that all of the coefficients of variation for each design parameter are greater than 30%. For layer thicknesses, the NCHRP research indicated that for unbound layers the 85th percentile thickness variation would be 0.5 inches and 0.3 inches for asphalt bound layers.

For the evaluation of the reliability of the MEPDG process, data from the NCHRP project discussed above along with data obtained from quality control information from the Kentucky Transportation Cabinet was utilized. The data from the Kentucky Transportation Cabinet included both historical material quality control reports within Kentucky and their current quality control standards (KYTC, 2008). Based on these sources of data, reasonable variation of selected input parameters was determined.

Since the goal of this study was to evaluate the variability of a specific design, in addition to these asphalt volumetric parameters, information regarding the aggregate structure of the mix is also necessary. A single gradation for the surface was utilized, while two gradations for the HMA base were used. This decision was made based on review of several QC/QA reports for Kentucky projects, which indicated that the

variation on gradation for the surface was very small, while greater variation in the base layer gradation was observed.

Aggregate specific gravities were selected for a given aggregate source typical for Kentucky. It was assumed that this would remain constant for a specific construction project. Therefore, it was assumed, that constant values of maximum specific gravity (G_{mm}) and bulk specific gravity of the aggregate (G_{sb}) could be utilized. Based on these assumptions, in conjunction with the parameters listed in Table 13, the bulk specific gravity of the mix (G_{mb}) and resulting unit weight at various void contents may be determined. In addition, once the G_{mb} is known, the mixture VMA may then be calculated for each G_{mb} and asphalt content. Once the VMA is known, it may be used in conjunction with air voids to determine the effective binder content (by volume) used in Level 3 of the MEPDG software. These properties are linked together to provide realistic information regarding the mix instead of just varying each parameter across a range independently

In addition to the HMA mix parameters, variability in Average Annual Daily Truck Traffic (AADTT), dense-graded-aggregate (DGA) base (thickness and strength), HMA base thickness, and subgrade strength were included. The discrete values used for the normal distribution for each is given in Table 14.

Table 14. Summary of HMA Input Parameters

Input Parameter	Average	Standard Deviation	Values Used in Simulation
3/8" (9.5 mm) Surface Air Voids (%)	6.5	1.5	2.5, 3.5, 4.5, 5.5, 6.5, 7.5, 8.5, 9.5, 10.5,
3/8" (9.5 mm) Surface AC Content (%)	5.5	0.26	4.9, 5.1, 5.3, 5.5, 5.7, 5.9, 6.1, 6.3
1.0" (25 mm) Base Air Voids (%)	7.0	1.5	3, 4, 5, 6, 7, 8, 9, 10, 11
1.0" (25 mm) Base AC Content (%)	4.5	0.26	3.7, 3.9, 4.1, 4.3, 4.5, 4.7, 4.9, 5.1
AADTT TTC 1	6,000	1,200	2,000, 3,000, 4,000, 5,000, 6,000,7,000, 8,000, 9,000, 10,000
HMA Base Thickness (in)	7	0.5	5.67, 6.0, 6.33, 6.67, 7.0, 7.33, 7.67, 8.0, 8.33
DGA Thickness (in)	8	0.5	5.67, 6.0, 6.33, 6.67, 7.0, 7.33, 7.67, 8.0, 8.33
DGA Modulus (psi)	30,000	7,500	10,000, 15,000, 20,000, 25,000, 30,000, 35,000, 40,000, 45,000, 50,000
Subgrade Modulus (psi) A-7-6	8,000	2,000	3,500, 5,000, 6,500, 8,000, 9,500, 11,000, 12,500, 14,000

The remainder of the input parameters for the MEPDG was set to the default values

provided by the guide.

3.4 Monte Carlo Simulation

Input parameters given in Table 14 were defined using a discrete normal

distribution. This type of distribution provides a benefit, in that since it is discrete, during

the simulation process one of the nine discrete values is selected for each simulation. An

example of this type of distribution is given in Figure 29 for AADTT.
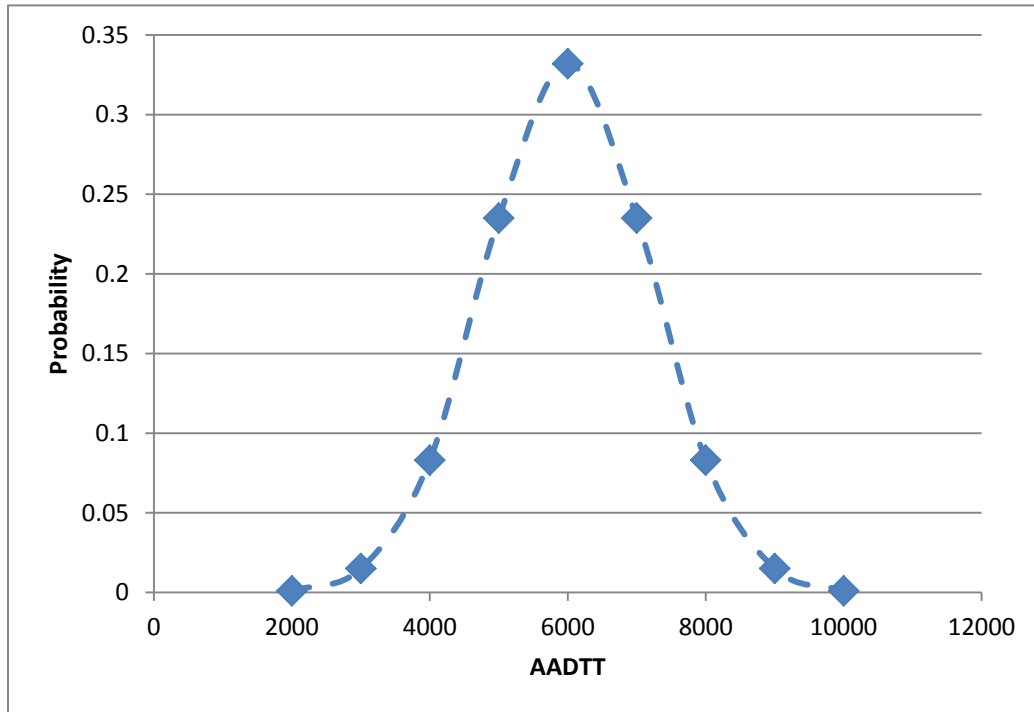
Figure 29. Example discrete normal distribution

With a typical normal distribution, during simulation the number of values which could be selected is theoretically infinite. The use of the discrete normal distribution provides a means to sample the entire space of a given variable with fewer simulations. These discrete distributions were then sampled using a Monte Carlo random sampling routine (Helton, 2004), to produce 100 different design scenarios covering the complete range of the input parameter space. The remaining variables necessary to evaluate the design were assigned default values based on the MEPDG software. These 100 scenarios were then processed through the MEPDG software to produce a matrix of outputs for the following distresses: fatigue cracking, HMA rutting, total rutting, transverse cracking

and IRI. For this particular design section, less than 5 percent of the scenarios showed any longitudinal cracking or transverse cracking. Therefore, these distresses were not included in the remainder of the analysis.

3.5 Evaluation of Distress Prediction Reliability

To evaluate the variability of the predicted distresses, a cumulative distribution was calculated for each predicted distress at the 10-year level. From these distributions the reliability at a given distress level may be determined. Cumulative distributions are illustrated in Figure 30 through Figure 32. In each figure, the 90th percent reliability is also noted. Some are nearly normally distributed, while others appear to be skewed.
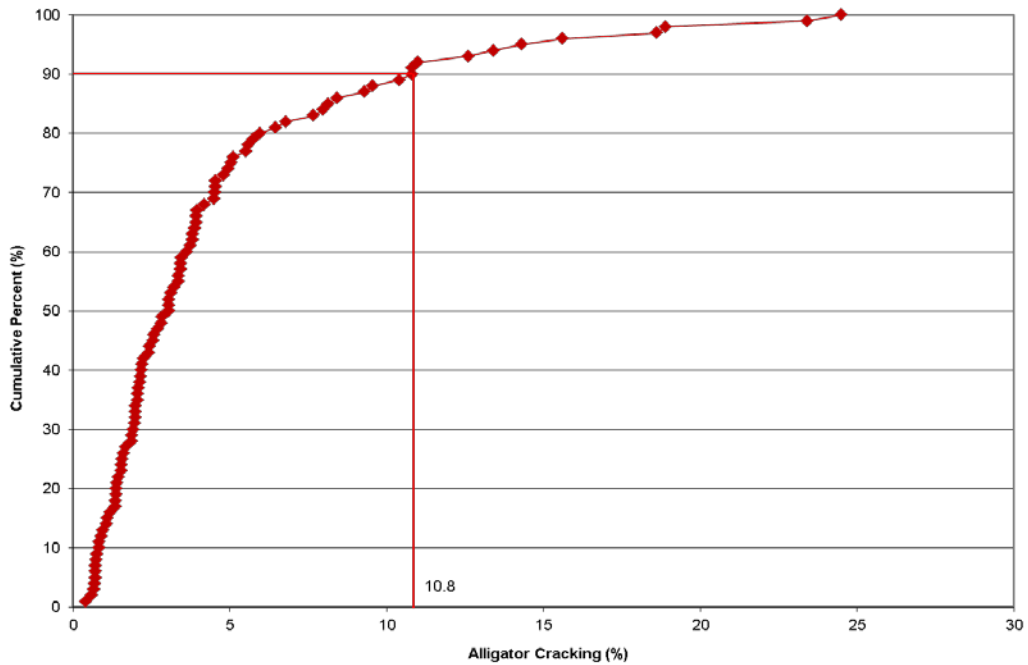
Figure 30. Cumulative distribution of fatigue cracking
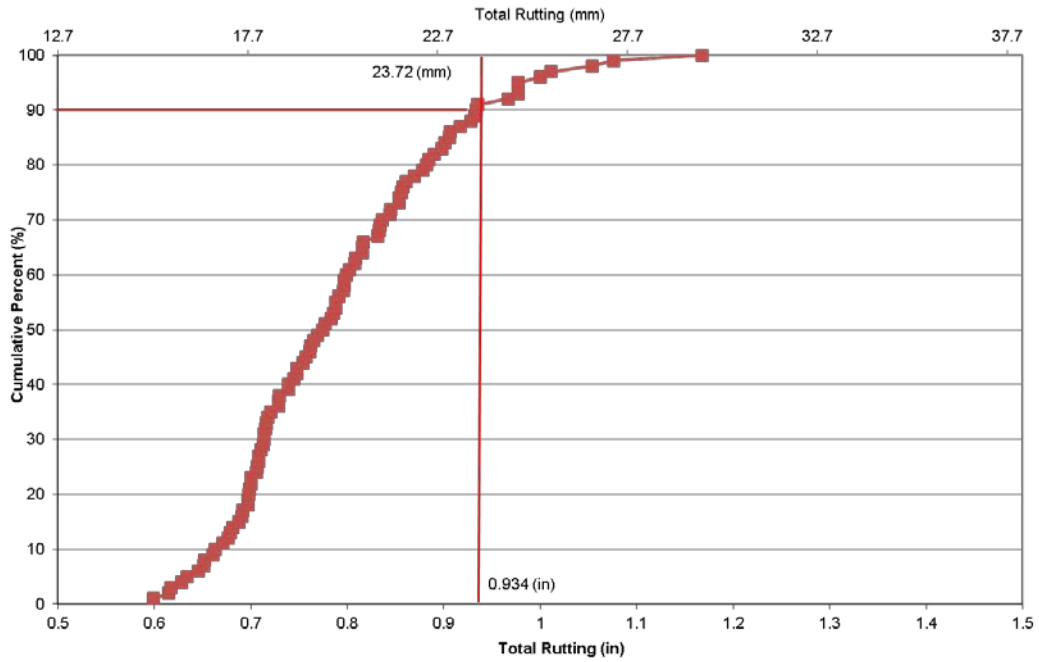
Figure 31. Cumulative distribution of total rutting
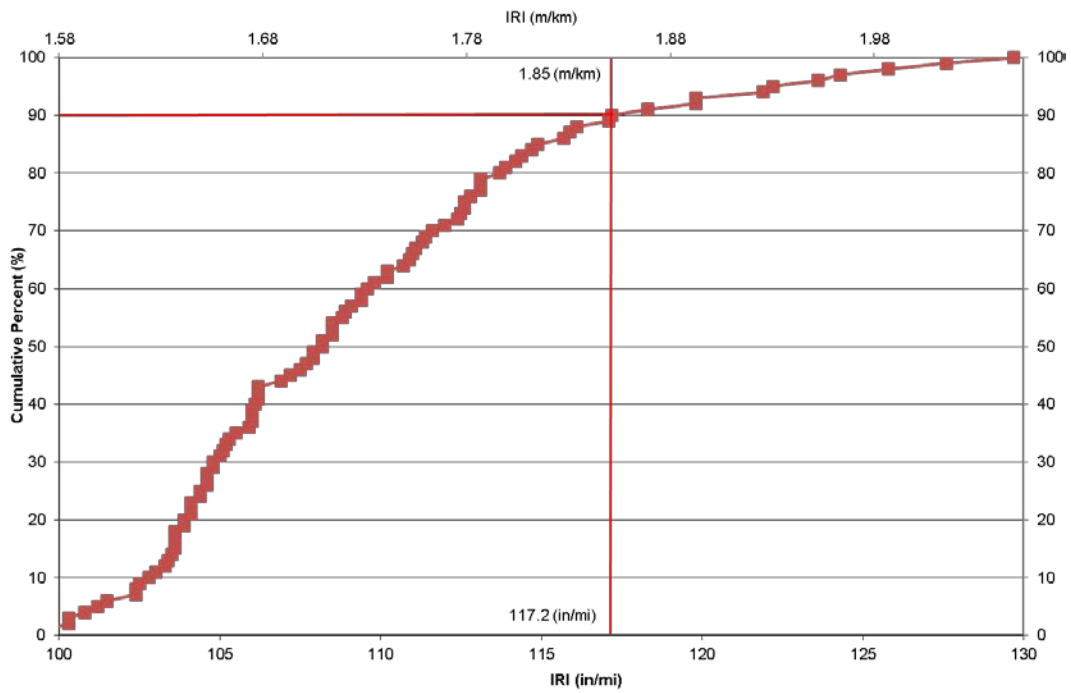
Figure 32. Cumulative distribution of IRI

There are a variety of methods to evaluate the normality of a given distribution. One such graphical method is presented in Figure 33 through Figure 35. This method involves plotting the cumulative distribution of a given distress against the standard normal quantiles of a normal distribution (Park, 2012). This quantile – quantile (Q-Q) is a plot of the percentiles (or quintiles) of a standard normal distribution versus the corresponding percentiles of the observed data. If the observations follow approximately a normal distribution, the resulting plot should be roughly a straight line with a positive slope.

Mean	4.55
Standard Deviation	4.77
Skewness	2.26
Kurtosis	5.46
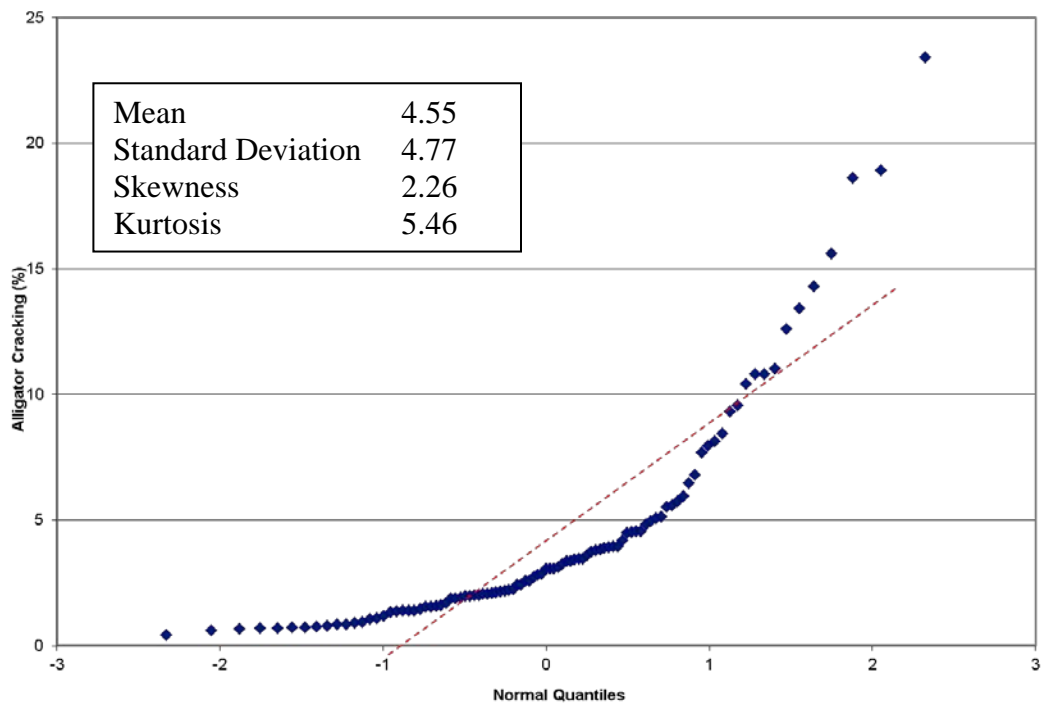
Figure 33. Normal quantiles, fatigue cracking

Mean	0.79
Standard Deviation	0.11
Skewness	0.79
Kurtosis	0.54
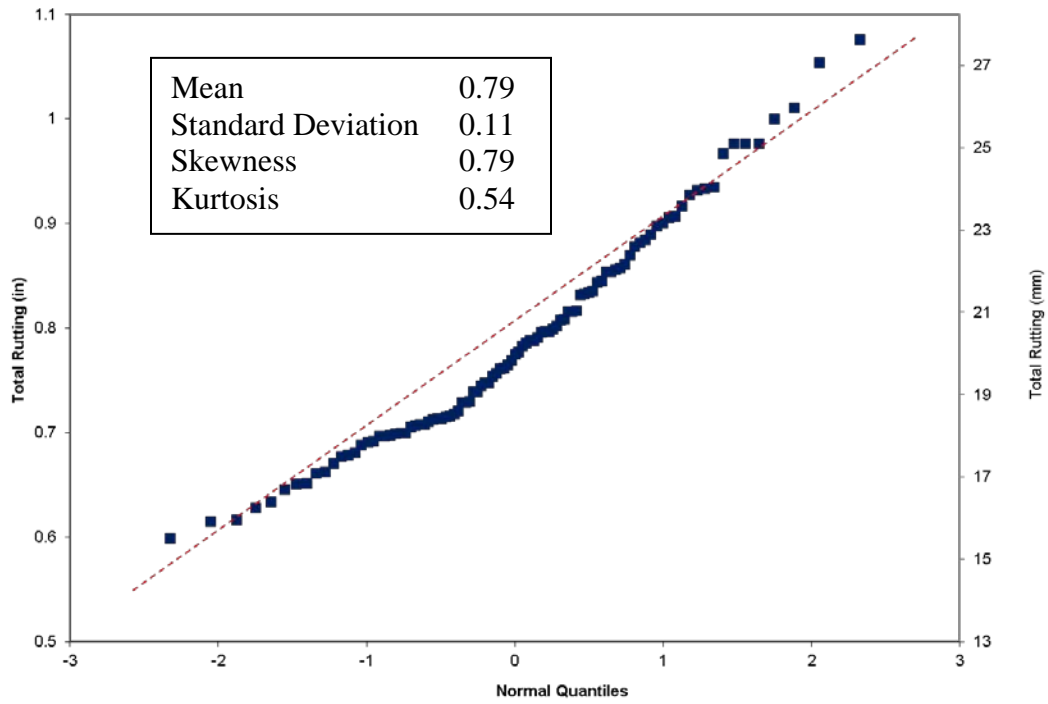
Figure 34. Normal quantiles, total rutting

Mean	109.34
Standard Deviation	6.37
Skewness	1.05
Kurtosis	0.91
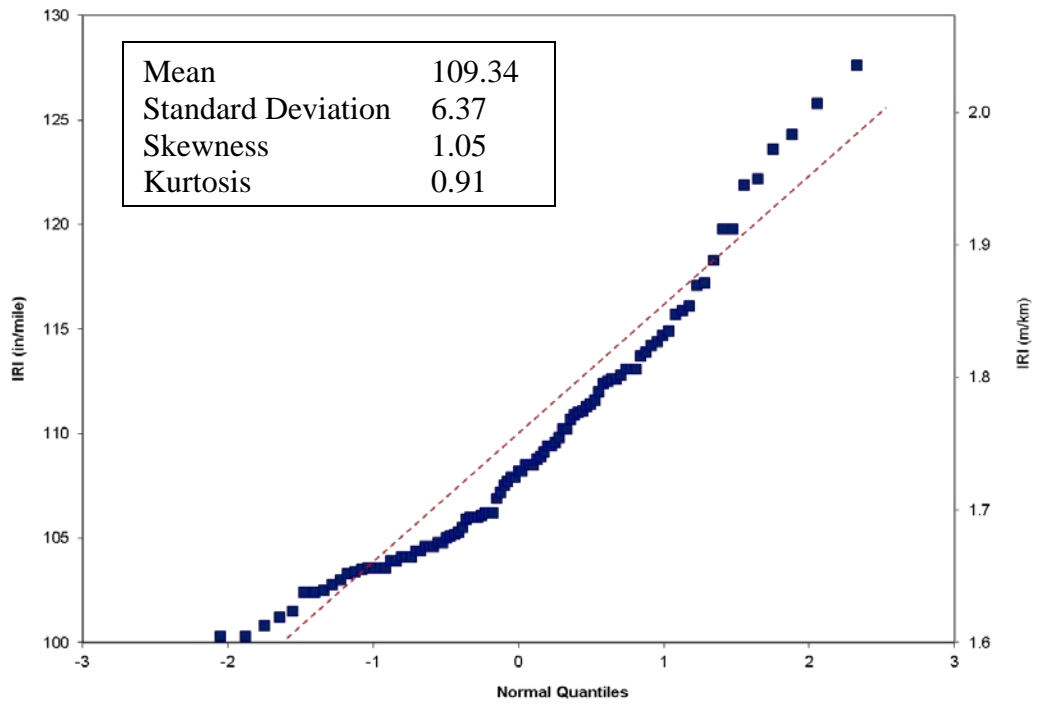
Figure 35. Normal Quantiles, IRI

In Figure 33 through Figure 35 the dashed line is a reference for what the data should look like if it were normally distributed. It may be seen that from these figures that fatigue cracking is somewhat skewed to the lower cracking values, while total rutting along with IRI are more near the reference line, but still indicate that they may not be normally distributed.

To further evaluate the normality of the predicted tests, the Skewness and Kurtosis for each predicted distress were determined. Skewness and Kurtosis are terms that describe the shape and symmetry of the distributions.

Skewness is a measure of symmetry, or lack thereof. A value greater than 1 or less than -1 indicates a highly skewed distribution, between 0.5 and 1.0 or -0.5 and -1.0 is moderately skewed, and between -0.5 and 0.5 indicates a fairly symmetric distribution, or nearly normally distributed. Positive skewness indicate distributions are skewed to the left, or lower values, while negative skewness are skewed to the right indicating higher values.

Kurtosis is a measure of the heaviness of the tails of a distribution. A normal distribution has its kurtosis equal to zero. Extremely non-normal distributions may have high positive or negative kurtosis values, while nearly normal distributions will have kurtosis values close to zero. Kurtosis is positive if the tails are "heavier" than for a normal distribution and negative if the tails are "lighter" than for a normal distribution (SAS, 2006).

The Skewness and Kurtosis for each predicted distress are given in Figure 33 through Figure 35. In review of these statistics, it may be seen that all the distress types

69

have Skewness that is greater than 0.5, indicating that the data are skewed toward lower

levels. Two of the distresses, IRI and fatigue cracking have Skewness greater than 1.0

indicating that they are significantly skewed toward lower values. All of the distributions

except AC rutting have high positive Kurtosis, which would indicate the tails of the

distribution are heavier than a normal distribution.   The Kurtosis for AC rutting is nearly

zero, indicating that it is approaching the symmetry of a normal distribution.

 Another method to test for normality is to perform a Shapiro-Wilk test (Park,

2012). This test examines the null hypothesis that a particular sample came from a

normally distributed population. For each of the distributions given in Figure 33 through

Figure 35, the null hypothesis that the data are normally distributed is rejected.

These results are interesting in that each of the input levels were normally

distributed, but the predicted distresses do not appear to be normally distributed. This is

not entirely unexpected since the MEPDG is a very complex model, which has many

interactions between input variables which may or may not be linear. However, the

reliability in the current MEPDG is based on assumptions that the residual error

associated with mean inputs compared to actual measured distress is normally distributed.

A comparison of 90 percent reliability given by the MEPDG for mean inputs of the

variables in this study and the reliability given from the simulation results may be seen in

Table 15.

Table 15. Comparison of 90 percent Reliability from MEPDG and Simulation Model

Distress	MEPDG	Simulation
Fatigue Cracking (%)	15.4	10.8
Total Rutting (in)	0.970	0.934
IRI (in/mi)	147.4	117.2

Some of the distresses have significant differences between the MEPDG and Simulation reliability at the 90 percent level. For fatigue cracking, the MEPDG value was 50% higher than that of the simulation results, while rutting and IRI were somewhat closer together. This may be explained to some extent by the fact that the prediction models for rutting and IRI generally have less model error as indicated by higher R^2 and lower standard errors than do fatigue cracking models, as described in the recently released NCHRP Research Results Digest (NCHRP, 2006). A full understanding of this difference is necessary, so that designers can have the best possible confidence in the predictions provided by the MEPDG software. Additionally, the observed departure from normality of various distress modes may impact the reliability of the design. High-type pavements are designed to perform without distresses exceeding a low threshold. It is indeed at these low thresholds levels where significant departures from normality take place under the current models. Therefore, any reliability-based analysis for high-type pavement facilities would seem suspect at this time. A similar argument can be made for the low-volume roads, in which distress thresholds are much higher. Only the mid-ranges of the distress modes seem to follow normal distributions.

As was discussed earlier, the reliability in the MEPDG is assumed to be all inclusive and account for all errors, such as: input error, distress measurement error, pure error, and model fitting error. It may be seen from these results that the 90 percent reliability based on simulation of the variation in input parameters is less in all cases than that predicted by the MEPDG. This would indicate that some of the other errors in the

prediction model (measurement error, pure error or model fitting error) have some significant impact on the MEPDG reliability.

These results may also indicate that continued refinement of the reliability portion of the MEPDG may be useful. It is not apparent at the time of preparation of this report what changes may have been made to the reliability calculations during the recalibration of distress models included in Version 1.1 of the MEPDG software. Data were not readily available in the literature regarding the distributions of the residuals for the measured versus predicted distresses for the new models. Therefore, continued work in this area is recommended.

This analysis provides a means to quantify the variability of the MEPDG distress predictions based on the variation in typical design inputs. It would indicate that for some of the distresses (fatigue cracking, and IRI) the variability not associated with input variability may be quite significant.

3.5 Summary of Results

This study has illustrated that the variability of the MEPDG predicted output for a given design section may not be normally distributed across typical variations of project input parameters. This was evident from the use of quantile plots to evaluate the shape of the predicted distributions. In addition, Skewness and Kurtoses statistics indicate that the predicted distresses were not normally distributed. The Shapiro-Wilk test also indicated the distributions were not normal. Since the current MEPDG reliability relies on assumption of normality for the performance prediction errors or residuals to determine reliability, further work may be necessary to develop alternative methods to address

reliability. One method may be to follow the same process which is currently utilized, but instead of making the assumption of normality, actual distributions of error/residuals could be used.

The departure from normality of various distress modes has the potential to impact the reliability of designs. Since high-type pavements are designed with very low distress thresholds, where the departures from normality take place under the current models, designs of this type of projects could be suspect. The same argument could also be made for lower volume facilities, which are designed for high distress levels which also exhibit departure from normal distributions. Further understanding of this variability is necessary to insure pavement designers can effectively utilize the correct reliability in design, and achieve the pavement performance they are expecting.

As computational efficiency and streamlining of the MEPDG software continues, the use of additional simulation techniques will become more feasible. Similar methodologies (Darter, Khazanovich, Yu, & Mallela, 2005) have been suggested in the literature, but have not been implemented due to the computationally intensive analysis required.

This study has outlined the potential contribution of material input variability to the overall reliability predicted by the design guide. As computational efficiency continues to increase, this type of process could be utilized to further investigate the reliability portion of the design guide.

4.0 Streamlined Model Development

4.1 Introduction

The Mechanistic Empirical Pavement Design Guide (MEPDG) (NCHRP, 2004), developed by the National Cooperative Highway Research Program (NCHRP) is a very robust and powerful tool for the analysis and design of highway pavements. The software does require some trial and error processing to determine the optimal design based on selected required performance. The user will select a trial design, allow the software to predict performance and then adjust design parameters if the required performance is not met.

The ability to streamline this process and reduce the potential number of required interactions would improve the use of the design guide on routine designs. The streamlining process outlined in this project will provide a means to determine a better starting point for determining the optimal design. It will provide the designer with an estimate of the required design thicknesses which can then be run through the full MEPDG model for performance final prediction.

The recently released DARWin-ME (AASHTO, 2011) software does include an optimization routine which automates the process of evaluating different structural thicknesses around a base design. However, it still requires multiple runs of the DARWin-ME software. The procedure is still an analysis procedure which does not allow for a direct solution for pavement thickness. The most recent version of the software still requires more than fifteen minutes of runtime, for a single flexible

pavement analysis. Rigid pavement projects run somewhat faster, but still require at least

five minutes to complete a single analysis. Both of these runtimes are achieved using a

very high end, six-core personnel computer with 12 MB of RAM. For an average user

the process can still be quite cumbersome and time consuming.

The factors mentioned above illustrate the need to develop some type of

streamlined procedure to utilize this new methodology. The development of a

streamlined process will allow designers to more effectively utilize the tools they have at

their disposal, by optimizing the amount of time needed to conduct pavement designs.

4.2 Selection of Modeling Methodology

As has been discussed the MEPDG model is a very complex procedure, in

addition, all of the underlying analysis algorithms and source code are not available.

Therefore, a direct evaluation of all the models and streamlining their use is not a viable

alternative. The lack of access to all of these models also forces the streamlining to take

place using some form of nonparametric model. Nonparametric models are developed

with no understanding of the underlying model form or the interactions between

variables. All of this information is derived from the actual data set being modeled.

In working to streamline the MEPDG several methodologies were investigated as

potential means to develop the streamline model, one was the use of Neural Networks

another was Multiple Adaptive Regression Splines (MARS). Many comparative studies

have been conducted (Francis, 2003; Cogger, 2001; Abraham & Steinberg, 2004; De

Veauz, Pischogios, & Ungar, 1993), these studies have identified some of the strengths

and weaknesses of each method. Neural Networks are very powerful tools in looking at complex problems; one of their drawbacks has been that they are generally "Black Box" analysis procedures, in that their results are generally very complex and not easily understood and can be difficult to implement into practical solutions.

The MARS technique (Friedman, 1991) is a multivariate, nonparametric regression technique which has been used in a variety of applications in many disciplines. It does not require any assumptions about the relation between dependent and independent variables and develops the relationship between those variables in a piecewise regression function.

Nonparametric regression techniques not only relax the assumption of linearity and normality of relationships, they do not require the functional relationship between the response and repressor variables to be known.   Nonparametric models typically grow in size to accommodate the complexity of the data. This is a form of regression analysis in which the predictor does not take a predetermined form but is constructed according to information derived from the data.   This method only connects the input variables to the output results. In the case of the MARS models developed during the research, no information is necessary regarding the transfer functions which are included in the MEPDG software, the MARS models developed are completely independent of what may be occurring within the "black box" of the MEPDG software. Nonparametric regression is a form of regression analysis in which the predictor does not take a predetermined form but is constructed according to information derived from the data.

Nonparametric regression requires larger sample sizes than regression based on parametric models because the data must supply the model structure as well as the model estimates.

This method has the ability to easily analyze complex situations and include both nonlinear relationships and interactions among variables. One key advantage to the MARS method is the ability to take the model results and implement them into a variety of applications. The basis functions in the MARS model provide information on the breakpoints or changes in the input parameter space which impact the model result.

4.3 Overview of Multiple Adaptive Regression Splines Model

The MARS methodology was introduced by Stanford physicist and statistician Jerome Friedman (Friedman, 1991). MARS is an innovative modeling tool that provides an excellent tool in finding optimal variable transformations and interactions.

There are three main steps to fit a MARS model. First is the construction phase, where basis functions (BF) are introduced in several regions of the predictors (independent variables). These basis functions are then combined into a weighted sum to define the global MARS model. These basis functions generally define where the piece-wise regression model changes or "hinges". This model normally contains many basis functions, which can cause over-fitting of the model. The second step is to prune the basis functions that have caused the over-fitting. The third and final step is to select the optimal model from the remaining smaller models which have resulted from the pruning. A more detailed discussion of the MARS technique is outlined by Friedmen (Friedman, 1991).

The procedure is a form of nonparametric regression, therefore making no assumptions about the underlying functional relationship between the dependent and independent variables. Some have described the process as the "Divide and Conquer" strategy where the input space is divided into regions each with its own regression equation. It provides a means to develop flexible regression models by fitting separate splines (or basis functions) to intervals of the predictor variables. The variables used and the end points of the intervals for each variable, referred to as knots are found via a brute force mathematical routine. Variables, knots and interactions are optimized simultaneously by evaluating a "loss of fit" (LOF) criterion. MARS chooses the LOF that most improves the model at each step. In addition to searching variables one by one, it also searches for interactions between variables, allowing any degree of interaction to be considered.

The output from the MARS procedure is a model that can be easily understood. Others have concluded that MARS has specific advantages over more complicated techniques such as neural networks, in that it has the ability to be easily implemented into other applications.

The general model of the MARS technique may be represented by the following

equations. MARS can be viewed as a generalization of stepwise linear regression

method. Which uses expansions in piecewise linear basis functions of the form (Haleem,

Abdel-Aty, & Santos, 2010):

$(x - t)+$ and $(t - x)+$. The "+" means positive part, so

$$(x-t)_+ = \begin{cases} x-t, & \textit{if } x > t \\ 0, & \textit{otherwise} \end{cases} \qquad \textit{and} \qquad (t-x)_+ = \begin{cases} t-x, & \textit{if } x < t \\ 0, & \textit{otherwise} \end{cases}$$

A graphical representation of this is given in Figure 36.
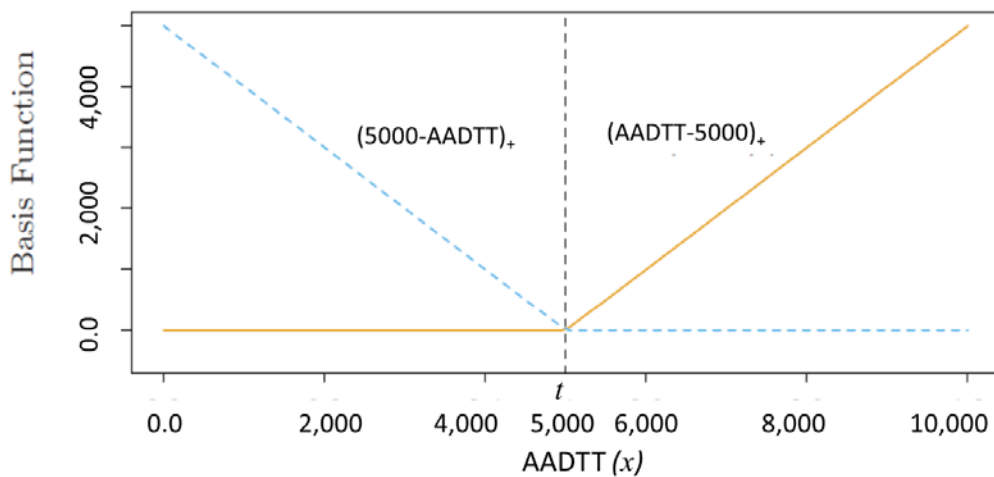
Figure 36. Basis function used by MARS (Hastie, Tibshirani, & Friedman, 2001)

In the example the location where $t = 5,000$ is called the knot with a pair of

splines intersecting at this location. The model-building follows a pattern like a forward

79

stepwise linear regression, with the exception that instead of using the original input

values, we us functions which are developed using the Basis Functions created from the

input values. The general form of the model is as follows:

$$\hat{y} = a_0 + \sum_{m=1}^{M} a_m \ B_m\,(x)$$

Where:

$\hat{y}$ is the predicted response:

a_0 is the coefficient of the constant basis function:

$B_m(x)$ is the mth basis function, which can be a single spline function or an interaction of two (or more) spline functions;

a_m is the coefficient of the mth basis function; and

M is the number of basis functions included in the MARS model

Generalized cross-validation (GVC) is used to evaluate the quality of the fit of the

models. This procedure is used to determine which variables to keep within the model,

therefore, producing the best fit. The GVC is also used to rank the variables in terms of

importance; the GVC is computed with and without each variable in the model to

determine their importance.   The general form of the GVC is as follows:

$$GVC = \frac{1}{N}\sum_{i=1}^{N}\left[\frac{y_i - \hat{f}(x_i)}{1 - \frac{k}{N}}\right]^2$$

Where:

> N is the number of observations
>
> y is the dependent variable
>
> x is the independent variable(s)
>
> k is the effective number of parameters or degrees of freedom in the model

The MARS process was implemented using the MARS 2.0 (Salford Systems, 2009) software developed by Salford Systems. This software provides an interactive interface to the MARS algorithms which facilitate the model development. The models developed by the MARS procedure can be easily programed in a variety of languages including C, visual basic for applications (VBA). Visual Basic has been utilized for this research to facilitate the use of the MARS models developed. . An example of a typical MARS model is given in the following equation:

Fatigue Cracking = 5.0646 - 0.627951 * BF1 + 2.25994 * BF2 + 0.000231766 * BF3
– 0.000604024 * BF4 - 5.77597E-005 * BF5 + 0.000333157 * BF6 - 5.7591E-005 *
BF7- 0.00100138 * BF8 - 0.000245137 * BF9 + 0.000296165 * BF10 + 8.62713E-009 * BF11-
3.56426E-007 * BF12 - 0.0891434 * BF13 + 0.196097 * BF14 - 2.94177E-005 *
 BF15 - 1.23361E-008 * BF16 + 9.40696E-009 * BF17 + 1.05724E-007 * BF18 +
 0.000236021 * BF20 - 1.4413E-005 * BF22 + 2.98929E-005 * BF23 + 0.582007 * BF24

where:

Fatigue Cracking = predicted fatigue cracking from MARS model.
BF1 = max (0, AC_THICKNESS - 6);
BF2 = max (0, 6 - AC_THICKNESS);
BF3 = max (0, AADTT - 5000);
BF4 = max (0, 5000 - AADTT);
*BF5 = max (0, AC_THICKNESS - 10) * BF3;*
*BF6 = max (0, 10 - AC_THICKNESS) * BF3;*
BF7 = max (0, DGA_MODULUS - 30000);
BF8 = max (0, 30000 - DGA_MODULUS);
*BF9 = max (0, AC_THICKNESS - 12) * BF8;*
*BF10 = max (0, 12 - AC_THICKNESS) * BF8;*
*BF11 = max (0, AADTT - 2500) * BF8;*
*BF12 = max (0, 2500 - AADTT) * BF8;*
BF13 = max (0, DGA_THICKNESS - 10);
BF14 = max (0, 10 - DGA_THICKNESS);
*BF15 = max (0, SUBGRADE_MODULUS - 6000) * BF1;*
*BF16 = max (0, DGA_MODULUS - 30000) * BF6;*
*BF17 = max (0, 30000 - DGA_MODULUS) * BF6;*
*BF18 = max (0, AC_THICKNESS - 6) * BF12;*
*BF20 = max (0, AC_THICKNESS - 8) * BF8;*
*BF22 = max (0, DGA_THICKNESS - 10) * BF6;*
*BF23 = max (0, 10 - DGA_THICKNESS) * BF6;*
BF24 = max (0, AC_THICKNESS - 12);

AC_THICKNESS = Asphalt Concrete Thickness
AADTT = Average Annual Daily Truck Traffic
DGA_MODULUS = Dense Graded Aggregate Modulus
DGA_THICKNESS = Dense Graded Aggregate Thickness
SUBGRADE_MODULUS = Subgrade Modulus

4.4 Overview of Datasets used for Modeling

       The datasets used for the development of the streamlined model are based on the

MEPDG program that was developed during the NCHRP 1-37A project. These data sets

consist of multiple analysis runs over a range of values for selected design inputs. The

selection of these variables was based on the sensitivity analysis outlined in the previous

chapter and experience working with Kentucky's mechanistic-empirical pavement design

procedure.   Streamlined models have been developed for both flexible pavements (HMA

pavements) and rigid pavements (PCC pavements).

       A summary of the variables utilized in each of these designs is given in Table 16.

For the development of these models all required input values for climate, bound and

unbound materials, and traffic which are not included in Table 16, were held constant,

information regarding these default values may be found in previous research by the

authors (Graves & Mahboub, 2006).

Table 16. Summary of Variables in the Streamlined Model

Flexible Pavement	Rigid Pavements
AADTT	AADTT
HMA Thickness	PCC Thickness
DGA Thickness	DGA Thickness
DGA Modulus	DGA Modulus
Subgrade Modulus	Dowell Bar Diameter

       To develop the streamlined models, a series of designs were developed and

processed through the NCHRP design software, these designs were randomly selected

from the input parameter set of possible design combinations. Table 17and Table 18

provide a summary of the input variable combinations possible for each type of pavement. The AADT levels indicated were the current year AADTT and this traffic level was projected for 20-years at two percent growth per year. Therefore, the distresses predicted are those which occur at the end of a 20-year design life.

A full factorial matrix of the input parameters would require several thousand different design runs to be completed. Each of these design runs takes in excess of 30 minutes to complete. There are multiple methods which could be utilized to minimize the number of design runs to be completed. One such method would be to conduct a fractional factorial design, which would reduce the number of required MEPDG design runs by the selected fraction ½, ¼, etc. Once the fractional number was selected, some type of methodology would be necessary to insure the entire input parameter space is included. A second method, which was used in this analysis was a random sampling technique using discrete uniform distributions, which would allow for equal probability in sampling across the entire input parameter space. The final result was a set of 1,500 different pavement designs for each of the pavement types, these designs were utilized to develop the streamlined models. With this large dataset of solutions, one could simply utilize some type of search routine to determine the design which most closely fits the required performance parameters for design. However, this may not provide the most efficient design since the thickness increments are at least one inch apart.

Table 17. Flexible Pavement Input Variables

AADTT (Average Annual Daily Truck Traffic)	500, 2,500, 5,000, 7,500, 10,000, 15,000, 20,000, 25,000
HMA Thickness (in)	4, 6, 8, 10, 12, 14
DGA Thickness (in)	6, 8, 10, 12, 14, 16
DGA Modulus (psi)	20,000, 25,000, 30,000, 35,000, 40,000
Subgrade Modulus (psi)	6,000, 7,500, 9,000, 10,500, 12,000, 13,500

Table 18. Rigid Pavement Input Variables

AADTT (Average Annual Daily Truck Traffic)	500, 2,500, 5,000, 7,500, 10,000, 15,000, 20,000, 25,000
PCC Thickness (in)	6, 8, 10, 12, 14
DGA Thickness (in)	6, 8, 10, 12, 14, 16
DGA Modulus (psi)	20,000, 25,000, 30,000, 35,000, 40,000
Subgrade Modulus (psi)	6,000, 7,500, 9,000, 10,500, 12,000, 13,500
Dowel Bar Diameter (in)	1.25, 1.5, 1.70

The streamlined model provides a means to go from a discrete set of solutions to a

continuous solution space which will allow the designer to determine the most efficient

design.

The development of these design scenarios is a very time consuming process.

Two Master's Degree students (Ganapathy Palanisamy and Salman Hakimzadeh) assisted

in the operation of the design software to process the design scenarios selected.   Each

design scenario must be entered into the design software and processed. Once all of the

designs had been processed, the resulting predicted performance (output files) must be

combined into a database which provides a listing of the input parameters and the output parameters for each design evaluated.

To facilitate the input of the information into the design software, an automation program, Automation Anywhere 4.0 (Automation Anywhere, 2006) was utilized. This program read information from the spreadsheet of desired input values and input it into the interactive design software.
These input files were then processed through a batch process available in the software.

The resulting predicted distresses are stored in an Excel spreadsheet for use by the designer. An Excel macro was developed to extract data from each of these spreadsheets and combine it with the database of input solutions. The advantage of utilizing this type of process was that the potential of user input error was reduced, and the speed of developing the input files was increased. Once completed, this database provided the necessary data used to develop the streamlined models.

4.5 Development Model for Flexible Pavements

The database of design scenarios which was previously discussed was used as the
input information for the streamlined MARS models. Two different sets of models have
been developed. The first set of models was developed to predict individual distresses of
rutting, fatigue cracking, and roughness (IRI). The general form of the models which
were developed are given below, the actual models for each is given in Appendix A:

*Fatigue Cracking (%) = f (AC thickness, DGA thickness, subgrade modulus,
DGA modulus, and AADTT)*

*Rutting (in) = f (AC thickness, DGA thickness, subgrade modulus, DGA modulus,
and AADTT)*

*Roughness, IRI (in/mi) = f (AC thickness, DGA thickness, subgrade modulus,
DGA modulus, and AADTT)*

where:
Fatigue Cracking (%) = predicted flexible pavement fatigue cracking
Rutting (in) = predicted flexible pavement rutting
Roughness (in/mi) = predicted flexible pavement roughness
AC Thickness (in) = thickness of asphalt bound surface layer
DGA Thickness (in) = thickness of unbound dense graded aggregate
Subgrade modulus (psi) = subgrade strength in terms of resilient modulus
*DGA modulus (psi) = unbound dense graded aggregate base in terms of
resilient modulus*
AADTT = average annual daily truck traffic

These models will predict pavement performance based on the input parameters
similar to the results of the full MEPDG software. They can be utilized as a pavement
analysis tool by predicting anticipated pavement performance. MARS models were
developed for each of the above listed relationships; the resulting R^2 for each of these
models was in excess of 0.9. Once the models were developed they were used to

compute the specified distress and then compared to the actual distress in the input

database as determined by the MEPDG model. These results are given graphically in

Figure 37 through Figure 39. It may be seen from each comparison that the predicted

distress from the MARS model and the actual distress from the MEPDG model correlate

very well.
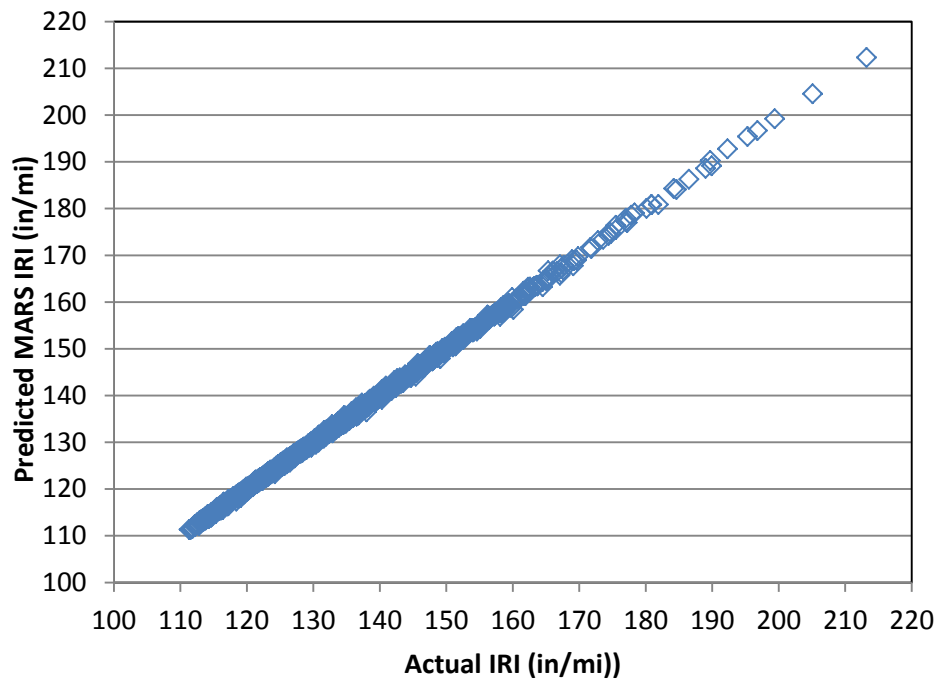
Figure 37. Comparison of actual IRI and MARS predicted IRI
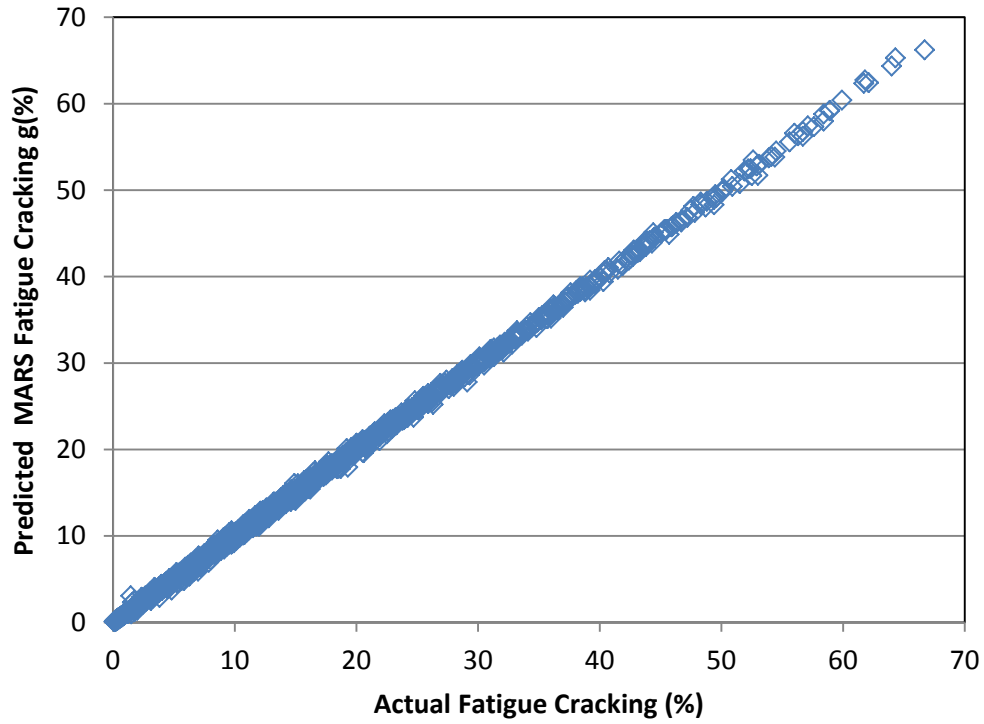
Figure 38. Comparison of total rutting with MARS predicted total rutting
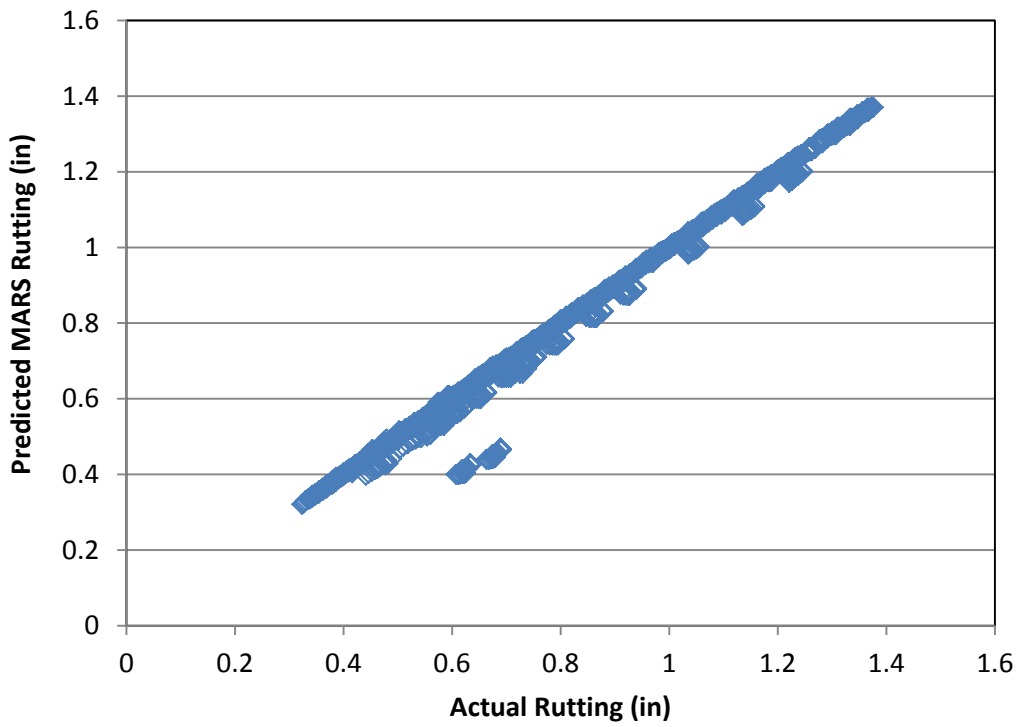
Figure 39. Comparison of fatigue cracking with MARS predicted fatigue cracking

To further evaluate these MARS models a series of random designs were chosen which were not included in the subset used for model development. For these designs, the MARS models were used to predict the pavement distresses and then compared to the distresses predicted by the MEPDG. A comparison of a portion of these results for fatigue cracking is shown in Figure 40. It may be seen from this figure that there is generally good agreement between the MARS distresses and the MEPDG distresses.
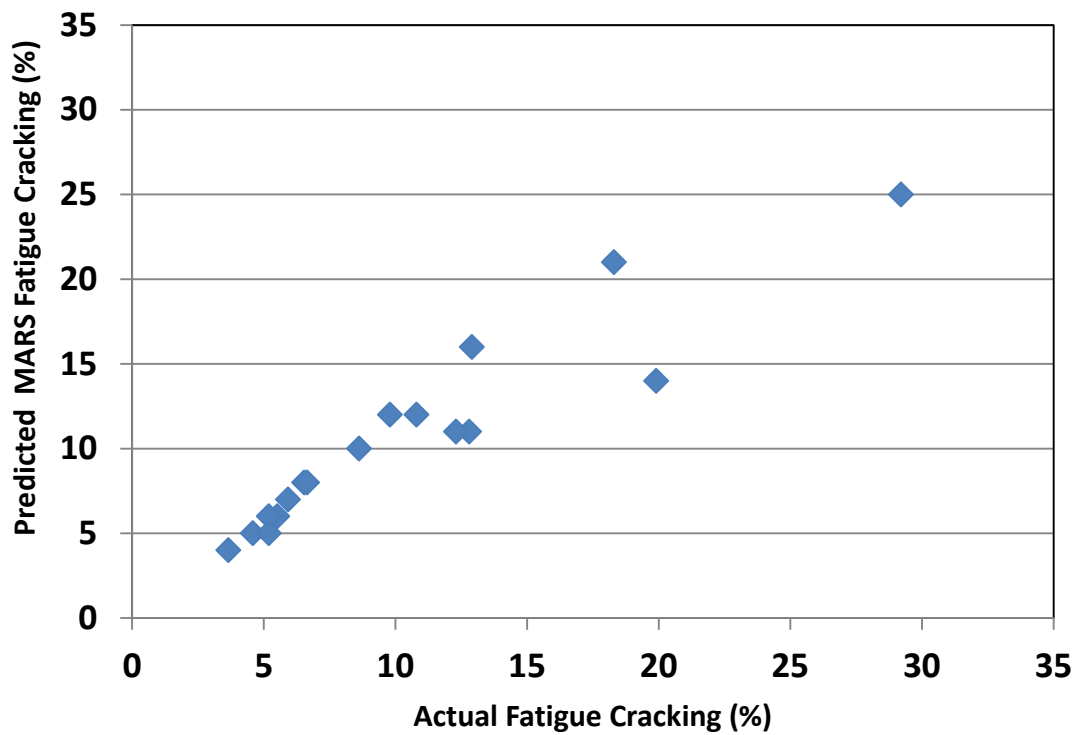
Figure 40. Comparison of actual MEPDG fatigue cracking to MARS model fatigue cracking

The second phase of utilization of this type of modeling is to develop an "Efficient Design Solution" to allow the designer to predict the thickness of the roadway needed to achieve a desired level of performance. This method was developed to be

similar to the methods used today where the ultimate result is a pavement thickness. This solution is independent of the previous MARS models developed to predict pavement performance.

Traditional pavement design typically considers the strength of subgrade materials, anticipated traffic, and some standardized granular base thickness and strength based on various constructability issues. Once these granular base thicknesses have been set, the final surface thickness of bound material is determined in a single step. As has been previously discussed, the current MEPDG only predicts performance, the designer is responsible for analyzing multiple pavement structures and then determining the final thickness of the surface layer based on "trial and error". The "trial and error" process can be very inefficient and time consuming. This raises the need for some type of streamlined model to calculate the surface thickness, once the designer has selected the desired performance, along with information about the traffic, and underlying materials (subgrade and granular base).

In the development of this solution it was determined that a solution which allows the user to input all distress types (cracking, rutting, and IRI) into one model was not feasible since there are many interactions between each distress. The models developed for this all-inclusive approach did not seem to perform as well as models that allowed the designer to select an individual distress and predict a thickness to achieve that distress.

91

The following models were developed to predict AC thickness; the detailed MARS

model for each is given in Appendix A.

AC Thickness $_{Fatigue\ Cracking\ model}$ (in) =
f (Fatigue Cracking, DGA thickness, subgrade modulus, DGA modulus, and AADTT)

AC Thickness $_{Total\ Rutting\ model}$ (in) =
f (Total Rutting, DGA thickness, subgrade modulus, DGA modulus, and AADTT)

AC Thickness $_{IRI}$ (in) =
f (IRI, DGA thickness, subgrade modulus, DGA modulus, and AADTT)

where:

      AC Thickness $_{Fatigue\ Cracking\ model}$ (in) =
        calculated surface thickness using fatigue cracking model
      AC Thickness $_{Total\ Rutting\ model}$ (in) =
        calculated surface thickness using total rutting model
      AC Thickness $_{IRI}$ (in) = calculated surface thickness using IRI model
      Fatigue Cracking (%) = predicted flexible pavement fatigue cracking
      Rutting (in) = predicted flexible pavement rutting
      Roughness (in/mi) = predicted flexible pavement roughness
      DGA Thickness (in) = thickness of unbound dense graded aggregate
      Subgrade modulus (psi) = subgrade strength in terms of resilient modulus
      DGA modulus (psi) =
        unbound dense graded aggregate base resilient modulus
      AADTT = average annual daily truck traffic

This essentially provides three solutions for each design. The designer can select

the most conservative design (thickest structure), or utilize the models developed in the

previous section to determine the distress characteristics of each thickness and then

choose the design which best fits their design situation.

To evaluate these "Efficient Design Solution" models, the predicted performance

results from the subset of MEPDG solutions were use as input into the MARS models,

along with the corresponding information on traffic and material properties. The

thicknesses determined by the models were compared to the actual original input

thicknesses used in the MEPDG predictions.   These results are given in Figure 41

through Figure 43.
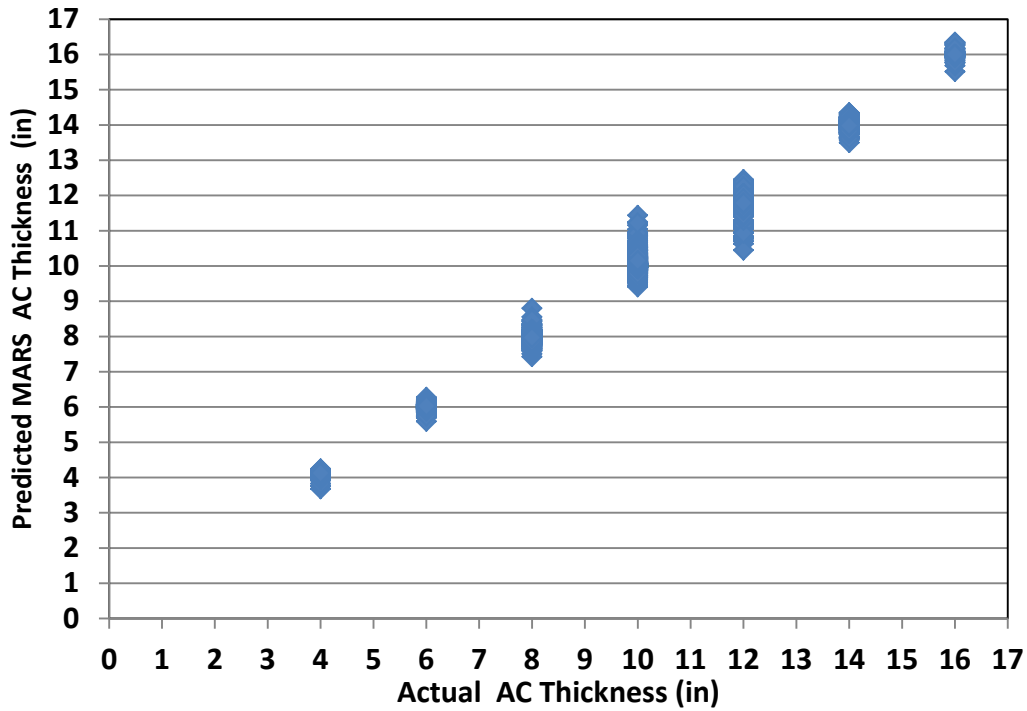
Figure 41. Comparison of actual thickness to MARS predicted thickness – total rutting
model
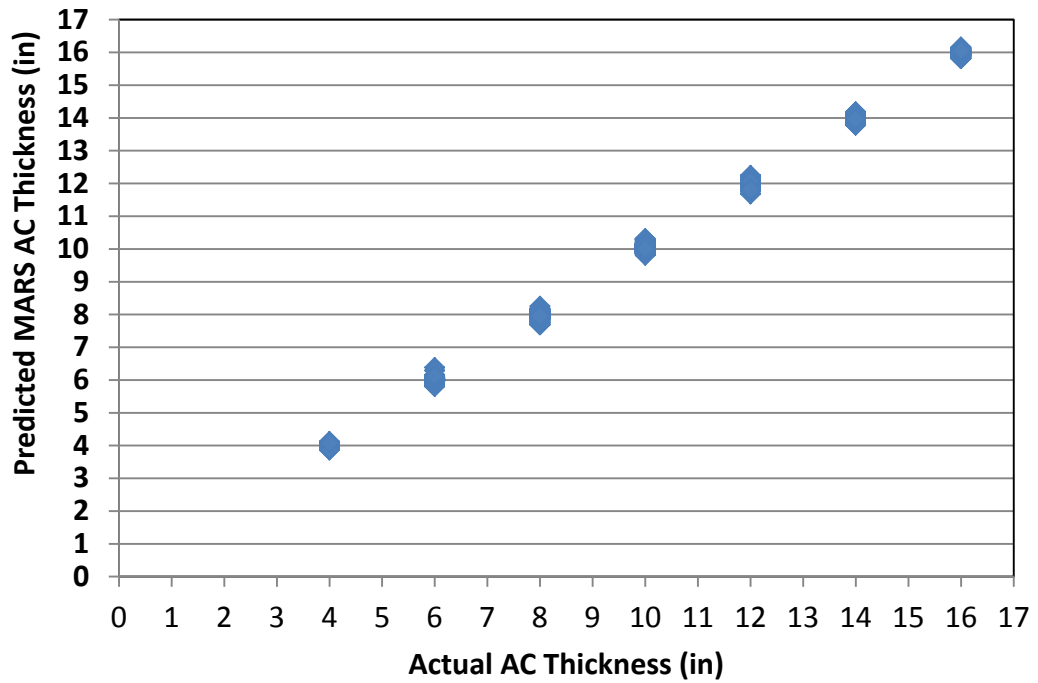
Figure 42. Comparison of actual thickness to MARS predicted thickness—IRI model
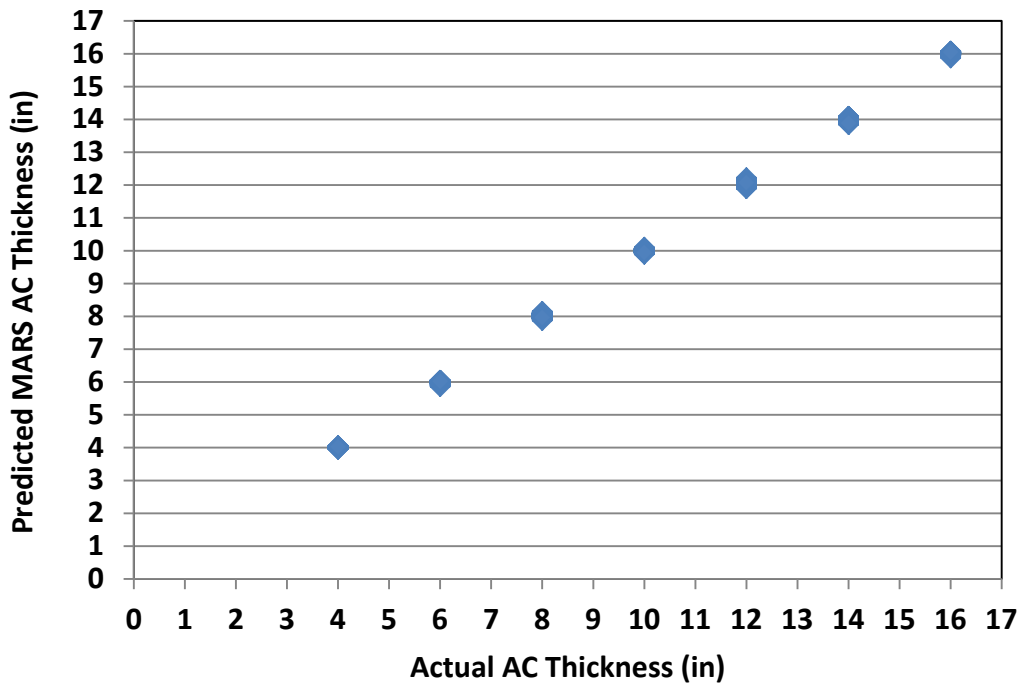
Figure 43. Comparison of actual thickness to MARS predicted thickness—fatigue cracking model

The actual and predicted thickness agreed very well in the previous figures. As a means to evaluate the effectiveness of these models another series of MEPDG designs were developed at various thickness and distress levels which were not included in the original subset used for model development. These designs were selected across a range of thicknesses and traffic levels within the overall range of the original MEPDG solutions used for the model development. The predicted distress results were then input into the MARS models for each type of distress, providing three predicted thickness results. A comparison of these predicted thickness for each distress model are shown in Figure 44. These results illustrate good agreement between the actual and predicted distress for each distress type.
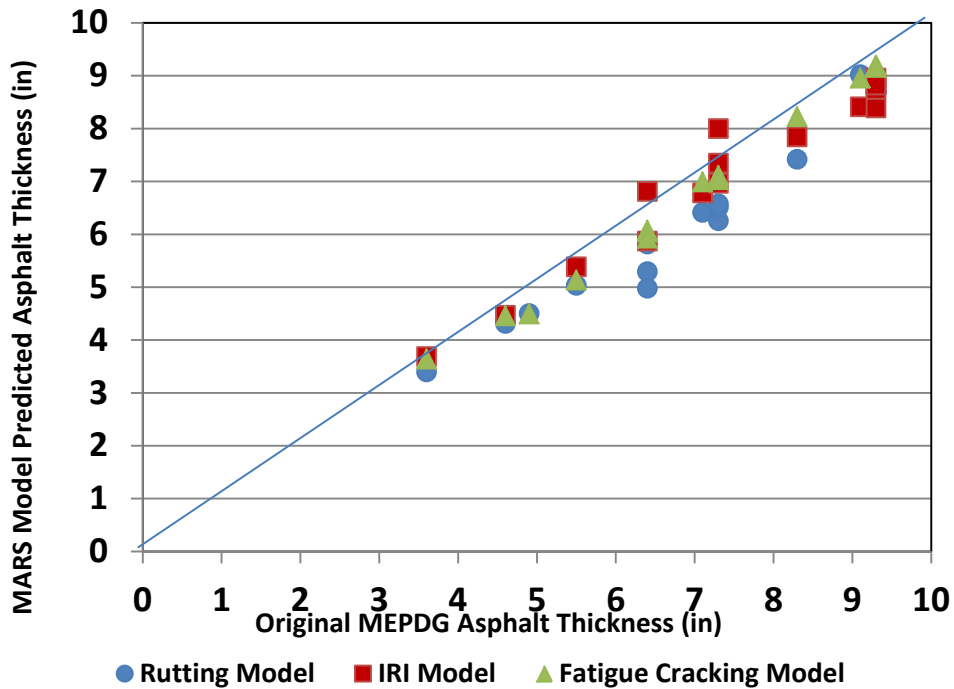
Figure 44. Comparison of original MEPDG thickness with MARS predicted AC thickness

4.6 Development of Model for Rigid Pavements

The same process outlined for the flexible pavements has been used to develop two sets of models for rigid pavements. The first set of models predict the pavement distresses of faulting, cracking and IRI, the second set of models determine the required thickness for a given distress.

The models developed for prediction of performance are given below, the detailed MARS model for each is given in Appendix A:

> *Faulting (in) = f (PCC thickness, DGA thickness, subgrade modulus,*
> *DGA modulus, Dowel Diameter and AADTT)*

> *Cracking (%) = f (PCC thickness, DGA thickness, subgrade modulus,*
> *DGA modulus, Dowel Diameter and AADTT)*

> *Roughness, IRI (in/mi) = f (PCC thickness, DGA thickness, subgrade modulus,*
> *DGA modulus, Dowel Diameter and AADTT)*

> *where:*
> *Faulting (in) =transverse joint faulting*
> *Cracking (%) = percent of slabs with transverse cracks*
> *Roughness (in/mi) = predicted rigid pavement roughness*
> *PCC Thickness (in) = thickness of PCC surface layer*
> *DGA Thickness (in) = thickness of unbound dense graded aggregate*
> *Subgrade modulus (psi) = subgrade strength in terms of resilient modulus*
> *DGA modulus (psi) = unbound dense graded aggregate base in terms of*
> *resilient modulus*
> *Dowel Diameter (in) = diameter of transverse joint dowel bars*
> *AADTT = average annual daily truck traffic*

MARS models were developed for each of the above listed relationships; the resulting R^2 for each of these models was in excess of 0.9. Once the models were developed they were used to compute the specified distress and then compared to the actual distress in the input database as determined by the MEPDG model. These results are given graphically in Figure 45through Figure 47.

The agreement between the distresses calculated using the MEPDG (cracking, faulting, and IRI) and those predicted by the MARS model is excellent. Cracking is somewhat clustered above 80 percent level and the below 10 percent level. This is a function of the sharp break in the distress prediction curve in the MEPDG software. An example showing the relationship between slab cracking and PCC pavement thickness is given in Figure 48.
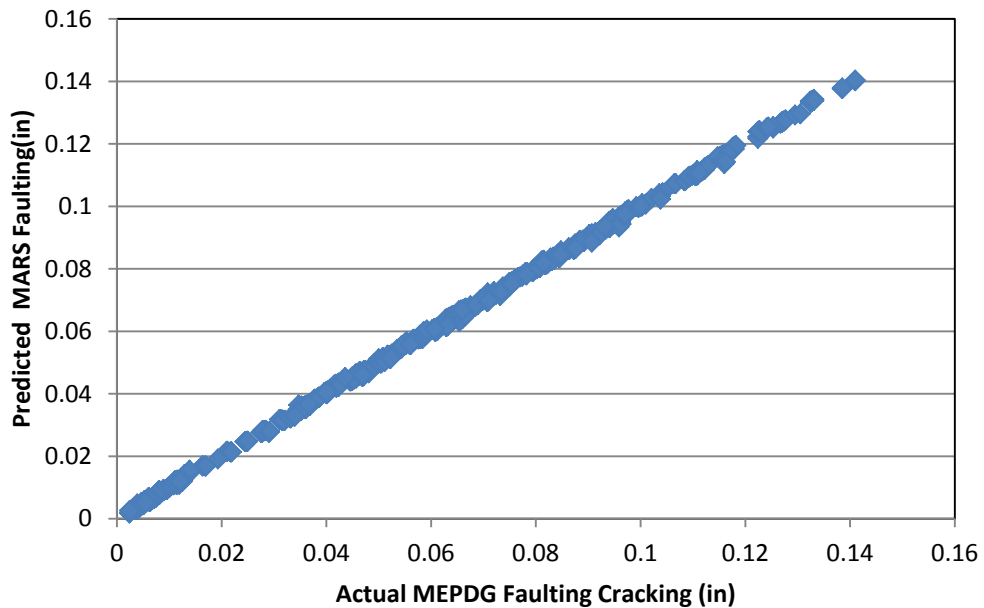
Figure 45. Comparison of actual MEPDG faulting with predicted MARS faulting
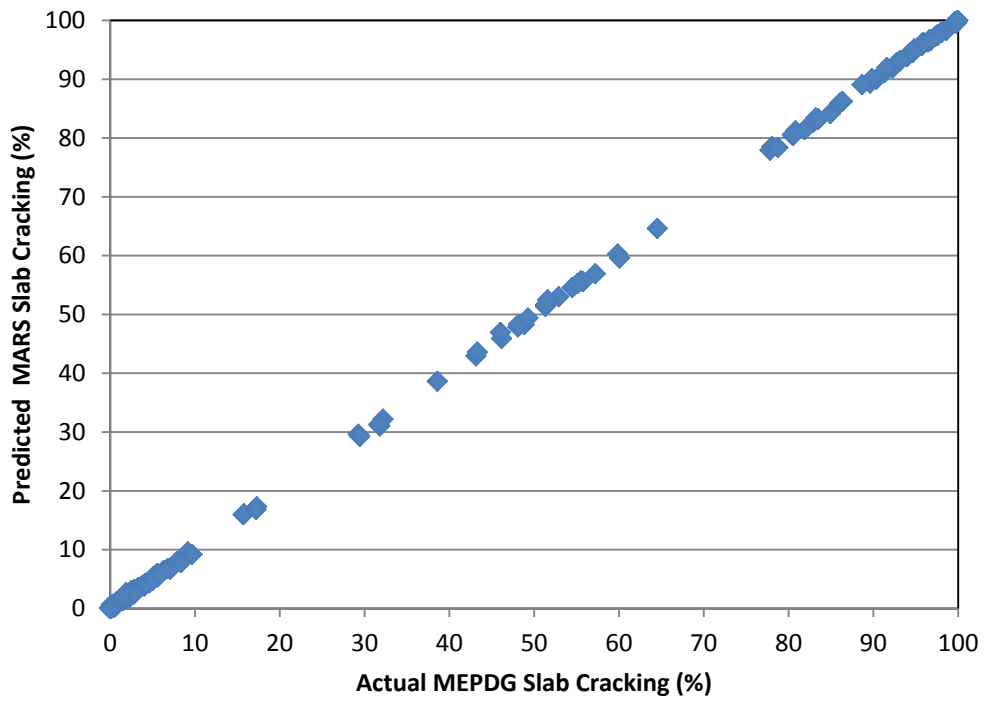
Figure 46. Comparison of actual MEPDG slab cracking with predicted MARS slab cracking
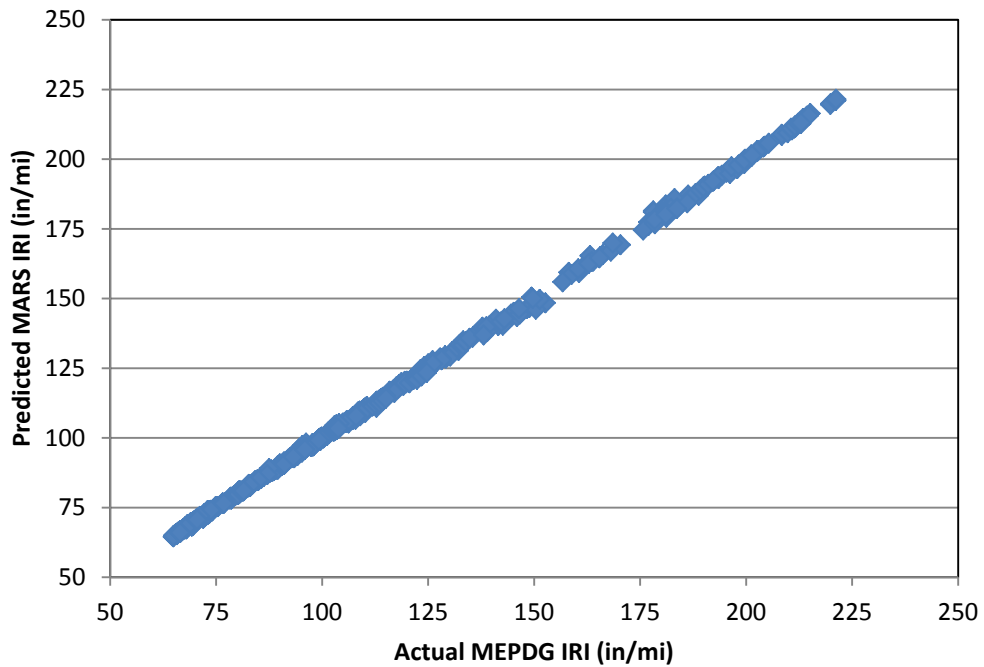
Figure 47. Comparison of actual MEPDG IRI with predicted MARS IRI
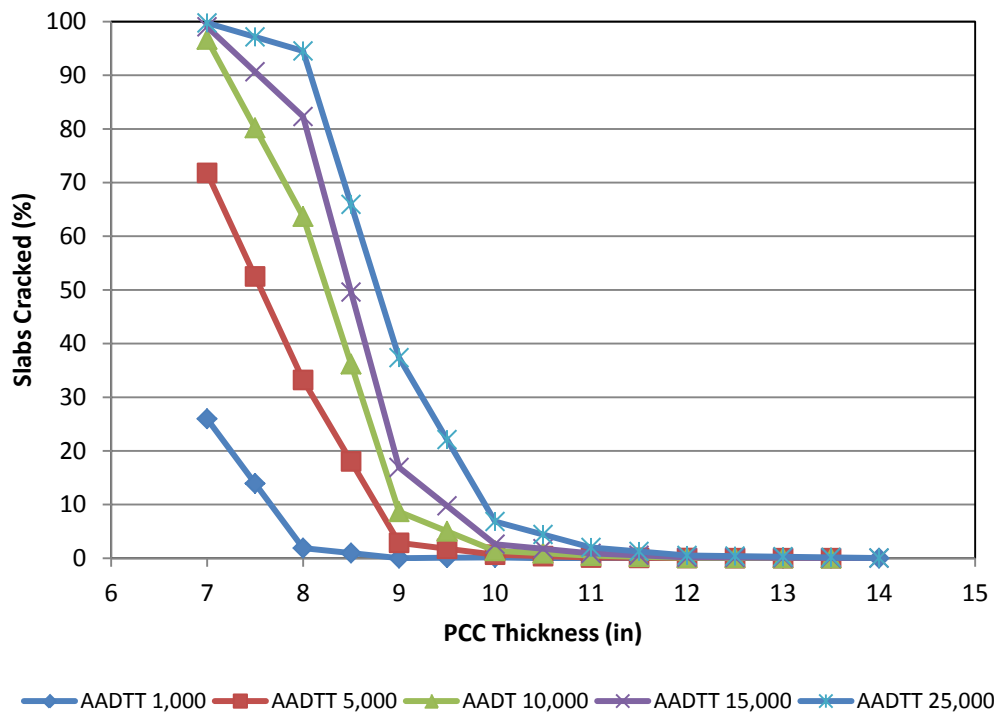
Figure 48. Example of slab cracking model

In Figure 48 there is a sharp break occurring between seven and nine inches, depending on the level of traffic. For a pavement thickness less than ten inches the MEPDG model prediction of slab cracking is very sensitive to pavement thickness, while above that level it is very insensitive.

As was done for flexible pavements in the previous section an "Efficient Design Solution" has been developed for rigid pavements utilizing the same concept where the pavement thicknesses is determined based on a given type of distress. This again gives the designer the option to select the most conservative design (thickest structure), or utilize the models developed in the previous section to determine the distress

characteristics of each thickness and then choose the design which best fits their design

situation and provides the most efficient design.

The models which make up this "Efficient Design Solution" for rigid pavements

are given below, the detailed MARS model for each is included in Appendix A.

Thickness $_{Faulting\ Model}$ (in) =
  f (Faulting, DGA thickness, subgrade modulus, DGA modulus, Dowel
  Diameter and AADTT)

Thickness $_{Cracking\ Model}$ (in) =
  f (Cracking, DGA thickness, subgrade modulus, DGA modulus, Dowel
  Diameter and AADTT)

Thickness $_{Roughness,\ IRI}$ (in) =
  f (IRI, DGA thickness, subgrade modulus, DGA modulus, Dowel Diameter
  and AADTT)

where:
  Thickness $_{Faulting\ Model}$ (in) = calculated PCC thickness -- Faulting Model
  Thickness $_{Cracking\ Model}$ (in) = calculated PCC Thickness – Cracking Mode
  Thickness $_{Roughness,\ IRI}$ (in) = calculated PCC Thickness – IRI Model
  Faulting (in) =transverse joint faulting
  Cracking (%) = percent of slabs with transverse cracks
  Roughness (in/mi) = predicted rigid pavement roughness
  DGA Thickness (in) = thickness of unbound dense graded aggregate
  Subgrade modulus (psi) = subgrade strength in terms of resilient modulus
  DGA modulus (psi) = unbound dense graded aggregate base in terms of
                      resilient modulus
  Dowel Diameter (in) = diameter of transverse joint dowel bars
  AADTT = average annual daily truck traffic

To evaluate these models the predicted performance results from the subset of

MEPDG solutions were use as input into the MARS models, along with the

corresponding information on traffic and material properties. The thicknesses determined

by the models were compared to the actual original input thicknesses used in the MEPDG

predictions.   These results are given in Figure 49 through Figure 50.
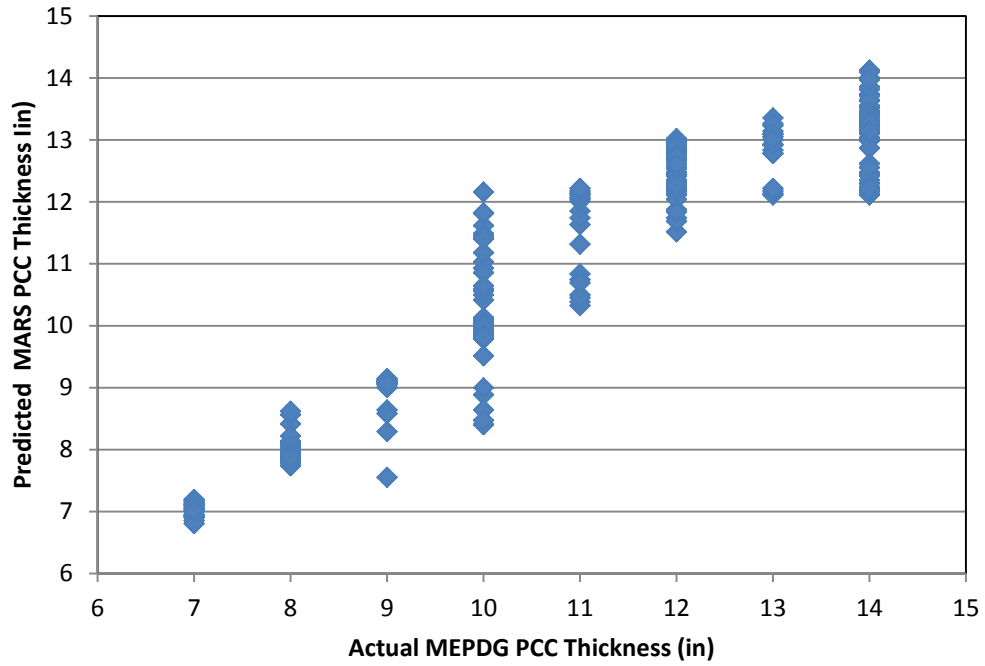
Figure 49. Comparison of actual MEPDG thickness with MARS predicted
thickness using the slab cracking model
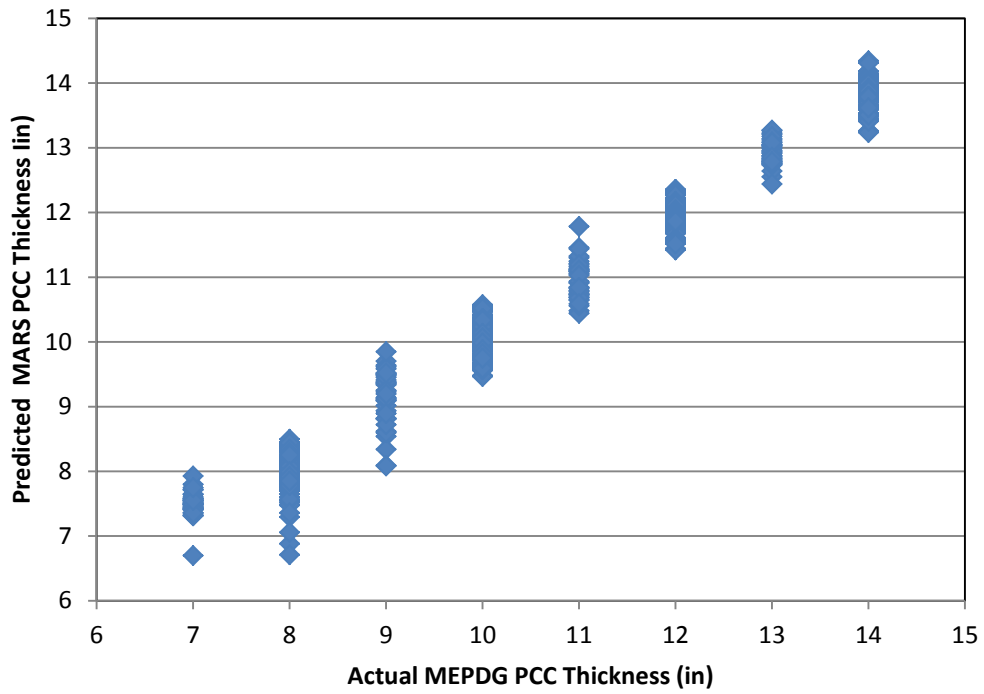
Figure 50. Comparison of actual MEPDG thickness with MARS predicted thickness using the IRI model
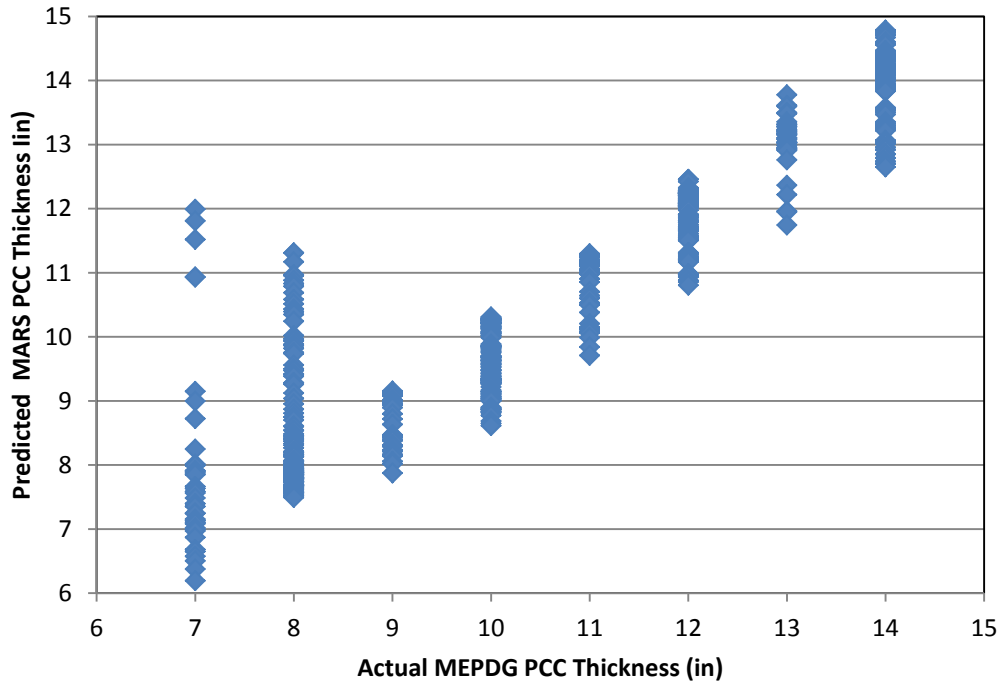
Figure 51. Comparison of actual MEPDG thickness with MARS predicted thickness using the faulting model

102

It may be seen from Figure 49 Figure 50 that the MARS thickness prediction models have quite bit of variability in the predicted thickness. This variability is generally within one inch of the target thickness with the exception of a few isolated areas. In Figure 48 the slab-cracking model within the MEPDG has a very sharp break just prior to ten inches and predicts very little cracking for thicknesses greater than 10 inches. These very small predicted distress levels, in many cases actually zero, make it very difficult to accurately predict the design thickness. For example in Figure 48, a level of zero percent cracking could yield a thickness anywhere from 10 to 14 inches.

To further illustrate the difficulties in predicting pavement thickness for rigid pavements, an analysis was conducted to look at the MEPDG faulting model results. A set of calculated faulting results for a given subgrade strength, traffic level, and base strength is plotted versus pavement thickness at various dowel bar diameters in Figure 52.
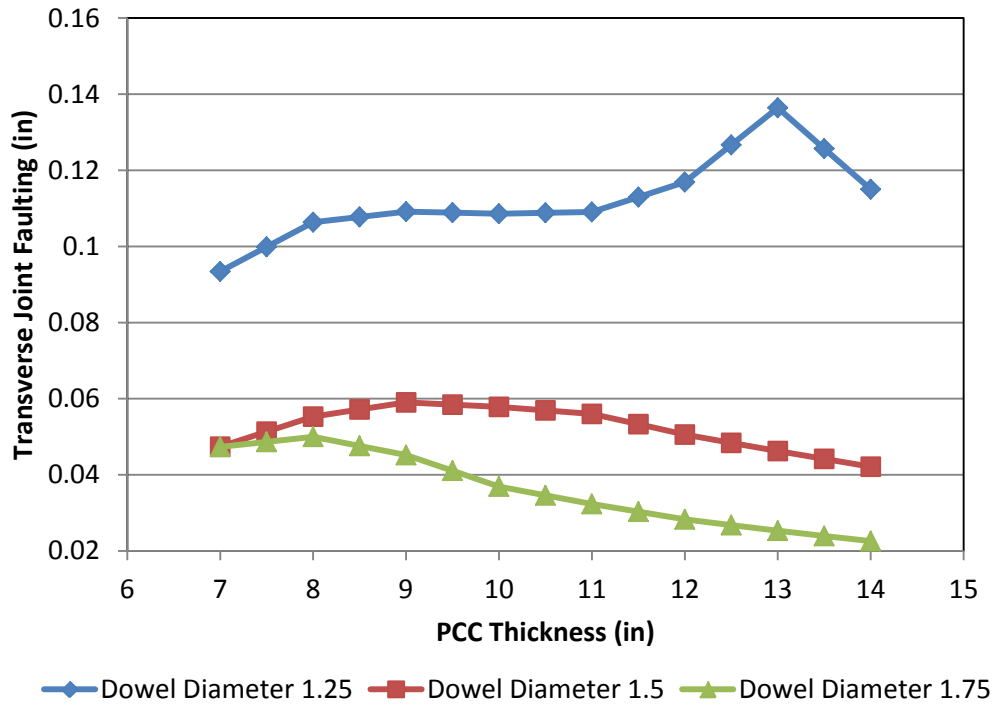
Figure 52. Example of faulting model

The faulting models appear to be providing faulting predictions that are not correct. Specifically for a 1.25-inch diameter dowel, the MEPDG model actually predicts worse performance as the pavement gets thicker, which is certainly not the case (Figure 52). Even for 1.5-inch diameter dowel bars for thicknesses less than nine inches the performance decreases as thickness increases. The effect of this anomaly in the original MEPDG model can clearly be seen in Figure 50, specifically for thicknesses less than nine inches.

5.0 Development of Streamlined Design Process

5.1 Overview of Need for Streamlined Design Process

As has been previously discussed, the most widely used pavement design

procedure in the United States is the AASHTO 1993 pavement design guide. This

procedure has relatively few input parameters and the final result is a thickness of either

Hot-Mix-Asphalt or Portland Cement Concrete. The new NCHRP procedure has many

more potential input parameters and the output is pavement performance, not pavement

thickness. Additional information outlining the individual parameters required for the

NCHRP procedure is contained in Table 1 through Table 4. A comparison of the number

of input requirements for the AASHTO 1993 method and the NCHRP method is given in

Table 19.   Depending on the number of layers that are used in the system, the NCHRP

design process could easily have more than 100 input parameters for a single analysis.

Table 19. Summary of Number of Design Inputs

Design Input	AASHTO 1993 Number of Inputs Required	Number of Inputs Required NCHRP MEPDG
Climate	None	three
Hot-Mix Asphalt Materials	one per layer	more than 20 per layer
PCC Materials	one per layer 1	more than 10 per layer
Unbound Materials Granular and Subgrade	one per layer	eight per layer
Traffic	1	50
Thickness	Predicted by Design	one per layer
Performance	One Reduction in Serviceability (i.e. performance)	Predicted by Design/Analysis Procedure

As has been mentioned the new NCHRP process is an analysis tool and not a direct design process. A schematic of the process is given in Figure 53.

.
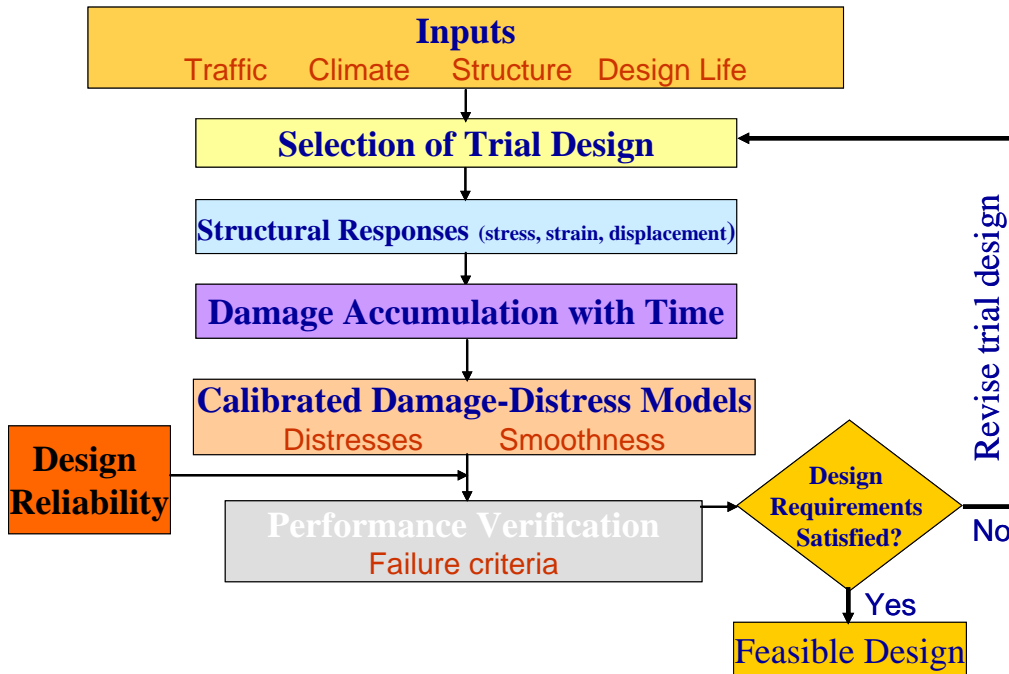
Figure 53. Schematic of NCHRP design/analysis process

This figure illustrates the iterative nature of the NCHRP process, in that design, thicknesses are assumed, performance is predicted and then an evaluation is made to see if the design requirements are satisfied.

The concept of an iterative process and the need for a large number of input parameters (many of which may not be significant) illustrates the need for a streamlined "Efficient Design Solution" as has been discussed in the previous chapter. This streamlined procedure will allow a designer to very quickly determine a pavement thickness and an estimate of the performance of that pavement design in a single step.

5.2 Comparison of Actual Pavement Design Processes

To illustrate the need of a streamlined design procedure, the following flexible pavement design scenario will be processed through both the NCHRP Software and the "Efficient Design Solution" developed during this work. The known design parameters are given in Table 20.

Table 20. Summary of Pavement Design Inputs

Design Input	Value
Average Annual Daily Traffic (AADTT)	14,000
Subgrade Strength (psi)	8,000
Dense Graded Aggregate (DGA) strength (psi)	30,000
Dense Graded Aggregate (DGA) thickness (in)	8.0
Desired Level of Rutting (in)	1.0
Desired Level of Fatigue Cracking (%)	15.0
Desired Level of IRI (in/mi)	150

Since the NCHRP process does not provide any starting point for the designer, they are left to make assumptions on potential designs based on their experience. These potential designs are processed through the NCHRP software and the pavement performance is predicted in terms of fatigue cracking, rutting, and IRI.

To evaluate this design using the NCHRP procedure, potential HMA thickness of 7.25, 9.25, and 11.25 inches were chosen. These thicknesses along with the additional information provided in Table 20 along with software defaults for the remaining design

inputs were processed by the NCHRP software. This software requires approximately

thirty minutes to process each different proposed design thickness. Once the

computational time has been competed the designer will have results as illustrated in

Table 21.

Table 21. Typical NCHRP Process Results

Proposed Thickness (in)	Predicted Fatigue Cracking (%)	Predicted Total Rutting (in)	Predicted IRI (in/mi)
7.25	26.9	1.398	169
9.25	8.62	1.221	150.9
11.25	2.92	1.041	140.8

The designer must now review these results and determine the appropriate design

thickness to meet each of their performance criteria. If none of these results meet the

necessary criteria directly, the designer must now interpolate between the designs to

select the optimum thickness required for each distress.

As was discussed in previous sections, two different sets of MARS models have

been developed during this study. One set of models essentially becomes a surrogate for

the existing NCHRP program, in that they predict pavement performance based on a set

of input values, the second set of models developed the "Efficient Design Solution"

which provides a direct calculation of thickness for a given desired distress. Both of

these sets of models are used to evaluate the design in this example.

Using the design solution developed from the MARS models ("Efficient Design

Solution"), the information contained in Table 20 is used directly to calculate an estimate

of the required thickness for each desired distress. This solution is essentially

instantaneous, in that as soon as each input is entered into the procedure, the results are

displayed. The results contain the estimated thickness based on the desired distress and

the predicted performance for this distress. If the procedure were perfect, then the

resulting predicted distress would be exactly what was used to find the estimated

thickness. The results from this procedure are given in Table 22. The predicted distress

levels are very close to the desired distress levels, indicating that the estimated

thicknesses are reasonable estimates which could be used for design and further refined

by the NCHRP process as needed.

Table 22. Pavement Design Results using "Efficient Design Solution"

Distress	Desired Level	Estimated Thickness	Predicted Distress Level
Fatigue Cracking (%)	15.0	8.0	17
Total Rutting (in)	1.0	11.4	0.98
IRI (in/mi)	150	9.0	151

To illustrate how these designs may compare to those that could be determined

using the full NCHRP process, graphs illustrating the predicted distresses at various

thicknesses were developed. Included in these graphs are the thicknesses which were

estimated using the "Efficient Design Solution" along with their corresponding predicted

distress along with the results from the full MEPDG model. These results are given in

Figure 54 through Figure 56. The designs determined using the "Efficient Design

Solution" are in very good agreement with those from the full NCHRP Procedure.
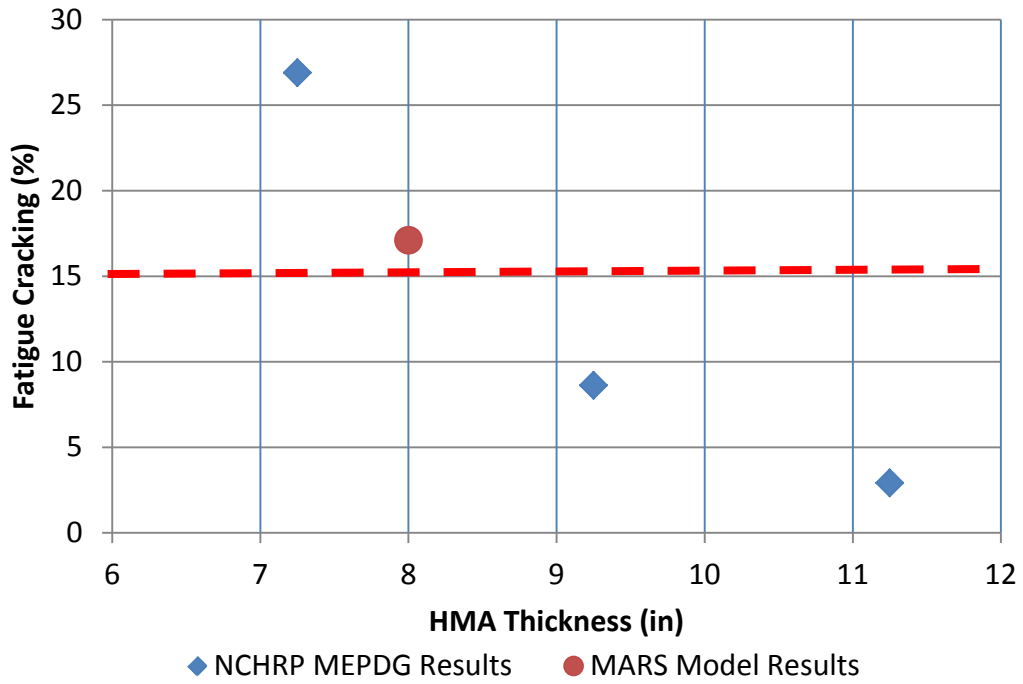
Figure 54. Comparison of MEPDG iterations with MARS model prediction, fatigue cracking
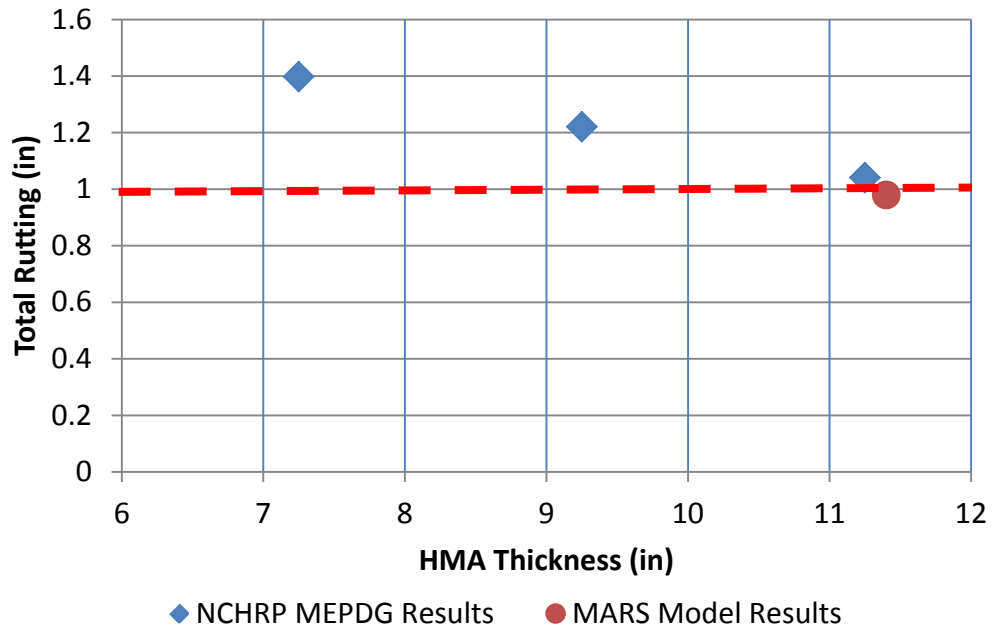
Figure 55. Comparison of MEPDG iterations with MARS model prediction, total rutting
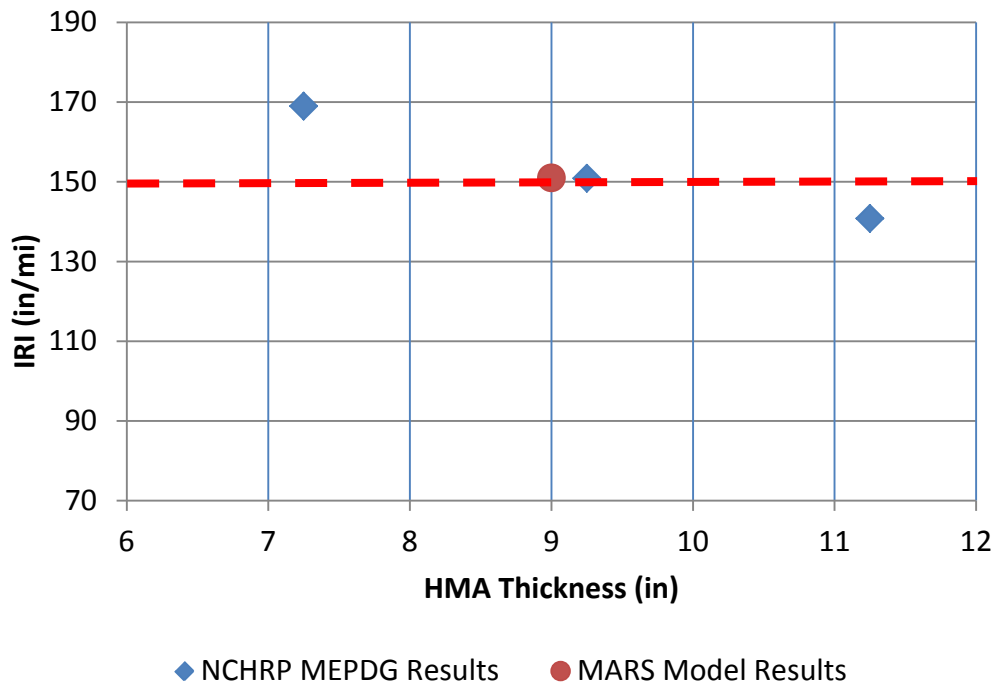
Figure 56. Comparison of MEPDG iterations with MARS model prediction, IRI

5.3 Overview of Streamlined Design Process Software

To facilitate the use of the models which have been developed during this work, an interactive computer program has been developed called "KYPDT". This software has been developed using Microsoft Visual Studio as a self-contained software application. It provides a number of advantages over the NCHRP software. One such advantage is the direct comparison between the both flexible and rigid pavement designs for the same design inputs. Using the NCHRP procedure multiple separate designs must be run for each type of pavement and the comparisons made outside the software provided.

The NCHRP procedure does not provide any method to directly calculate the cost any design; this must be done by the designer outside the design process. The solution

developed in this study provides the user the opportunity to input basic cost information for each material and calculate an estimated total cost based on the estimated thickness determined for each desired distress. It is anticipated that this program will be utilized by designers to provide a first estimate of a potential pavement thickness design; they would then have the option to utilize the full MEPDG model to further refine their design as necessary. A complete User's Guide for the software is included in Appendix B.

6.0 Summary of Recommendations

6.1 Review of information from Sensitivity Analysis

This study has demonstrated that the global sensitivity analysis is a powerful tool, which will help to identify potentially important variables for the input parameter studies. It has also illustrated that default values may be used for the least significant variables and still achieve acceptable results. It must be kept in mind that the global sensitivity analysis does not necessarily deal with individual model inputs and how they may impact individual output values. This method provides a means to screen variables over a wide range of values and evaluate their relative importance to individual model outputs. This method has been used successfully to evaluate both flexible and rigid pavement to identify the most influential variables for which the designer actually has control over or has the ability to easily determine. This sensitivity analysis did not set out to determine the sensitivity for every input value within the model, since many of these values are not readily available in practice.

6.2 Recommended Guidelines for use of Streamlined Model

This study has outlined a method to develop a regression model which can accurately predict the results of the NCHRP MEPDG software. In addition, an "Efficient Design Solution" for pavement thickness, given specific distress inputs has been achieved. The accuracy in these predictions is certainly within acceptable ranges for initial structural thickness determination, which will make the use of the NCHRP MEPDG design procedure more efficient due to the reduction in the overall number of solutions necessary to make a design decision.

The new DARWin-ME software (AASHTO, 2011) can facilitate the development of these subsets through its sensitivity analysis procedure. These sensitivity analysis solutions can be modeled with the MARS process to produce an "Efficient Design Solution" of pavement thickness along with a quick prediction of performance for specific pavement thickness.

Due to the nature of the MARS procedure, models can be easily developed for any subset of designs necessary, such as typical designs for a state or local agency. This procedure could be utilized as a replacement for "catalog" designs by providing a method to determine agency specific designs for any combination of input variables desired or for the development of very specific design catalogs quickly.

This procedure has the potential to significantly reduce the MEPDG iterations necessary to develop a viable design, to as few as two to three iterations on either side of the predicted MARS model thickness. It could then be merged with a smart decision tree structure to provide very efficient execution of the MEPDG procedure.

The utilization of the streamlined procedure has the potential to provide cost savings in various areas, including a reduction in the time to complete a potential design, due to less iteration and less demand for input information which could be costly to obtain for a wide variety of projects.

The ability for the MARS models to accurately predict the results of the full MEPDG software provide many advantages to pavement designers. As additional information becomes available, the MARS models could be expanded to provide

performance prediction using various construction quality control results to predict the change in performance very quickly. This could then be potentially utilized in performance related specifications.

The MARS models also have the ability to allow for analysis of many different combinations of variables which can assist in determining potential anomalies in the MEPDG process as was outlined previously for rigid pavements.

The streamlined model developed in this study is not intended to replace the NCHRP procedure. Rather it is intended to be a complement to the process by providing the designer a starting point, or estimated design for which a complete analysis can be completed using the NCHRP procedure.

6.3 Recommendations for Future Research

The methodologies presented in this study can be expanded to develop very specific streamlined design processes from a given subset of designs. These methods could be utilized by agencies who desire to have the robust nature of the NCHRP MEPDG process, but would like to streamline its use.

One of the more exciting areas where the streamlined model could be expanded is in the potential for a probabilistic design solution. As was mentioned earlier, this idea was abandoned in the NCHRP project due to the long computational time required for a single analysis. By having a model that can be evaluated in seconds, the potential to have the input values be distributions of likely values and thus providing a distribution of likely outputs exists. This could provide a means to develop a "true" design reliability

based on real variation in input values, instead of relying on the: "surrogate" reliability that is currently in the NCHRP process.

The continued development of this procedure and subsequent software will open up the area of mechanistic-empirical design and analysis to a much wider audience. At the present time the cost of the AASHTO Darwin-ME is approximately $5,000 for a single user license which could make this procedure somewhat difficult for many agencies and academic institutions to evaluate.

Appendix A -- MARS Models for all Pavement Types

MARS Model for HMA Thickness – Fatigue Cracking Model

BF1 = Max(0, AADTT - 7500)
BF2 = Max(0, 7500 - AADTT)
BF3 = Max(0, ALLIGATOR_CRACKING - 1.59)
BF4 = Max(0, 1.59 - ALLIGATOR_CRACKING)
BF5 = Max(0, SUBGRADE_MODULUS - 9000)
BF6 = Max(0, 9000 - SUBGRADE_MODULUS)
BF7 = Max(0, DGA_MODULUS - 20000)
BF8 = Max(0, AADTT - 2500)
BF9 = Max(0, 2500 - AADTT)
BF10 = Max(0, DGA_THICKNESS - 10)
BF11 = Max(0, 10 - DGA_THICKNESS)
BF12 = Max(0, ALLIGATOR_CRACKING - 5.03) * BF8
BF13 = Max(0, 5.03 - ALLIGATOR_CRACKING) * BF8
BF14 = Max(0, ALLIGATOR_CRACKING - 0.6)
BF17 = Max(0, 1.15 - ALLIGATOR_CRACKING) * BF9
BF18 = Max(0, ALLIGATOR_CRACKING - 3.29)
BF19 = Max(0, 3.29 - ALLIGATOR_CRACKING)
BF20 = Max(0, AADTT - 10000) * BF6
BF21 = Max(0, 10000 - AADTT) * BF6
BF22 = Max(0, DGA_THICKNESS - 12) * BF7
BF23 = Max(0, 12 - DGA_THICKNESS) * BF7
BF24 = Max(0, SUBGRADE_MODULUS - 7500) * BF10
BF25 = Max(0, 7500 - SUBGRADE_MODULUS) * BF10
BF26 = Max(0, ALLIGATOR_CRACKING - 0.273) * BF6
BF27 = Max(0, 0.273 - ALLIGATOR_CRACKING) * BF6
BF28 = Max(0, ALLIGATOR_CRACKING - 10.2) * BF5
BF30 = Max(0, ALLIGATOR_CRACKING - 0.907) * BF8
BF31 = Max(0, 0.907 - ALLIGATOR_CRACKING) * BF8
BF32 = Max(0, AADTT - 5000)
BF33 = Max(0, 5000 - AADTT)
BF34 = Max(0, AADTT - 15000)
BF35 = Max(0, 15000 - AADTT)
BF36 = Max(0, DGA_THICKNESS - 10) * BF31
BF37 = Max(0, 10 - DGA_THICKNESS) * BF31
BF38 = Max(0, DGA_MODULUS - 30000) * BF31
BF39 = Max(0, 30000 - DGA_MODULUS) * BF31
BF40 = Max(0, SUBGRADE_MODULUS - 10500) * BF11
BF41 = Max(0, 10500 - SUBGRADE_MODULUS) * BF11
BF43 = Max(0, 0.561 - ALLIGATOR_CRACKING) * BF33
BF44 = Max(0, DGA_MODULUS - 30000) * BF6
BF45 = Max(0, 30000 - DGA_MODULUS) * BF6
BF46 = Max(0, ALLIGATOR_CRACKING - 0.409) * BF7

BF47 = Max(0, 0.409 - ALLIGATOR_CRACKING) * BF7
BF48 = Max(0, DGA_THICKNESS - 8) * BF13
BF49 = Max(0, 8 - DGA_THICKNESS) * BF13
BF50 = Max(0, SUBGRADE_MODULUS - 7500) * BF4
BF51 = Max(0, 7500 - SUBGRADE_MODULUS) * BF4
BF52 = Max(0, SUBGRADE_MODULUS - 9000) * BF13
BF53 = Max(0, 9000 - SUBGRADE_MODULUS) * BF13
BF54 = Max(0, ALLIGATOR_CRACKING - 8.49)
BF55 = Max(0, 8.49 - ALLIGATOR_CRACKING)
BF56 = Max(0, AADTT - 10000) * BF19
BF58 = Max(0, ALLIGATOR_CRACKING - 0.989) * BF35
BF59 = Max(0, 0.989 - ALLIGATOR_CRACKING) * BF35
BF60 = Max(0, ALLIGATOR_CRACKING - 2.42) * BF32
BF62 = Max(0, DGA_MODULUS - 30000) * BF14
BF63 = Max(0, 30000 - DGA_MODULUS) * BF14
BF64 = Max(0, DGA_MODULUS - 30000) * BF13
BF65 = Max(0, 30000 - DGA_MODULUS) * BF13
BF66 = Max(0, AADTT - 2500) * BF4
BF68 = Max(0, AADTT - 7500) * BF51
BF69 = Max(0, 7500 - AADTT) * BF51
BF71 = Max(0, 9000 - SUBGRADE_MODULUS) * BF23
BF72 = Max(0, AADTT - 20000)
BF73 = Max(0, 20000 - AADTT)
BF74 = Max(0, AADTT - 2500) * BF41
BF75 = Max(0, 2500 - AADTT) * BF41
BF76 = Max(0, AADTT - 10000) * BF55
BF77 = Max(0, 10000 - AADTT) * BF55
BF80 = Max(0, ALLIGATOR_CRACKING - 5.21)
BF82 = Max(0, ALLIGATOR_CRACKING - 2.22)
BF83 = Max(0, 2.22 - ALLIGATOR_CRACKING)
BF84 = Max(0, DGA_MODULUS - 30000) * BF24
BF86 = Max(0, DGA_THICKNESS - 6) * BF27
BF87 = Max(0, ALLIGATOR_CRACKING - 0.43) * BF6
BF88 = Max(0, 0.43 - ALLIGATOR_CRACKING) * BF6
BF89 = Max(0, AADTT - 2500) * BF27
BF90 = Max(0, 2500 - AADTT) * BF27
BF91 = Max(0, SUBGRADE_MODULUS - 9000) * BF47
BF92 = Max(0, 9000 - SUBGRADE_MODULUS) * BF47
BF94 = Max(0, 0.199 - ALLIGATOR_CRACKING) * BF21
BF96 = Max(0, 14 - DGA_THICKNESS) * BF66
BF97 = Max(0, ALLIGATOR_CRACKING - 16.8)
BF99 = Max(0, SUBGRADE_MODULUS - 7500) * BF19
BF100 = Max(0, 7500 - SUBGRADE_MODULUS) * BF19
BF101 = Max(0, AADTT - 5000) * BF25

BF102 = Max(0, 5000 - AADTT) * BF25
BF104 = Max(0, 0.723 - ALLIGATOR_CRACKING) * BF71
BF105 = Max(0, DGA_MODULUS - 30000) * BF102
BF107 = Max(0, SUBGRADE_MODULUS - 7500) * BF96
BF108 = Max(0, 7500 - SUBGRADE_MODULUS) * BF96
BF109 = Max(0, DGA_THICKNESS - 8) * BF83
BF110 = Max(0, 8 - DGA_THICKNESS) * BF83
BF111 = Max(0, SUBGRADE_MODULUS - 10500) * BF19
BF112 = Max(0, 10500 - SUBGRADE_MODULUS) * BF19
BF113 = Max(0, AADTT - 5000) * BF91
BF114 = Max(0, 5000 - AADTT) * BF91
BF116 = Max(0, 0.428 - ALLIGATOR_CRACKING) * BF25
BF118 = Max(0, 30000 - DGA_MODULUS) * BF35
BF120 = Max(0, 1.23 - ALLIGATOR_CRACKING) * BF73
BF121 = Max(0, AADTT - 2500) * BF83
BF122 = Max(0, 2500 - AADTT) * BF83
BF123 = Max(0, DGA_MODULUS - 20000) * BF52
BF124 = Max(0, DGA_THICKNESS - 14) * BF53
BF125 = Max(0, 14 - DGA_THICKNESS) * BF53
BF126 = Max(0, AADTT - 20000) * BF112
BF127 = Max(0, 20000 - AADTT) * BF112
BF128 = Max(0, AADTT - 2500) * BF10
BF129 = Max(0, 2500 - AADTT) * BF10
BF130 = Max(0, DGA_THICKNESS - 8) * BF7
BF132 = Max(0, DGA_MODULUS - 20000) * BF121
BF133 = Max(0, DGA_THICKNESS - 14)
BF135 = Max(0, AADTT - 7500) * BF88
BF136 = Max(0, 7500 - AADTT) * BF88
BF137 = Max(0, AADTT - 2500) * BF5
BF138 = Max(0, 2500 - AADTT) * BF5
BF139 = Max(0, ALLIGATOR_CRACKING - 1.64) * BF34
BF141 = Max(0, ALLIGATOR_CRACKING - 3.95)
BF143 = Max(0, ALLIGATOR_CRACKING - 6.43) * BF8
BF145 = Max(0, AADTT - 7500) * BF27
BF148 = Max(0, 1.23 - ALLIGATOR_CRACKING) * BF20
BF149 = Max(0, SUBGRADE_MODULUS - 7500) * BF39
BF150 = Max(0, 7500 - SUBGRADE_MODULUS) * BF39

allcrack_drain_0 = 13.1355 + 0.00113966 * BF1 - 0.00122041 * BF2 - 3.74709 * BF3
+ 4.14962 * BF4 - 0.000068255 * BF5 + 0.000296141 * BF6 - 0.0000708209 * BF7
- 0.00138207 * BF8 - 0.0727677 * BF10 + 0.0781646 * BF11 - 0.00014892 * BF12
+ 0.000151419 * BF13 + 2.18065 * BF14 - 0.000113179 * BF17 + 0.212216 * BF18
+ 0.0000000047076 * BF20 - 0.00000000850912 * BF21 - 0.00000362552 * BF22
+ 0.00000445556 * BF23 + 0.000005184 * BF24 - 0.0000207563 * BF25

- 0.000966547 * BF26 + 0.00160266 * BF27 + 0.00000781016 * BF28
+ 0.000154065 * BF30 - 0.000182606 * BF32 - 0.0000510239 * BF34
- 0.00000662715 * BF36 + 0.0000136714 * BF37 - 0.00000000186975 * BF38
+ 0.00000000599187 * BF39 - 0.00000448542 * BF40 + 0.0000103693 * BF41
- 0.000275742 * BF43 - 0.00000000323229 * BF44 + 0.0000000037792 * BF45
+ 0.0000335673 * BF46 + 0.000141792 * BF47 - 0.00000029566 * BF48
+ 0.000000644883 * BF49 - 0.0000324771 * BF50 + 0.0000638516 * BF51
- 0.000000000818329 * BF52 - 0.00000000104293 * BF53 + 0.104811 * BF54
+ 0.00000285529 * BF56 + 0.0000179223 * BF58 + 0.0000260377 * BF59
+ 0.0000104522 * BF60 - 0.0000334501 * BF62 + 0.000033906 * BF63
- 9.96897E-11 * BF64 + 0.00000000023986 * BF65 + 0.0000224086 * BF66
- 0.00000000669878 * BF68 - 0.0000000213097 * BF69 + 0.000000000253166 * BF71
- 0.0000215622 * BF72 + 0.0000000001621 * BF74 - 0.00000000221213 * BF75
- 0.00000295211 * BF76 - 0.00000582606 * BF77 + 0.0912604 * BF80
+ 0.350733 * BF82 + 0.000000000237907 * F84 + 0.0000633759 * BF86
+ 0.000955862 * BF87 + 0.000000261164 * BF89 - 0.000000134052 * BF90
- 0.0000000563975 * BF91 - 0.0000000508487 * BF92 + 0.00000023726 * BF94
+ 0.00000320634 * BF96 + 0.0519829 * BF97 - 0.0000272267 * BF99
+ 0.0000744313 * BF100 + 0.000000000817261 * BF101 + 0.00000000312414 * BF102
+ 0.00000000131106 * BF104 + 7.0961E-13 * BF105 - 0.000000000693289 * BF107
- 0.00000000154212 * BF108 - 0.00486935 * BF109 + 0.00952931 * BF110
+ 0.000030758 * BF111 + 1.07041E-11 * BF113 + 1.17895E-11 * BF114
- 0.000102005 * BF116 + 0.00000000240567 * BF118 + 0.0000237499 * BF120
- 0.00008349 * BF122 + 3.08638E-14 * BF123 - 0.00000000015773 * BF124
+ 0.000000000200888 * BF125 + 0.000000000745265 * BF126
- 0.00000000148787 * BF127 - 0.000000239459 * BF128 + 0.00000402042 * BF129
+ 0.00000147312 * BF130 - 0.000000000299643 * BF132 + 0.0145845 * BF133
+ 0.000000103081 * BF135 - 0.00000003695 * BF136 - 0.000000000809332 * BF137
+ 0.0000000104058 * BF138 - 0.0000208569 * BF139 + 0.0980544 * BF141
+ 0.00000322751 * BF143 - 0.000000360997 * BF145 + 0.00000000991327 * BF148
- 1.16614E-12 * BF149 - 1.1454E-12 * BF150

MARS Model for HMA Thickness – IRI Model

BF1 = Max(0, AADTT - 7500)
BF2 = Max(0, 7500 - AADTT)
BF3 = Max(0, IRI - 135.2)
BF4 = Max(0, 135.2 - IRI)
BF5 = Max(0, SUBGRADE_MODULUS - 7500)
BF6 = Max(0, 7500 - SUBGRADE_MODULUS)
BF7 = Max(0, AADTT - 2500) * BF4
BF8 = Max(0, 2500 - AADTT) * BF4
BF9 = Max(0, IRI - 124.5) * BF2
BF10 = Max(0, 124.5 - IRI) * BF2
BF12 = Max(0, 7500 - SUBGRADE_MODULUS) * BF1
BF13 = Max(0, DGA_MODULUS - 20000)
BF14 = Max(0, AADTT - 5000) * BF4
BF15 = Max(0, 5000 - AADTT) * BF4
BF16 = Max(0, AADTT - 10000)
BF17 = Max(0, 10000 - AADTT)
BF19 = Max(0, 12000 - SUBGRADE_MODULUS) * BF15
BF20 = Max(0, IRI - 119.3) * BF17
BF21 = Max(0, 119.3 - IRI) * BF17
BF22 = Max(0, AADTT - 5000) * BF13
BF23 = Max(0, 5000 - AADTT) * BF13
BF24 = Max(0, IRI - 129.2) * BF12
BF25 = Max(0, 129.2 - IRI) * BF12
BF26 = Max(0, IRI - 152.4) * BF5
BF27 = Max(0, 152.4 - IRI) * BF5
BF28 = Max(0, DGA_THICKNESS - 6) * BF23
BF29 = Max(0, AADTT - 20000)
BF30 = Max(0, 20000 - AADTT)
BF31 = Max(0, IRI - 122.8)
BF32 = Max(0, 122.8 - IRI)
BF33 = Max(0, SUBGRADE_MODULUS - 7500) * BF14
BF34 = Max(0, 7500 - SUBGRADE_MODULUS) * BF14
BF35 = Max(0, SUBGRADE_MODULUS - 9000) * BF17
BF36 = Max(0, 9000 - SUBGRADE_MODULUS) * BF17
BF37 = Max(0, IRI - 132.4) * BF35
BF38 = Max(0, 132.4 - IRI) * BF35
BF39 = Max(0, AADTT - 5000)
BF40 = Max(0, 5000 - AADTT)
BF41 = Max(0, AADTT - 2500) * BF5
BF42 = Max(0, 2500 - AADTT) * BF5
BF43 = Max(0, IRI - 126.3) * BF6
BF44 = Max(0, 126.3 - IRI) * BF6

BF45 = Max(0, AADTT - 5000) * BF44
BF46 = Max(0, 5000 - AADTT) * BF44
BF47 = Max(0, AADTT - 5000) * BF6
BF48 = Max(0, 5000 - AADTT) * BF6
BF49 = Max(0, DGA_MODULUS - 20000) * BF25
BF50 = Max(0, DGA_THICKNESS - 6) * BF34
BF51 = Max(0, DGA_MODULUS - 30000) * BF45
BF52 = Max(0, 30000 - DGA_MODULUS) * BF45
BF53 = Max(0, AADTT - 10000) * BF6
BF54 = Max(0, 10000 - AADTT) * BF6
BF55 = Max(0, DGA_MODULUS - 30000) * BF31
BF56 = Max(0, 30000 - DGA_MODULUS) * BF31
BF57 = Max(0, SUBGRADE_MODULUS - 12000) * BF20
BF58 = Max(0, 12000 - SUBGRADE_MODULUS) * BF20
BF59 = Max(0, AADTT - 20000) * BF31
BF60 = Max(0, 20000 - AADTT) * BF31
BF61 = Max(0, DGA_THICKNESS - 6) * BF45
BF62 = Max(0, SUBGRADE_MODULUS - 10500) * BF39
BF63 = Max(0, 10500 - SUBGRADE_MODULUS) * BF39
BF64 = Max(0, IRI - 136.9) * BF41
BF65 = Max(0, 136.9 - IRI) * BF41
BF66 = Max(0, DGA_THICKNESS - 12) * BF27
BF67 = Max(0, 12 - DGA_THICKNESS) * BF27
BF68 = Max(0, DGA_THICKNESS - 6) * BF49
BF69 = Max(0, DGA_THICKNESS - 10) * BF30
BF70 = Max(0, 10 - DGA_THICKNESS) * BF30
BF71 = Max(0, IRI - 117.4) * BF23
BF72 = Max(0, 117.4 - IRI) * BF23
BF73 = Max(0, SUBGRADE_MODULUS - 10500) * BF60
BF74 = Max(0, 10500 - SUBGRADE_MODULUS) * BF60
BF75 = Max(0, AADTT - 15000) * BF27
BF77 = Max(0, IRI - 128.7) * BF42
BF78 = Max(0, 128.7 - IRI) * BF42
BF79 = Max(0, IRI - 126.8) * BF40
BF81 = Max(0, AADTT - 2500) * BF32
BF82 = Max(0, 2500 - AADTT) * BF32
BF83 = Max(0, DGA_THICKNESS - 12) * BF8
BF84 = Max(0, 12 - DGA_THICKNESS) * BF8
BF85 = Max(0, DGA_MODULUS - 30000) * BF69
BF86 = Max(0, 30000 - DGA_MODULUS) * BF69
BF87 = Max(0, IRI - 130.2) * BF23
BF89 = Max(0, DGA_THICKNESS - 6) * BF10
BF90 = Max(0, IRI - 125.5) * BF6
BF91 = Max(0, 125.5 - IRI) * BF6

BF92 = Max(0, AADTT - 5000) * BF91
BF94 = Max(0, DGA_MODULUS - 30000) * BF92
BF95 = Max(0, 30000 - DGA_MODULUS) * BF92
BF96 = Max(0, DGA_MODULUS - 30000) * BF61
BF97 = Max(0, 30000 - DGA_MODULUS) * BF61
BF98 = Max(0, DGA_MODULUS - 30000) * BF8
BF99 = Max(0, 30000 - DGA_MODULUS) * BF8
BF100 = Max(0, DGA_THICKNESS - 8) * BF3
BF101 = Max(0, 8 - DGA_THICKNESS) * BF3
BF102 = Max(0, SUBGRADE_MODULUS - 7500) * BF81
BF103 = Max(0, 7500 - SUBGRADE_MODULUS) * BF81
BF104 = Max(0, AADTT - 2500) * BF91
BF105 = Max(0, 2500 - AADTT) * BF91
BF106 = Max(0, SUBGRADE_MODULUS - 7500) * BF21
BF109 = Max(0, 7500 - SUBGRADE_MODULUS) * BF69
BF110 = Max(0, DGA_MODULUS - 30000) * BF2
BF111 = Max(0, 30000 - DGA_MODULUS) * BF2
BF112 = Max(0, SUBGRADE_MODULUS - 9000) * BF82
BF113 = Max(0, 9000 - SUBGRADE_MODULUS) * BF82
BF114 = Max(0, IRI - 138.4) * BF5
BF115 = Max(0, 138.4 - IRI) * BF5
BF116 = Max(0, SUBGRADE_MODULUS - 10500) * BF23
BF117 = Max(0, 10500 - SUBGRADE_MODULUS) * BF23
BF118 = Max(0, IRI - 122.6) * BF54
BF119 = Max(0, 122.6 - IRI) * BF54
BF120 = Max(0, IRI - 123.7) * BF54
BF122 = Max(0, DGA_MODULUS - 20000) * BF70
BF125 = Max(0, IRI - 137.7) * BF22
BF126 = Max(0, 137.7 - IRI) * BF22
BF127 = Max(0, AADTT - 2500) * BF67
BF128 = Max(0, 2500 - AADTT) * BF67
BF129 = Max(0, AADTT - 15000) * BF13
BF131 = Max(0, DGA_THICKNESS - 6) * BF9
BF132 = Max(0, IRI - 129) * BF2
BF134 = Max(0, IRI - 117.5) * BF69
BF135 = Max(0, 117.5 - IRI) * BF69
BF136 = Max(0, AADTT - 15000) * BF100
BF138 = Max(0, IRI - 122.8) * BF54
BF140 = Max(0, SUBGRADE_MODULUS - 9000)
BF141 = Max(0, 9000 - SUBGRADE_MODULUS)
BF142 = Max(0, AADTT - 15000) * BF141
BF143 = Max(0, 15000 - AADTT) * BF141
BF144 = Max(0, SUBGRADE_MODULUS - 10500) * BF30
BF145 = Max(0, 10500 - SUBGRADE_MODULUS) * BF30

BF146 = Max(0, DGA_THICKNESS - 14) * BF141
BF147 = Max(0, 14 - DGA_THICKNESS) * BF141
BF148 = Max(0, IRI - 157.7) * BF140
BF149 = Max(0, 157.7 - IRI) * BF140
BF150 = Max(0, AADTT - 500) * BF115

IRI_Draini_0 = 10.2431 + 0.000956761 * BF1 - 0.00121258 * BF2 - 0.329257 * BF3
+ 0.37384 * BF4 - 0.00187586 * BF5 + 0.00110821 * BF6 - 0.00000585863 * BF7
- 0.000131539 * BF8 + 0.00000367024 * BF9 + 0.00000129877 * BF12
- 0.00000508463 * BF13 - 0.000230611 * BF16 + 0.000000000640121 * BF19
+ 0.0000181612 * BF20 + 0.0000400117 * BF21 + 0.00000000186738 * BF22
+ 0.000000000805772 * BF24 - 0.0000680218 * BF26 + 0.0000904455 * BF27
- 0.000000000459619 * BF28 - 0.000139161 * BF29 + 0.125606 * BF31
- 0.00000000325205 * BF33 - 0.00000010445 * BF35 + 0.000000164859 * BF36
+ 0.00000000684486 * BF37 - 0.00000000359774 * BF38 - 0.000429299 * BF39
+ 0.000000123827 * BF42 + 0.00046961 * BF43 + 0.000569872 * BF44
- 0.0000000483349 * BF45 - 0.000000415091 * BF46 - 0.000000686603 * BF47
+ 0.0000000854554 * BF48 - 5.70313E-13 * BF49 - 7.73792E-11 * BF50
- 4.91131E-12 * BF51 + 1.17614E-11 * BF52 - 0.000000590413 * BF53
- 0.00000135468 * BF55 + 0.00000157488 * BF56 + 0.00000000746813 * BF57
- 0.00000000692815 * BF58 + 0.00000404208 * BF59 - 0.00000102236 * BF60
- 0.0000000080072 * BF61 + 0.0000000398633 * BF62 - 0.0000000368262 * BF63
- 0.00000000231371 * BF64 - 0.00000000248158 * BF65 + 0.000000159309 * BF66
- 0.000000107885 * BF67 - 1.28336E-13 * BF68 - 0.00000092758 * BF69
- 8.32453E-11 * BF71 + 0.00000000190864 * BF72 + 0.000000000857133 * BF73
- 0.000000000708659 * BF74 - 0.00000000213034 * BF75 - 0.000000028809 * BF77
+ 0.00000000441369 * BF78 + 0.0000293637 * BF79 - 0.0000637828 * BF81
- 0.0000198705 * BF82 - 0.0000016848 * BF83 + 0.00000247618 * BF84
- 2.73409E-11 * BF85 + 9.80311E-11 * BF86 + 0.00000000219391 * BF87
+ 0.000000860885 * BF89 - 0.000471098 * BF90 + 0.00000107695 * BF92
+ 2.27258E-12 * BF94 - 0.0000000000118 * BF95 - 2.80104E-13 * BF96
+ 6.89492E-13 * BF97 - 0.000000000607294 * BF98 + 0.000000000499643 * BF99
- 0.000890849 * BF100 + 0.002564 * BF101 + 0.0000000108428 * BF102
+ 0.000000190378 * BF103 - 0.00000050842 * BF104 + 0.000000429713 * BF105
- 0.00000000830773 * BF106 - 0.000000000277217 * BF109
- 0.00000000163059 * BF110 + 0.00000000311248 * BF111
- 0.0000000107599 * BF112 + 0.0000000385213 * BF113 + 0.000120361 * BF114
- 2.73344E-13 * BF116 + 4.19601E-13 * BF117- 0.0000000879177 * BF118
+ 0.0000000371198 * BF119 + 0.000000194454 * BF120 + 8.36832E-11 * BF122
+ 3.33084E-11 * BF125 - 0.000000000108579 * BF126 - 1.33202E-11 * BF127
- 6.71344E-11 * BF128 - 0.0000000138799 * BF129 - 0.000000902901 * BF131
+ 0.0000193757 * BF132 + 0.0000000742015 * BF134 + 0.000000637464 * BF135
+ 0.000000129692 * BF136 - 0.0000000982426 * BF138 + 0.0000603609 * BF140

- 0.00000000748308 * BF142 - 0.0000000222126 * BF143 - 0.0000000126426 * BF144
+ 0.0000000158054 * BF145 - 0.00000642383 * BF146 + 0.00000194495 * BF147
+ 0.0000074903 * BF148 + 0.00000220845 * BF149 - 0.00000000421066 * BF150

MARS Model for HMA Thickness – Total Rutting Model

BF1 = Max(0, AADTT - 7500)
BF2 = Max(0, 7500 - AADTT)
BF3 = Max(0, total_rutting - 0.579)
BF4 = Max(0, 0.579 - total_rutting)
BF5 = Max(0, SUBGRADE_MODULUS - 7500)
BF6 = Max(0, 7500 - SUBGRADE_MODULUS)
BF7 = Max(0, AADTT - 2500)
BF8 = Max(0, 2500 - AADTT)
BF9 = Max(0, SUBGRADE_MODULUS - 9000) * BF7
BF10 = Max(0, 9000 - SUBGRADE_MODULUS) * BF7
BF11 = Max(0, AADTT - 10000) * BF3
BF12 = Max(0, 10000 - AADTT) * BF3
BF13 = Max(0, AADTT - 5000)
BF14 = Max(0, 5000 - AADTT)
BF15 = Max(0, DGA_MODULUS - 30000) * BF2
BF16 = Max(0, 30000 - DGA_MODULUS) * BF2
BF17 = Max(0, total_rutting - 0.634) * BF5
BF18 = Max(0, 0.634 - total_rutting) * BF5
BF19 = Max(0, total_rutting - 0.552) * BF8
BF20 = Max(0, 0.552 - total_rutting) * BF8
BF21 = Max(0, AADTT - 20000) * BF5
BF22 = Max(0, 20000 - AADTT) * BF5
BF23 = Max(0, total_rutting - 0.703) * BF14
BF24 = Max(0, 0.703 - total_rutting) * BF14
BF25 = Max(0, DGA_THICKNESS - 6) * BF17
BF26 = Max(0, total_rutting - 0.774) * BF10
BF27 = Max(0, 0.774 - total_rutting) * BF10
BF29 = Max(0, 9000 - SUBGRADE_MODULUS) * BF14
BF30 = Max(0, total_rutting - 0.692) * BF2
BF31 = Max(0, 0.692 - total_rutting) * BF2
BF32 = Max(0, DGA_THICKNESS - 6) * BF15
BF33 = Max(0, AADTT - 15000)
BF34 = Max(0, 15000 - AADTT)
BF35 = Max(0, total_rutting - 0.822)
BF36 = Max(0, 0.822 - total_rutting)
BF37 = Max(0, SUBGRADE_MODULUS - 9000) * BF36
BF38 = Max(0, 9000 - SUBGRADE_MODULUS) * BF36
BF40 = Max(0, 2500 - AADTT) * BF37
BF41 = Max(0, DGA_MODULUS - 20000) * BF27
BF42 = Max(0, total_rutting - 0.719) * BF10
BF43 = Max(0, 0.719 - total_rutting) * BF10
BF44 = Max(0, AADTT - 7500) * BF38
BF45 = Max(0, 7500 - AADTT) * BF38

BF46 = Max(0, AADTT - 10000) * BF6
BF47 = Max(0, 10000 - AADTT) * BF6
BF48 = Max(0, SUBGRADE_MODULUS - 7500) * BF34
BF49 = Max(0, 7500 - SUBGRADE_MODULUS) * BF34
BF50 = Max(0, DGA_THICKNESS - 6) * BF38
BF53 = Max(0, total_rutting - 1.062)
BF55 = Max(0, SUBGRADE_MODULUS - 10500) * BF12
BF56 = Max(0, 10500 - SUBGRADE_MODULUS) * BF12
BF57 = Max(0, AADTT - 5000) * BF6
BF60 = Max(0, 20000 - AADTT) * BF35
BF61 = Max(0, DGA_MODULUS - 30000) * BF44
BF62 = Max(0, 30000 - DGA_MODULUS) * BF44
BF63 = Max(0, total_rutting - 0.576) * BF29
BF64 = Max(0, 0.576 - total_rutting) * BF29
BF65 = Max(0, SUBGRADE_MODULUS - 9000) * BF2
BF66 = Max(0, 9000 - SUBGRADE_MODULUS) * BF2
BF67 = Max(0, total_rutting - 0.728) * BF49
BF69 = Max(0, total_rutting - 0.689) * BF6
BF70 = Max(0, 0.689 - total_rutting) * BF6
BF71 = Max(0, DGA_THICKNESS - 6) * BF41
BF73 = Max(0, 10500 - SUBGRADE_MODULUS) * BF30
BF74 = Max(0, DGA_THICKNESS - 6)
BF75 = Max(0, AADTT - 2500) * BF74
BF76 = Max(0, 2500 - AADTT) * BF74
BF77 = Max(0, DGA_MODULUS - 30000) * BF76
BF78 = Max(0, 30000 - DGA_MODULUS) * BF76
BF79 = Max(0, total_rutting - 0.481) * BF74
BF80 = Max(0, 0.481 - total_rutting) * BF74
BF81 = Max(0, SUBGRADE_MODULUS - 12000) * BF74
BF82 = Max(0, 12000 - SUBGRADE_MODULUS) * BF74
BF83 = Max(0, AADTT - 10000) * BF38
BF85 = Max(0, DGA_MODULUS - 30000) * BF74
BF86 = Max(0, 30000 - DGA_MODULUS) * BF74
BF87 = Max(0, DGA_MODULUS - 30000) * BF43
BF88 = Max(0, 30000 - DGA_MODULUS) * BF43
BF89 = Max(0, total_rutting - 0.662) * BF6
BF91 = Max(0, total_rutting - 0.728) * BF47
BF92 = Max(0, 0.728 - total_rutting) * BF47
BF93 = Max(0, total_rutting - 0.678) * BF29
BF95 = Max(0, SUBGRADE_MODULUS - 12000) * BF24
BF96 = Max(0, 12000 - SUBGRADE_MODULUS) * BF24
BF97 = Max(0, AADTT - 5000) * BF85
BF98 = Max(0, 5000 - AADTT) * BF85
BF100 = Max(0, 1.253 - total_rutting) * BF86

BF101 = Max(0, total_rutting - 0.687) * BF32
BF103 = Max(0, total_rutting - 0.629) * BF22
BF104 = Max(0, 0.629 - total_rutting) * BF22
BF105 = Max(0, SUBGRADE_MODULUS - 9000) * BF11
BF106 = Max(0, 9000 - SUBGRADE_MODULUS) * BF11
BF107 = Max(0, SUBGRADE_MODULUS - 7500) * BF79
BF108 = Max(0, 7500 - SUBGRADE_MODULUS) * BF79
BF109 = Max(0, SUBGRADE_MODULUS - 12000)
BF112 = Max(0, 12 - DGA_THICKNESS) * BF14
BF113 = Max(0, total_rutting - 0.497) * BF112
BF114 = Max(0, 0.497 - total_rutting) * BF112
BF116 = Max(0, 10500 - SUBGRADE_MODULUS) * BF16
BF117 = Max(0, DGA_THICKNESS - 10) * BF43
BF118 = Max(0, 10 - DGA_THICKNESS) * BF43
BF119 = Max(0, DGA_THICKNESS - 10) * BF27
BF121 = Max(0, total_rutting - 1.214) * BF7
BF124 = Max(0, 7500 - SUBGRADE_MODULUS) * BF86
BF125 = Max(0, AADTT - 7500) * BF50
BF126 = Max(0, 7500 - AADTT) * BF50
BF127 = Max(0, DGA_MODULUS - 30000) * BF17
BF128 = Max(0, 30000 - DGA_MODULUS) * BF17
BF129 = Max(0, AADTT - 7500) * BF124
BF130 = Max(0, 7500 - AADTT) * BF124
BF131 = Max(0, DGA_THICKNESS - 10) * BF18
BF132 = Max(0, 10 - DGA_THICKNESS) * BF18
BF133 = Max(0, SUBGRADE_MODULUS - 10500) * BF75
BF134 = Max(0, 10500 - SUBGRADE_MODULUS) * BF75
BF135 = Max(0, DGA_MODULUS - 20000) * BF8
BF137 = Max(0, 7500 - AADTT) * BF128
BF138 = Max(0, AADTT - 15000) * BF124
BF140 = Max(0, DGA_THICKNESS - 6) * BF88
BF142 = Max(0, 30000 - DGA_MODULUS) * BF14
BF143 = Max(0, DGA_MODULUS - 20000) * BF67
BF144 = Max(0, total_rutting - 0.703)
BF146 = Max(0, SUBGRADE_MODULUS - 10500)
BF148 = Max(0, total_rutting - 0.461) * BF135
BF149 = Max(0, 0.461 - total_rutting) * BF135
BF150 = Max(0, DGA_THICKNESS - 6) * BF87

totalrut_drain_0 = 28.1067 + 0.00329821 * BF1 - 0.00350442 * BF2 - 8.45495 * BF3
+ 14.8171 * BF4 - 0.0029254 * BF5 - 0.00366096 * BF6 - 0.00215979 * BF7
+ 0.000000163066 * BF9 - 0.000000496841 * BF10 + 0.000321779 * BF11
- 0.00103076 * BF12 - 0.000723493 * BF13 - 0.00000000191416 * BF15
- 0.000657002 * BF17 - 0.00140932 * BF18 + 0.00809587 * BF19 - 0.00273971 * BF20

- 0.000000174914 * BF21 + 0.000000145272 * BF22 + 0.00209759 * BF23
+ 0.000435807 * BF24 + 0.000123695 * BF25 - 0.00000613233 * BF26
+ 0.00000303238 * BF27 + 0.000000208601 * BF29 - 0.000707227 * BF30
+ 0.000965066 * BF31 + 0.000000000628148 * BF32 - 0.000161857 * BF33
+ 0.000360048 * BF37 - 0.00163343 * BF38 - 0.000000250937 * BF40
- 3.76474E-11 * BF41 + 0.00000616447 * BF42 + 0.00000147555 * BF44
- 0.00000227987 * BF45 - 0.000000722238 * BF46 - 0.000000110167 * BF47
+ 0.00000000427238 * BF48 + 0.000000455174 * BF49 - 0.0000428305 * BF50
- 1.83169 * BF53 - 0.0000000670946 * BF55 + 0.000000135158 * BF56
+ 0.000000894616 * BF57 - 0.000254134 * BF60 + 1.19295E-11 * BF61
- 1.18937E-11 * BF62 - 0.00000442253 * BF63 + 0.00000399545 * BF64
- 0.000000014337 * BF65 + 0.000000526511 * BF66 - 0.0000426377 * BF67
- 0.0198867 * BF69 + 0.0293042 * BF70 - 4.57047E-12 * BF71
- 0.000000343313 * BF73 + 0.0947603 * BF74 - 0.00000120411 * BF75
- 0.0000300161 * BF76 - 0.00000000038338 * BF77 + 0.00000000110166 * BF78
+ 0.0689348 * BF79 + 1.11562 * BF80 + 0.0000219319 * BF81 - 0.0000237441 * BF82
- 0.00000253145 * BF83- 0.00000117232 * BF85 + 4.24832E-11 * BF87
- 3.52057E-11 * BF88 + 0.0204752 * BF89 + 0.0000756819 * BF91
- 0.00000331816 * BF92 - 0.00000559208 * BF93 - 0.000000245808 * BF95
+ 0.000000360106 * BF96 + 4.55699E-11 * BF97 - 0.00000000141391 * BF98
+ 0.00000322256 * BF100 - 0.00000000677274 * BF101 + 0.0000000473393 * BF103
+ 0.0000000700681 * BF104 + 0.000000031683 * BF105 - 0.0000000730102 * BF106
- 0.00011908 * BF107 + 0.0000188122 * BF108 + 0.0000425199 * BF109
+ 0.000039193 * BF113 + 0.000136233 * BF114 - 3.9875E-13 * BF116
+ 0.000000143182 * BF117 - 0.0000000790285 * BF118 - 0.0000000615178 * BF119
- 0.000062567 * BF121 + 0.00000000318563 * BF124 + 0.0000000373987 * BF125
+ 0.00000000898896 * BF126 + 0.00000000198051 * BF127 - 3.8653E-13 * BF129
- 3.84632E-13 * BF130 - 0.0000848086 * BF131 + 0.0000569042 * BF132
- 0.000000000250491 * BF133 + 0.000000000167906 * BF134
- 0.0000000024485 * BF135 + 6.46856E-12 * BF137 + 4.04418E-13 * BF138
- 6.34324E-12 * BF140 + 0.00000000585812 * BF142 - 6.79267E-11 * BF143
- 2.14065 * BF144 + 0.0000467373 * BF146 - 0.0000000213074 * BF148
+ 0.000000132115 * BF149 + 3.86891E-12 * BF150

MARS Model for HMA Fatigue Cracking

BF1 = Max(0, AC_THICKNESS - 6)
BF2 = Max(0, 6 - AC_THICKNESS)
BF3 = Max(0, AADTT - 5000)
BF4 = Max(0, 5000 - AADTT)
BF5 = Max(0, AC_THICKNESS - 10) * BF3
BF6 = Max(0, 10 - AC_THICKNESS) * BF3
BF7 = Max(0, DGA_MODULUS - 30000)
BF8 = Max(0, 30000 - DGA_MODULUS)
BF9 = Max(0, AC_THICKNESS - 12) * BF8
BF10 = Max(0, 12 - AC_THICKNESS) * BF8
BF11 = Max(0, AADTT - 2500) * BF8
BF12 = Max(0, 2500 - AADTT) * BF8
BF13 = Max(0, SUBGRADE_MODULUS - 6000) * BF1
BF14 = Max(0, DGA_THICKNESS - 10) * BF13
BF15 = Max(0, 10 - DGA_THICKNESS) * BF13
BF16 = Max(0, DGA_MODULUS - 30000) * BF6
BF17 = Max(0, 30000 - DGA_MODULUS) * BF6
BF18 = Max(0, DGA_THICKNESS - 10) * BF6
BF19 = Max(0, 10 - DGA_THICKNESS) * BF6
BF20 = Max(0, DGA_THICKNESS - 10)
BF21 = Max(0, 10 - DGA_THICKNESS)
BF22 = Max(0, AC_THICKNESS - 6) * BF12
BF23 = Max(0, 6 - AC_THICKNESS) * BF12
BF24 = Max(0, AC_THICKNESS - 12)
BF25 = Max(0, 12 - AC_THICKNESS)
BF26 = Max(0, AADTT - 2500) * BF25
BF27 = Max(0, 2500 - AADTT) * BF25
BF28 = Max(0, DGA_THICKNESS - 10) * BF26
BF29 = Max(0, 10 - DGA_THICKNESS) * BF26
BF30 = Max(0, AC_THICKNESS - 8) * BF21
BF31 = Max(0, 8 - AC_THICKNESS) * BF21
BF32 = Max(0, AADTT - 500) * BF31
BF33 = Max(0, DGA_MODULUS - 30000) * BF26
BF34 = Max(0, 30000 - DGA_MODULUS) * BF26
BF36 = Max(0, 6 - AC_THICKNESS) * BF7
BF37 = Max(0, AADTT - 5000) * BF13
BF38 = Max(0, 5000 - AADTT) * BF13
BF39 = Max(0, AADTT - 5000) * BF21
BF40 = Max(0, 5000 - AADTT) * BF21
BF41 = Max(0, SUBGRADE_MODULUS - 6000) * BF26
BF42 = Max(0, DGA_THICKNESS - 10) * BF1
BF43 = Max(0, 10 - DGA_THICKNESS) * BF1
BF44 = Max(0, AC_THICKNESS - 10) * BF20

131

BF45 = Max(0, 10 - AC_THICKNESS) * BF20
BF46 = Max(0, AADTT - 5000) * BF44
BF48 = Max(0, AC_THICKNESS - 10) * BF11
BF49 = Max(0, 10 - AC_THICKNESS) * BF11
BF50 = Max(0, AC_THICKNESS - 10)
BF52 = Max(0, DGA_MODULUS - 30000) * BF50
BF53 = Max(0, 30000 - DGA_MODULUS) * BF50
BF54 = Max(0, AC_THICKNESS - 8)
BF55 = Max(0, 8 - AC_THICKNESS)
BF56 = Max(0, AADTT - 500) * BF55
BF57 = Max(0, DGA_MODULUS - 20000) * BF56
BF58 = Max(0, AADTT - 10000) * BF1
BF59 = Max(0, 10000 - AADTT) * BF1
BF60 = Max(0, AADTT - 2500) * BF7
BF61 = Max(0, 2500 - AADTT) * BF7
BF62 = Max(0, SUBGRADE_MODULUS - 10500) * BF11
BF63 = Max(0, 10500 - SUBGRADE_MODULUS) * BF11
BF64 = Max(0, AC_THICKNESS - 10) * BF4
BF65 = Max(0, 10 - AC_THICKNESS) * BF4
BF66 = Max(0, DGA_THICKNESS - 14) * BF41
BF67 = Max(0, 14 - DGA_THICKNESS) * BF41
BF68 = Max(0, DGA_THICKNESS - 8) * BF27
BF69 = Max(0, 8 - DGA_THICKNESS) * BF27
BF70 = Max(0, AADTT - 2500) * BF42
BF71 = Max(0, 2500 - AADTT) * BF42
BF72 = Max(0, SUBGRADE_MODULUS - 12000) * BF25
BF73 = Max(0, 12000 - SUBGRADE_MODULUS) * BF25
BF74 = Max(0, AADTT - 15000) * BF25
BF75 = Max(0, 15000 - AADTT) * BF25
BF76 = Max(0, DGA_MODULUS - 20000) * BF31
BF77 = Max(0, AC_THICKNESS - 14) * BF63
BF78 = Max(0, 14 - AC_THICKNESS) * BF63
BF79 = Max(0, SUBGRADE_MODULUS - 9000) * BF3
BF80 = Max(0, 9000 - SUBGRADE_MODULUS) * BF3
BF81 = Max(0, DGA_THICKNESS - 10) * BF80
BF82 = Max(0, 10 - DGA_THICKNESS) * BF80
BF83 = Max(0, AC_THICKNESS - 14) * BF82
BF84 = Max(0, 14 - AC_THICKNESS) * BF82
BF85 = Max(0, SUBGRADE_MODULUS - 12000) * BF7
BF86 = Max(0, 12000 - SUBGRADE_MODULUS) * BF7
BF87 = Max(0, AC_THICKNESS - 10) * BF60
BF88 = Max(0, 10 - AC_THICKNESS) * BF60
BF90 = Max(0, 30000 - DGA_MODULUS) * BF67
BF92 = Max(0, 12000 - SUBGRADE_MODULUS) * BF68

BF93 = Max(0, SUBGRADE_MODULUS - 6000) * BF19
BF94 = Max(0, DGA_MODULUS - 30000) * BF54
BF95 = Max(0, 30000 - DGA_MODULUS) * BF54
BF96 = Max(0, DGA_THICKNESS - 8) * BF25
BF97 = Max(0, 8 - DGA_THICKNESS) * BF25
BF98 = Max(0, DGA_THICKNESS - 6) * BF36
BF99 = Max(0, DGA_MODULUS - 20000) * BF74
BF100 = Max(0, AC_THICKNESS - 14) * BF80
BF101 = Max(0, 14 - AC_THICKNESS) * BF80
BF102 = Max(0, DGA_THICKNESS - 12) * BF65
BF103 = Max(0, 12 - DGA_THICKNESS) * BF65
BF104 = Max(0, SUBGRADE_MODULUS - 7500) * BF39
BF105 = Max(0, 7500 - SUBGRADE_MODULUS) * BF39
BF106 = Max(0, DGA_THICKNESS - 8) * BF33
BF107 = Max(0, 8 - DGA_THICKNESS) * BF33
BF108 = Max(0, SUBGRADE_MODULUS - 12000) * BF10
BF109 = Max(0, 12000 - SUBGRADE_MODULUS) * BF10
BF110 = Max(0, DGA_THICKNESS - 12) * BF54
BF111 = Max(0, 12 - DGA_THICKNESS) * BF54
BF112 = Max(0, SUBGRADE_MODULUS - 12000) * BF27
BF113 = Max(0, 12000 - SUBGRADE_MODULUS) * BF27
BF114 = Max(0, DGA_THICKNESS - 8) * BF50
BF115 = Max(0, 8 - DGA_THICKNESS) * BF50
BF116 = Max(0, SUBGRADE_MODULUS - 7500) * BF5
BF117 = Max(0, 7500 - SUBGRADE_MODULUS) * BF5
BF118 = Max(0, DGA_THICKNESS - 10) * BF10
BF119 = Max(0, 10 - DGA_THICKNESS) * BF10
BF120 = Max(0, DGA_THICKNESS - 10) * BF73
BF122 = Max(0, SUBGRADE_MODULUS - 6000) * BF2
BF123 = Max(0, DGA_THICKNESS - 10) * BF122
BF124 = Max(0, 10 - DGA_THICKNESS) * BF122
BF125 = Max(0, AC_THICKNESS - 8) * BF61
BF126 = Max(0, 8 - AC_THICKNESS) * BF61
BF128 = Max(0, 12000 - SUBGRADE_MODULUS) * BF69
BF129 = Max(0, DGA_MODULUS - 30000) * BF101
BF131 = Max(0, AADTT - 5000) * BF30
BF132 = Max(0, 5000 - AADTT) * BF30
BF133 = Max(0, SUBGRADE_MODULUS - 10500) * BF33
BF134 = Max(0, 10500 - SUBGRADE_MODULUS) * BF33
BF136 = Max(0, 15000 - AADTT) * BF72
BF138 = Max(0, 8 - DGA_THICKNESS) * BF3
BF139 = Max(0, DGA_THICKNESS - 6) * BF56
BF140 = Max(0, DGA_THICKNESS - 12) * BF26
BF143 = Max(0, 10 - DGA_THICKNESS) * BF49

BF144 = Max(0, DGA_THICKNESS - 6) * BF23
BF145 = Max(0, SUBGRADE_MODULUS - 10500) * BF21
BF146 = Max(0, 10500 - SUBGRADE_MODULUS) * BF21
BF147 = Max(0, AC_THICKNESS - 8) * BF146
BF148 = Max(0, 8 - AC_THICKNESS) * BF146
BF149 = Max(0, DGA_THICKNESS - 14) * BF75
BF150 = Max(0, 14 - DGA_THICKNESS) * BF75

all_cracking = 7.58414 - 2.86177 * BF1 + 4.01372 * BF2 + 0.000841954 * BF3
- 0.000991686 * BF4 + 0.000155313 * BF5 + 0.0000896338 * BF6 - 0.000059183 * BF7
- 0.000183277 * BF8 - 0.000064686 * BF9 + 0.0000726849 * BF10
+ 0.00000000570558 * BF11 - 0.0000000789771 * BF12 - 0.00000688099 * BF13
+ 0.000000609208 * BF14 + 0.00000490885 * BF15 + 0.00000000153644 * BF16
- 0.00000000427589 * BF17 - 0.00000877983 * BF18 + 0.00003163 * BF19
+ 0.794289 * BF20 - 0.809407 * BF21 + 0.0000000168257 * BF22
+ 0.0000000924546 * BF23 + 0.0983327 * BF24 + 0.000087442 * BF26
- 0.0000859762 * BF27 - 0.00000473212 * BF28 + 0.00000692308 * BF29
- 0.663782 * BF30 + 0.639015 * BF31 + 0.0000785336 * BF32
- 0.00000000261591 * BF33 + 0.0000000029167 * BF34 - 0.000125224 * BF36
+ 0.0000000128166 * BF37 + 0.0000000014677 * BF38 + 0.0000160939 * BF39
- 0.0000331687 * BF40 - 0.0000000011726 * BF41 - 0.191951 * BF42
+ 0.510994 * BF43 + 0.317169 * BF44 - 0.269829 * BF45 + 0.00000385687 * BF46
- 0.00000000110675 * BF48 + 0.0000000114408 * BF49 + 1.28372 * BF50
- 0.0000187924 * BF52 + 0.0000287851 * BF53 + 0.405599 * BF54
+ 0.00146015 * BF56 - 0.0000000467663 * BF57 - 0.000206246 * BF58
+ 0.000207061 * BF59 - 0.00000000323744 * BF60 + 0.0000000256638 * BF61
- 1.8311E-13 * BF62 + 2.28673E-13 * BF63 - 0.00020154 * BF64
+ 0.000000000616384 * BF66 - 0.000000000356977 * BF67
+ 0.00000375206 * BF68 - 0.00000201936 * BF70 + 0.00000188056 * BF71
+ 0.0000206384 * BF72 + 0.000021143 * BF73 - 0.0000119448 * BF74
– 0.00000173277 * BF76 + 2.28354E-13 * BF77 + 1.19161E-13 * BF78
- 0.0000000597744 * BF79 + 0.0000000618699 * BF80 - 0.00000000110954 * BF81
- 0.000000002436 * BF82 + 0.00000000109748 * BF83 + 0.00000000118049 * BF84
+ 0.00000000185971 * BF85 - 0.00000000162789 * BF86
+ 0.000000000434161 * BF87 - 0.00000000633535 * BF88 - 1.6768E-14 * BF90
+ 0.000000000521049 * BF92 - 0.00000000289952 * BF93 + 0.0000232062 * BF94
+ 0.0000336154 * BF95 - 0.01122 * BF96 + 0.0387939 * BF97
+ 0.00000486946 * BF98 + 0.000000000748092 * BF99 + 0.00000000889677 * BF100
+ 0.00000000283069 * BF101 + 0.0000113573 * BF102 - 0.00000879874 * BF103
- 0.00000000138127 * BF104 + 0.00000000297632 * BF105 + 6.12558E-11 * BF106
+ 0.0000000001468 * BF107 - 0.00000000171026 * BF108
+ 0.000000000642018 * BF109 - 0.0256852 * BF110 + 0.0297266 * BF111
+ 0.0000000125918 * BF112 - 0.000000007444 * BF113 - 0.0877621 * BF114
+ 0.0886054 * BF115 - 0.0000000103199 * BF116 + 0.0000000120419 * BF117

- 0.000000436257 * BF118 - 0.000000387875 * BF119 - 0.00000185361 * BF120
- 0.0000961601 * BF122 + 0.0000120579 * BF123 - 0.0000270324 * BF124
- 0.00000000746811 * BF125 - 0.00000000955476 * BF126
- 0.00000000374786 * BF128 - 1.65103E-13 * BF129 - 0.00000123903 * BF131
+ 0.00000685161 * BF132 + 1.75927E-13 * BF133 - 7.99126E-14 * BF134
- 0.00000000311151 * BF136 + 0.00000339838 * BF138 - 0.0000196353 * BF139
+ 0.00000157342 * BF140 - 0.000000000290126 * BF143 - 0.00000000119097 * BF144
- 0.0000262169 * BF145 + 0.0000291184 * BF146 + 0.0000025628 * BF147
+ 0.0000117145 * BF148 + 0.00000103814 * BF149 - 0.000000510708 * BF150

MARS Model for HMA IRI
BF1 = Max(0, AADTT - 15000)
BF2 = Max(0, 15000 - AADTT)
BF3 = Max(0, AC_THICKNESS - 10)
BF4 = Max(0, 10 - AC_THICKNESS)
BF5 = Max(0, AC_THICKNESS - 6) * BF2
BF6 = Max(0, 6 - AC_THICKNESS) * BF2
BF7 = Max(0, SUBGRADE_MODULUS - 7500) * BF3
BF8 = Max(0, 7500 - SUBGRADE_MODULUS) * BF3
BF9 = Max(0, AADTT - 2500) * BF4
BF10 = Max(0, 2500 - AADTT) * BF4
BF11 = Max(0, SUBGRADE_MODULUS - 7500)
BF12 = Max(0, 7500 - SUBGRADE_MODULUS)
BF13 = Max(0, AADTT - 5000)
BF14 = Max(0, 5000 - AADTT)
BF15 = Max(0, AC_THICKNESS - 14) * BF13
BF16 = Max(0, 14 - AC_THICKNESS) * BF13
BF17 = Max(0, DGA_MODULUS - 30000) * BF4
BF18 = Max(0, 30000 - DGA_MODULUS) * BF4
BF19 = Max(0, AC_THICKNESS - 8) * BF2
BF20 = Max(0, 8 - AC_THICKNESS) * BF2
BF21 = Max(0, DGA_MODULUS - 30000) * BF16
BF22 = Max(0, 30000 - DGA_MODULUS) * BF16
BF23 = Max(0, SUBGRADE_MODULUS - 9000) * BF16
BF25 = Max(0, AADTT - 5000) * BF3
BF26 = Max(0, 5000 - AADTT) * BF3
BF28 = Max(0, 12 - DGA_THICKNESS) * BF4
BF29 = Max(0, AADTT - 2500)
BF30 = Max(0, 2500 - AADTT)
BF31 = Max(0, AADTT - 7500)
BF32 = Max(0, 7500 - AADTT)
BF33 = Max(0, AC_THICKNESS - 14) * BF31
BF34 = Max(0, 14 - AC_THICKNESS) * BF31
BF36 = Max(0, AC_THICKNESS - 12)
BF37 = Max(0, 12 - AC_THICKNESS)
BF38 = Max(0, SUBGRADE_MODULUS - 10500)
BF39 = Max(0, 10500 - SUBGRADE_MODULUS)
BF40 = Max(0, AC_THICKNESS - 8) * BF30
BF41 = Max(0, 8 - AC_THICKNESS) * BF30
BF42 = Max(0, DGA_MODULUS - 30000) * BF6
BF43 = Max(0, 30000 - DGA_MODULUS) * BF6
BF44 = Max(0, DGA_THICKNESS - 6) * BF39
BF45 = Max(0, DGA_THICKNESS - 8) * BF11
BF46 = Max(0, 8 - DGA_THICKNESS) * BF11

136

BF47 = Max(0, DGA_MODULUS - 30000) * BF10
BF49 = Max(0, DGA_MODULUS - 30000) * BF44
BF50 = Max(0, 30000 - DGA_MODULUS) * BF44
BF51 = Max(0, DGA_THICKNESS - 10) * BF6
BF52 = Max(0, 10 - DGA_THICKNESS) * BF6
BF55 = Max(0, 30000 - DGA_MODULUS) * BF34
BF56 = Max(0, AADTT - 10000)
BF57 = Max(0, 10000 - AADTT)
BF58 = Max(0, AADTT - 20000)
BF59 = Max(0, 20000 - AADTT)
BF60 = Max(0, DGA_THICKNESS - 12) * BF37
BF61 = Max(0, 12 - DGA_THICKNESS) * BF37
BF62 = Max(0, AADTT - 15000) * BF18
BF63 = Max(0, 15000 - AADTT) * BF18
BF64 = Max(0, DGA_MODULUS - 30000) * BF45
BF65 = Max(0, 30000 - DGA_MODULUS) * BF45
BF66 = Max(0, SUBGRADE_MODULUS - 9000) * BF29
BF67 = Max(0, 9000 - SUBGRADE_MODULUS) * BF29
BF68 = Max(0, SUBGRADE_MODULUS - 9000) * BF20
BF69 = Max(0, 9000 - SUBGRADE_MODULUS) * BF20
BF70 = Max(0, DGA_MODULUS - 30000) * BF20
BF71 = Max(0, 30000 - DGA_MODULUS) * BF20
BF72 = Max(0, DGA_MODULUS - 30000) * BF2
BF73 = Max(0, 30000 - DGA_MODULUS) * BF2
BF75 = Max(0, 10 - AC_THICKNESS) * BF72
BF76 = Max(0, DGA_THICKNESS - 8) * BF16
BF77 = Max(0, 8 - DGA_THICKNESS) * BF16
BF78 = Max(0, DGA_MODULUS - 20000) * BF67
BF79 = Max(0, AC_THICKNESS - 14) * BF78
BF81 = Max(0, DGA_MODULUS - 20000) * BF66
BF82 = Max(0, DGA_MODULUS - 20000) * BF59
BF83 = Max(0, SUBGRADE_MODULUS - 9000) * BF82
BF84 = Max(0, 9000 - SUBGRADE_MODULUS) * BF82
BF85 = Max(0, DGA_THICKNESS - 6) * BF73
BF86 = Max(0, AADTT - 2500) * BF45
BF87 = Max(0, 2500 - AADTT) * BF45
BF88 = Max(0, DGA_THICKNESS - 14) * BF20
BF89 = Max(0, 14 - DGA_THICKNESS) * BF20
BF90 = Max(0, DGA_THICKNESS - 12) * BF11
BF91 = Max(0, 12 - DGA_THICKNESS) * BF11
BF92 = Max(0, AC_THICKNESS - 12) * BF64
BF93 = Max(0, 12 - AC_THICKNESS) * BF64
BF94 = Max(0, DGA_THICKNESS - 6) * BF12
BF95 = Max(0, AC_THICKNESS - 12) * BF57

BF96 = Max(0, 12 - AC_THICKNESS) * BF57
BF97 = Max(0, DGA_MODULUS - 30000) * BF36
BF98 = Max(0, 30000 - DGA_MODULUS) * BF36
BF99 = Max(0, AC_THICKNESS - 8) * BF91
BF100 = Max(0, 8 - AC_THICKNESS) * BF91
BF102 = Max(0, SUBGRADE_MODULUS - 9000) * BF2
BF103 = Max(0, 9000 - SUBGRADE_MODULUS) * BF2
BF104 = Max(0, SUBGRADE_MODULUS - 12000)
BF106 = Max(0, AADTT - 7500) * BF60
BF108 = Max(0, AC_THICKNESS - 10) * BF104
BF111 = Max(0, 10 - AC_THICKNESS) * BF84
BF112 = Max(0, DGA_THICKNESS - 8) * BF7
BF113 = Max(0, 8 - DGA_THICKNESS) * BF7
BF115 = Max(0, DGA_MODULUS - 30000) * BF41
BF116 = Max(0, 30000 - DGA_MODULUS) * BF41
BF117 = Max(0, SUBGRADE_MODULUS - 9000)
BF119 = Max(0, AC_THICKNESS - 12) * BF82
BF120 = Max(0, 12 - AC_THICKNESS) * BF82
BF122 = Max(0, 2500 - AADTT) * BF38
BF123 = Max(0, AADTT - 20000) * BF61
BF124 = Max(0, 20000 - AADTT) * BF61
BF125 = Max(0, AC_THICKNESS - 14) * BF44
BF126 = Max(0, 14 - AC_THICKNESS) * BF44
BF127 = Max(0, AC_THICKNESS - 8) * BF46
BF128 = Max(0, 8 - AC_THICKNESS) * BF46
BF129 = Max(0, DGA_MODULUS - 20000) * BF58
BF131 = Max(0, 12 - DGA_THICKNESS) * BF102
BF132 = Max(0, SUBGRADE_MODULUS - 10500) * BF4
BF134 = Max(0, DGA_THICKNESS - 10) * BF41
BF135 = Max(0, 10 - DGA_THICKNESS) * BF41
BF136 = Max(0, DGA_THICKNESS - 8) * BF72
BF137 = Max(0, 8 - DGA_THICKNESS) * BF72
BF138 = Max(0, DGA_THICKNESS - 10) * BF9
BF139 = Max(0, 10 - DGA_THICKNESS) * BF9
BF140 = Max(0, DGA_THICKNESS - 8) * BF66
BF141 = Max(0, 8 - DGA_THICKNESS) * BF66
BF142 = Max(0, AADTT - 5000) * BF18
BF144 = Max(0, DGA_THICKNESS - 10) * BF37
BF146 = Max(0, DGA_MODULUS - 20000) * BF14
BF147 = Max(0, SUBGRADE_MODULUS - 7500) * BF32
BF148 = Max(0, 7500 - SUBGRADE_MODULUS) * BF32
BF149 = Max(0, SUBGRADE_MODULUS - 10500) * BF85
BF150 = Max(0, 10500 - SUBGRADE_MODULUS) * BF85

IRI = 167.92 + 0.00318975 * BF1 - 0.00326001 * BF2 - 3.04757 * BF3 + 2.6349 * BF4
- 0.0000995931 * BF5 + 0.000303357 * BF6 + 0.0000633734 * BF7
- 0.0000594471 * BF8 + 0.000263281 * BF9 - 0.00114668 * BF10 - 0.00126243 * BF11
+ 0.00173072 * BF12 - 0.000605576 * BF13 + 0.00125569 * BF15
- 0.0000187738 * BF16 - 0.0000554149 * BF17 + 0.000124241 * BF18
+ 0.000123854 * BF19 - 0.0000000011571 * BF21 + 0.00000000222086 * BF22
- 0.00000000120985 * BF23 - 0.000183444 * BF25 + 0.000194943 * BF26
+ 0.0334299 * BF28 - 0.000823443 * BF29 - 0.000208294 * BF31
- 0.00100293 * BF33 - 0.0000433229 * BF34 - 0.794358 * BF36
+ 0.000236463 * BF38 - 0.000848937 * BF40 - 0.00000000634465 * BF42
+ 0.000000012001 * BF43 - 0.0000119686 * BF44 + 0.0000342688 * BF45
- 0.0000535999 * BF46 + 0.00000000227107 * BF47 - 0.000000000356712 * BF49
+ 0.00000000103476 * BF50 - 0.00000420569 * BF51 + 0.000019823 * BF52
- 0.00000000059273 * BF55 - 0.000228032 * BF56 - 0.000113145 * BF58
- 0.0321721 * BF60 + 0.070453 * BF61 + 0.00000000962645 * BF62
- 0.00000000844376 * BF63 + 0.000000000499757 * BF65 - 0.00000000241618 * BF66
+ 0.0000000113066 * BF67 - 0.00000000263112 * BF68 + 0.00000000698865 * BF69
- 0.00000000440911 * BF70 + 0.00000000801796 * BF71 + 0.00000000371189 * BF75
+ 0.000000403143 * BF76 + 0.0000020047 * BF77 - 1.33776E-13 * BF78
+ 4.95601E-13 * BF79 + 2.22805E-13 * BF81 - 0.00000000170021 * BF82
+ 1.25586E-13 * BF83 - 1.03163E-13 * BF84 + 0.000000000357681 * BF85
+ 0.000000000790155 * BF86 + 0.00000000430319 * BF87 - 0.00000428208 * BF88
+ 0.00000745558 * BF89 - 0.0000190466 * BF90 - 0.000000000454191 * BF92
+ 3.37283E-11 * BF93 - 0.0000250752 * BF94 + 0.0000379875 * BF95
- 0.0000170496 * BF96 - 0.0000193259 * BF97 + 0.0000203723 * BF98
+ 0.00000188031 * BF99 - 0.00000863028 * BF100 - 0.00000000413088 * BF103
+ 0.000145673 * BF104 - 0.000001045 * BF106 - 0.0000171234 * BF108
 - 7.42003E-14 * BF111 - 0.00000569062 * BF112 - 0.0000288513 * BF113
+ 0.0000000199823 * BF115 - 0.0000000403002 * BF116 + 0.000245274 * BF117
+ 0.00000000147481 * BF119 - 0.000000000408728 * BF120
+ 0.000000104308 * BF122 + 0.00000165709 * BF123 - 0.00000177448 * BF124
+ 0.00000414266 * BF125 + 0.00000201176 * BF126 + 0.0000214783 * BF127
+ 0.0000144876 * BF128 + 0.00000000183795 * BF129 + 0.00000000113768 * BF131
- 0.000069977 * BF132 + 0.0000220092 * BF134 - 0.0000733769 * BF135
- 0.000000000142925 * BF136 + 0.000000000353512 * BF137
- 0.00000278462 * BF138 + 0.00000992394 * BF139 - 0.00000000101723 * BF140
- 0.000000000997736 * BF141 - 0.0000000360298 * BF142 + 0.0173436 * BF144
+ 0.00000000434306 * BF146 + 0.0000000175126 * BF147
- 0.0000000267495 * BF148 - 5.23507E-14 * BF149 - 5.65979E-14 * BF150

MARS Model for HMA Total Rutting

BF1 = Max(0, AADTT - 15000)
BF2 = Max(0, 15000 - AADTT)
BF3 = Max(0, AC_THICKNESS - 10)
BF4 = Max(0, 10 - AC_THICKNESS)
BF5 = Max(0, AC_THICKNESS - 14) * BF10
BF6 = Max(0, 14 - AC_THICKNESS) * BF2
BF7 = Max(0, AADTT - 2500)
BF8 = Max(0, 2500 - AADTT)
BF9 = Max(0, SUBGRADE_MODULUS - 7500)
BF10 = Max(0, 7500 - SUBGRADE_MODULUS)
BF11 = Max(0, AADTT - 7500)
BF12 = Max(0, 7500 - AADTT)
BF13 = Max(0, AC_THICKNESS - 12) * BF11
BF14 = Max(0, 12 - AC_THICKNESS) * BF11
BF15 = Max(0, AC_THICKNESS - 6) * BF12
BF16 = Max(0, 6 - AC_THICKNESS) * BF12
BF17 = Max(0, DGA_MODULUS - 30000) * BF6
BF18 = Max(0, 30000 - DGA_MODULUS) * BF6
BF19 = Max(0, AC_THICKNESS - 12)
BF21 = Max(0, AC_THICKNESS - 14) * BF10
BF23 = Max(0, DGA_THICKNESS - 6) * BF14
BF24 = Max(0, AADTT - 5000) * BF3
BF26 = Max(0, SUBGRADE_MODULUS - 10500) * BF7
BF27 = Max(0, 10500 - SUBGRADE_MODULUS) * BF7
BF28 = Max(0, DGA_MODULUS - 20000) * BF3
BF29 = Max(0, DGA_THICKNESS - 14) * BF7
BF30 = Max(0, 14 - DGA_THICKNESS) * BF7
BF31 = Max(0, AC_THICKNESS - 10) * BF30
BF32 = Max(0, 10 - AC_THICKNESS) * BF30
BF33 = Max(0, DGA_MODULUS - 20000) * BF16
BF34 = Max(0, SUBGRADE_MODULUS - 10500) * BF2
BF35 = Max(0, 10500 - SUBGRADE_MODULUS) * BF2
BF36 = Max(0, AADTT - 5000)
BF38 = Max(0, DGA_THICKNESS - 12) * BF8
BF39 = Max(0, 12 - DGA_THICKNESS) * BF8
BF40 = Max(0, AADTT - 10000)
BF42 = Max(0, AADTT - 20000)
BF44 = Max(0, DGA_THICKNESS - 14) * BF10
BF45 = Max(0, 14 - DGA_THICKNESS) * BF10
BF46 = Max(0, SUBGRADE_MODULUS - 9000)
BF48 = Max(0, DGA_THICKNESS - 8) * BF9
BF49 = Max(0, 8 - DGA_THICKNESS) * BF9
BF50 = Max(0, DGA_THICKNESS - 6) * BF17

total_rutting = 2.31418 + 0.000130447 * BF1 - 0.000133777 * BF2 - 0.070995 * BF3
+ 0.0674614 * BF4 - 0.00000307676 * BF5 - 0.000000741493 * BF6
- 0.0000657549 * BF7 - 0.0000226296 * BF9 + 0.0000284758 * BF10
- 0.0000221393 * BF11 - 0.00000238974 * BF13 + 0.00000133248 * BF14
+ 0.00000260109 * BF15 + 0.00000251958 * BF16 + 0.000000000023435 * BF18
- 0.0229874 * BF19 + 0.0000708025 * BF21 - 0.0000000220797 * BF23
- 0.000000937015 * BF24 + 0.000000000121649 * BF26 + 0.000000000292982 * BF27
- 0.000000204456 * BF28 + 0.0000000610959 * BF29 - 0.000000211616 * BF30
+ 0.0000000524737 * BF31 - 0.0000000297929 * BF32 - 0.000000000172514 * BF33
+ 0.000000000152028 * BF34 + 0.000000000184548 * BF35 - 0.0000154411 * BF36
- 0.000000584107 * BF38 + 0.00000101095 * BF39 - 0.00000531626 * BF40
- 0.00000279347 * BF42 - 0.00000123436 * BF44 + 0.000000531415 * BF45
+ 0.00000588928 * BF46 + 0.000000323835 * BF48 - 0.000000140343 * BF49
- 2.42051E-12 * BF50

MARS Model for PCC Thickness – Cracked Slabs Model

BF1 = Max(0, DOWEL_DIAMETER - 1.5)
BF2 = Max(0, 1.5 - DOWEL_DIAMETER)
BF4 = Max(0, 10.4 - slabs_cracked) * BF2
BF5 = Max(0, AADTT - 2500) * BF2
BF6 = Max(0, 2500 - AADTT) * BF2
BF7 = Max(0, AADTT - 2500) * BF4
BF8 = Max(0, 2500 - AADTT) * BF4
BF10 = Max(0, 42 - slabs_cracked) * BF6
BF11 = Max(0, dga_modulus - 30000) * BF10
BF12 = Max(0, 30000 - dga_modulus) * BF10
BF13 = Max(0, Subgrade_modulus - 9000) * BF10
BF14 = Max(0, 9000 - Subgrade_modulus) * BF10
BF15 = Max(0, DGA_Thickness - 8) * BF10
BF16 = Max(0, 8 - DGA_Thickness) * BF10
BF17 = Max(0, Subgrade_modulus - 12000) * BF16
BF18 = Max(0, 12000 - Subgrade_modulus) * BF16
BF21 = Max(0, dga_modulus - 35000) * BF8
BF22 = Max(0, 35000 - dga_modulus) * BF8
BF23 = Max(0, DGA_Thickness - 14) * BF8
BF24 = Max(0, 14 - DGA_Thickness) * BF8
BF25 = Max(0, Subgrade_modulus - 7500) * BF8
BF26 = Max(0, 7500 - Subgrade_modulus) * BF8
BF27 = Max(0, dga_modulus - 30000) * BF13
BF28 = Max(0, 30000 - dga_modulus) * BF13
BF32 = Max(0, 25000 - dga_modulus) * BF23
BF33 = Max(0, Subgrade_modulus - 9000) * BF23
BF35 = Max(0, DGA_Thickness - 14) * BF10
BF38 = Max(0, 10500 - Subgrade_modulus) * BF35
BF42 = Max(0, 35000 - dga_modulus) * BF25
BF46 = Max(0, 25000 - dga_modulus) * BF33
BF47 = Max(0, DGA_Thickness - 14) * BF25
BF48 = Max(0, 14 - DGA_Thickness) * BF25
BF50 = Max(0, 25000 - dga_modulus) * BF47
BF52 = Max(0, 8 - DGA_Thickness) * BF28
BF54 = Max(0, 25000 - dga_modulus) * BF38
BF55 = Max(0, dga_modulus - 25000) * BF16
BF57 = Max(0, Subgrade_modulus - 9000) * BF55
BF63 = Max(0, DGA_Thickness - 8) * BF22
BF64 = Max(0, 8 - DGA_Thickness) * BF22
BF66 = Max(0, 9000 - Subgrade_modulus) * BF64
BF67 = Max(0, Subgrade_modulus - 6000) * BF32
BF70 = Max(0, DGA_Thickness - 6) * BF12
BF74 = Max(0, dga_modulus - 35000) * BF15

BF76 = Max(0, dga_modulus - 30000) * BF15
BF77 = Max(0, 30000 - dga_modulus) * BF15
BF78 = Max(0, dga_modulus - 35000) * BF26
BF79 = Max(0, 35000 - dga_modulus) * BF26
BF81 = Max(0, DGA_Thickness - 6) * BF21
BF82 = Max(0, dga_modulus - 35000) * BF2
BF84 = Max(0, slabs_cracked - 0.8) * BF82
BF85 = Max(0, 0.8 - slabs_cracked) * BF82
BF87 = Max(0, 2500 - AADTT) * BF85
BF88 = Max(0, DGA_Thickness - 8) * BF87
BF89 = Max(0, 8 - DGA_Thickness) * BF87
BF90 = Max(0, Subgrade_modulus - 6000) * BF87
BF92 = Max(0, 14 - DGA_Thickness) * BF90
BF93 = Max(0, dga_modulus - 35000) * BF5
BF94 = Max(0, 35000 - dga_modulus) * BF5
BF98 = Max(0, dga_modulus - 35000) * BF16
BF102 = Max(0, Subgrade_modulus - 6000) * BF7
BF104 = Max(0, 8 - DGA_Thickness) * BF102
BF105 = Max(0, DGA_Thickness - 8) * BF25
BF106 = Max(0, 8 - DGA_Thickness) * BF25
BF108 = Max(0, 12000 - Subgrade_modulus) * BF12
BF110 = Max(0, 8 - DGA_Thickness) * BF108
BF111 = Max(0, dga_modulus - 30000) * BF106
BF112 = Max(0, 30000 - dga_modulus) * BF106
BF113 = Max(0, Subgrade_modulus - 12000) * BF64
BF116 = Max(0, 8 - DGA_Thickness) * BF14
BF118 = Max(0, 8 - DGA_Thickness) * BF26
BF119 = Max(0, dga_modulus - 35000) * BF116
BF121 = Max(0, dga_modulus - 30000) * BF116
BF125 = Max(0, dga_modulus - 20000) * BF14

PCC_Thickness_cracked_slabs_model = 12 + 8 * BF1 - 16.0084 * BF2 + 0.777706 *
BF4 + 0.000561436 * BF5 - 0.00399322 * BF6 - 0.0000517686 * BF7
+ 0.00975634 * BF8 - 0.00179237 * BF10 - 0.0000000236489 * BF11
- 0.0000000150961 * BF12 - 0.0000000742646 * BF13 + 0.0000000695627 * BF14
- 0.0000529468 * BF15 + 0.000313783 * BF16 + 0.000000050279 * BF17
- 0.0000000514886 * BF18 + 0.000000723337 * BF21 - 0.0000000877283 * BF22
- 0.000362733 * BF24 + 0.00000148834 * BF25 - 0.000000311256 * BF26
- 0.000000000000415257 * BF27 + 0.000000000000883794 * BF28
+ 0.0000000735999 * BF32 + 0.0000878104 * BF35- 0.00000000000301694 * BF42
+ 0.0000000000335331 * BF46 + 0.000000195558 * BF47 - 0.000000195475 * BF48
- 0.0000000000178492 * BF50 + 0.0000000000351746 * BF52
- 0.0000000000401942 * BF54 - 0.000000000000914363 * BF57

- 0.0000000292792 * BF63 + 0.00000000462425 * BF64 - 0.0000000000194076 * BF66
- 0.0000000000157642 * BF67 + 0.0000000192396 * BF70 + 0.0000000835255 * BF74
- 0.00000000707161 * BF76 - 0.0000000121252 * BF77
- 0.00000000000510014 * BF78 + 0.00000000000210593 * BF79
- 0.00000032558 * BF81 - 0.0000883434 * BF82 + 0.00000162644 * BF84
+ 0.00011289 * BF85 + 0.000000308624 * BF87 + 0.000000215213 * BF88
- 0.000000462981 * BF89 + 0.0000000000348936 * BF92 + 0.0000000104462 * BF93
+ 0.00000000203336 * BF94 - 0.0000000744051 * BF98
+ 0.000000000816965 * BF102 + 0.000000000335712 * BF104
- 0.000000195126 * BF105 + 0.00000000000537115 * BF110
+ 0.00000000000407579 * BF111 + 0.00000000000522829 * BF112
 - 0.0000000000134177 * BF113 + 0.0000000296485 * BF116
+ 0.000000172384 * BF118 + 0.00000000000456128 * BF119
- 0.0000000000394567 * BF121 + 0.000000000000674217 * BF125

MARS Model for PCC Thickness – Faulting Model

BF1 = Max(0, DOWEL_DIAMETER - 1.5)
BF2 = Max(0, 1.5 - DOWEL_DIAMETER)
BF3 = Max(0, faulting - 0.012) * BF2
BF4 = Max(0, 0.012 - faulting) * BF2
BF5 = Max(0, Subgrade_modulus - 9000) * BF4
BF6 = Max(0, 9000 - Subgrade_modulus) * BF4
BF8 = Max(0, 2500 - AADTT) * BF2
BF9 = Max(0, DGA_Thickness - 6) * BF2
BF10 = Max(0, faulting - 0.06) * BF2
BF12 = Max(0, faulting - 0.01) * BF8
BF15 = Max(0, DGA_Thickness - 6) * BF10
BF17 = Max(0, 7500 - AADTT) * BF9
BF18 = Max(0, Subgrade_modulus - 6000) * BF17
BF19 = Max(0, faulting - 0.013) * BF17
BF21 = Max(0, dga_modulus - 20000) * BF17
BF22 = Max(0, faulting - 0.088) * BF9
BF24 = Max(0, faulting - 0.063) * BF2
BF25 = Max(0, 0.063 - faulting) * BF2
BF28 = Max(0, faulting - 0.052) * BF21
BF32 = Max(0, faulting - 0.058) * BF18
BF33 = Max(0, 0.058 - faulting) * BF18
BF34 = Max(0, faulting - 0.061) * BF17
BF37 = Max(0, 5000 - AADTT) * BF3
BF38 = Max(0, Subgrade_modulus - 6000) * BF37
BF39 = Max(0, DGA_Thickness - 10) * BF2
BF40 = Max(0, 10 - DGA_Thickness) * BF2
BF41 = Max(0, dga_modulus - 25000) * BF38
BF43 = Max(0, Subgrade_modulus - 9000) * BF25
BF44 = Max(0, 9000 - Subgrade_modulus) * BF25
BF45 = Max(0, AADTT - 499.999) * BF44
BF46 = Max(0, faulting - 0.013) * BF8
BF48 = Max(0, Subgrade_modulus - 6000) * BF19
BF50 = Max(0, 9000 - Subgrade_modulus) * BF37
BF51 = Max(0, DGA_Thickness - 10) * BF50
BF53 = Max(0, DGA_Thickness - 10) * BF41
BF54 = Max(0, 10 - DGA_Thickness) * BF41
BF55 = Max(0, faulting - 0.057) * BF17
BF57 = Max(0, faulting - 0.014) * BF8
BF58 = Max(0, 0.014 - faulting) * BF8
BF59 = Max(0, faulting - 0.088) * BF2
BF60 = Max(0, 0.088 - faulting) * BF2
BF61 = Max(0, AADTT - 499.999) * BF43
BF63 = Max(0, 9000 - Subgrade_modulus) * BF58

BF64 = Max(0, DGA_Thickness - 6) * BF58
BF65 = Max(0, dga_modulus - 20000) * BF33
BF66 = Max(0, AADTT - 2500) * BF60
BF69 = Max(0, 7500 - Subgrade_modulus) * BF46
BF70 = Max(0, dga_modulus - 20000) * BF69
BF71 = Max(0, dga_modulus - 20000) * BF50
BF72 = Max(0, faulting - 0.015) * BF40
BF74 = Max(0, DGA_Thickness - 8) * BF71
BF75 = Max(0, 8 - DGA_Thickness) * BF71
BF76 = Max(0, DGA_Thickness - 12) * BF50
BF78 = Max(0, DGA_Thickness - 14) * BF60
BF79 = Max(0, 14 - DGA_Thickness) * BF60
BF80 = Max(0, Subgrade_modulus - 10500) * BF37
BF81 = Max(0, 10500 - Subgrade_modulus) * BF37
BF83 = Max(0, 8 - DGA_Thickness) * BF81
BF84 = Max(0, faulting - 0.009) * BF21
BF86 = Max(0, faulting - 0.011) * BF8
BF88 = Max(0, dga_modulus - 20000) * BF78
BF89 = Max(0, Subgrade_modulus - 7500) * BF78
BF92 = Max(0, Subgrade_modulus - 7500) * BF79
BF97 = Max(0, Subgrade_modulus - 6000) * BF55
BF98 = Max(0, Subgrade_modulus - 7500) * BF37
BF99 = Max(0, 7500 - Subgrade_modulus) * BF37
BF100 = Max(0, DGA_Thickness - 8) * BF99
BF101 = Max(0, 8 - DGA_Thickness) * BF99
BF102 = Max(0, DGA_Thickness - 10) * BF99
BF106 = Max(0, dga_modulus - 30000) * BF51
BF108 = Max(0, Subgrade_modulus - 10500) * BF88
BF109 = Max(0, 10500 - Subgrade_modulus) * BF88
BF110 = Max(0, DGA_Thickness - 6) * BF4
BF111 = Max(0, Subgrade_modulus - 6000) * BF110
BF112 = Max(0, Subgrade_modulus - 10500) * BF79
BF116 = Max(0, dga_modulus - 20000) * BF111
BF117 = Max(0, dga_modulus - 20000) * BF112
BF118 = Max(0, dga_modulus - 20000) * BF37
BF120 = Max(0, 8 - DGA_Thickness) * BF118
BF122 = Max(0, 10500 - Subgrade_modulus) * BF120
BF123 = Max(0, DGA_Thickness - 12) * BF43
BF125 = Max(0, dga_modulus - 20000) * BF44

PCC_Thickness_faulting_model = 12 + 8.00001 * BF1 - 139.097 * BF2 + 4187.13 * BF3
+ 1157.47 * BF4 - 0.156667 * BF5 + 0.730625 * BF6 + 0.0531114 * BF8
+ 3.67628 * BF9 + 1914.55 * BF10 + 1.89596 * BF12 - 141.805 * BF15
- 0.000651119 * BF17 + 0.0000000500829 * BF18 + 0.00652995 * BF19

+ 140.192 * BF22 - 9589.61 * BF24 - 0.000000612097 * BF28
+ 0.00000645222 * BF32 - 0.0469388 * BF34 - 0.697294 * BF37
- 0.0000413693 * BF38 + 0.343742 * BF39 - 0.0331922 * BF43 + 0.0547768 * BF44
- 0.000232973 * BF45 - 3.47866 * BF46 - 0.00000116864 * BF48
- 0.000000000110622 * BF53 + 0.0000000000486958 * BF54 + 0.0454641 * BF55
- 3.15212 * BF57 + 3500.17 * BF59 + 0.0000640875 * BF61 - 0.000235981 * BF63
+ 0.199483 * BF64   + 0.0000000000813698 * BF65 - 2.04324 * BF66
- 0.0000000218102 * BF70 - 0.000000000456387 * BF71 - 3.30835 * BF72
+ 0.000000000189128 * BF74 + 0.00000000144799 * BF75 + 0.00000247006 * BF76
- 0.00000877569 * BF80 + 0.0000184677 * BF83 + 0.000000294459 * BF84
+ 1.19997 * BF86 - 0.00318687 * BF89 + 0.00326807 * BF92 - 0.00000502213 * BF97
+ 0.0000529829 * BF98 - 0.0000341075 * BF100 - 0.0000245216 * BF101
+ 0.0000332208 * BF102 - 0.000000000167578 * BF106 + 0.000000295593 * BF108
+ 0.000000195436 * BF109 - 584.217 * BF110 + 0.0116692 * BF111
 - 0.000000469721 * BF116 + 0.0000000431949 * BF117
- 0.000000000889326 * BF122 - 0.00252853 * BF123
- 0.000000343101 * BF125

MARS Model for PCC Thickness –IRI Model

BF1 = Max(0, DOWEL_DIAMETER - 1.5)

BF2 = Max(0, 1.5 - DOWEL_DIAMETER)

BF4 = Max(0, 5000 - AADTT) * BF2

BF5 = Max(0, IRI - 120) * BF2

BF6 = Max(0, 120 - IRI) * BF2

BF7 = Max(0, IRI - 78) * BF4

BF8 = Max(0, 78 - IRI) * BF4

BF9 = Max(0, Subgrade_modulus - 9000) * BF8

BF10 = Max(0, 9000 - Subgrade_modulus) * BF8

BF11 = Max(0, DGA_Thickness - 8) * BF8

BF12 = Max(0, 8 - DGA_Thickness) * BF8

BF13 = Max(0, DGA_Thickness - 8) * BF9

BF14 = Max(0, 8 - DGA_Thickness) * BF9

BF15 = Max(0, AADTT - 2500) * BF6

BF16 = Max(0, 2500 - AADTT) * BF6

BF17 = Max(0, IRI - 109.4) * BF2

BF18 = Max(0, 109.4 - IRI) * BF2

BF19 = Max(0, IRI - 102.5) * BF2

BF20 = Max(0, 102.5 - IRI) * BF2

BF21 = Max(0, dga_modulus - 30000) * BF14

BF22 = Max(0, 30000 - dga_modulus) * BF14

BF23 = Max(0, DGA_Thickness - 8) * BF6

BF24 = Max(0, 8 - DGA_Thickness) * BF6

BF25 = Max(0, Subgrade_modulus - 10500) * BF6

BF26 = Max(0, 10500 - Subgrade_modulus) * BF6

BF27 = Max(0, IRI - 105.8) * BF2

BF28 = Max(0, 105.8 - IRI) * BF2

BF29 = Max(0, dga_modulus - 25000) * BF28

BF30 = Max(0, 25000 - dga_modulus) * BF28

BF31 = Max(0, dga_modulus - 25000) * BF11

BF32 = Max(0, 25000 - dga_modulus) * BF11

BF33 = Max(0, Subgrade_modulus - 9000) * BF32

BF34 = Max(0, 9000 - Subgrade_modulus) * BF32

BF35 = Max(0, Subgrade_modulus - 10500) * BF32

BF37 = Max(0, DGA_Thickness - 6) * BF30

BF38 = Max(0, AADTT - 499.999) * BF20

BF39 = Max(0, Subgrade_modulus - 9000) * BF24

BF40 = Max(0, 9000 - Subgrade_modulus) * BF24

BF41 = Max(0, Subgrade_modulus - 9000) * BF16

BF42 = Max(0, 9000 - Subgrade_modulus) * BF16

BF43 = Max(0, DGA_Thickness - 8) * BF41

BF44 = Max(0, 8 - DGA_Thickness) * BF41

BF45 = Max(0, Subgrade_modulus - 9000) * BF37

BF47 = Max(0, dga_modulus - 30000) * BF44
BF48 = Max(0, 30000 - dga_modulus) * BF44
BF49 = Max(0, DGA_Thickness - 12) * BF29
BF50 = Max(0, 12 - DGA_Thickness) * BF29
BF51 = Max(0, Subgrade_modulus - 10500) * BF29
BF52 = Max(0, 10500 - Subgrade_modulus) * BF29
BF53 = Max(0, DGA_Thickness - 8) * BF28
BF54 = Max(0, 8 - DGA_Thickness) * BF28
BF55 = Max(0, dga_modulus - 25000) * BF38
BF57 = Max(0, Subgrade_modulus - 12000) * BF12
BF58 = Max(0, 12000 - Subgrade_modulus) * BF12
BF59 = Max(0, Subgrade_modulus - 12000) * BF54
BF61 = Max(0, DGA_Thickness - 8) * BF52
BF62 = Max(0, 8 - DGA_Thickness) * BF52
BF63 = Max(0, dga_modulus - 35000) * BF4
BF65 = Max(0, DGA_Thickness - 14) * BF16
BF66 = Max(0, 14 - DGA_Thickness) * BF16
BF67 = Max(0, dga_modulus - 20000) * BF23
BF68 = Max(0, Subgrade_modulus - 9000) * BF38
BF69 = Max(0, 9000 - Subgrade_modulus) * BF38
BF70 = Max(0, Subgrade_modulus - 7500) * BF20
BF76 = Max(0, dga_modulus - 35000) * BF14
BF78 = Max(0, Subgrade_modulus - 9000) * BF28
BF79 = Max(0, 9000 - Subgrade_modulus) * BF28
BF81 = Max(0, dga_modulus - 35000) * BF44
BF83 = Max(0, DGA_Thickness - 6) * BF55
BF85 = Max(0, 2500 - AADTT) * BF17
BF86 = Max(0, Subgrade_modulus - 10500) * BF31
BF88 = Max(0, DGA_Thickness - 10) * BF51
BF89 = Max(0, 10 - DGA_Thickness) * BF51
BF90 = Max(0, AADTT - 499.999) * BF88
BF92 = Max(0, 12 - DGA_Thickness) * BF10
BF93 = Max(0, Subgrade_modulus - 9000) * BF66
BF94 = Max(0, 9000 - Subgrade_modulus) * BF66
BF95 = Max(0, DGA_Thickness - 8) * BF18
BF97 = Max(0, dga_modulus - 25000) * BF9
BF98 = Max(0, 25000 - dga_modulus) * BF9
BF99 = Max(0, DGA_Thickness - 14) * BF98
BF100 = Max(0, 14 - DGA_Thickness) * BF98
BF102 = Max(0, 25000 - dga_modulus) * BF53
BF103 = Max(0, dga_modulus - 25000) * BF78
BF104 = Max(0, 25000 - dga_modulus) * BF78
BF105 = Max(0, Subgrade_modulus - 10500) * BF102
BF106 = Max(0, 10500 - Subgrade_modulus) * BF102

BF107 = Max(0, Subgrade_modulus - 7500) * BF54
BF109 = Max(0, DGA_Thickness - 14) * BF8
BF110 = Max(0, 14 - DGA_Thickness) * BF8
BF112 = Max(0, 25000 - dga_modulus) * BF109
BF113 = Max(0, Subgrade_modulus - 7500) * BF110
BF114 = Max(0, 7500 - Subgrade_modulus) * BF110
BF115 = Max(0, Subgrade_modulus - 6000) * BF112
BF116 = Max(0, Subgrade_modulus - 9000) * BF102
BF118 = Max(0, DGA_Thickness - 12) * BF42
BF120 = Max(0, Subgrade_modulus - 7500) * BF53
BF121 = Max(0, 7500 - Subgrade_modulus) * BF53
BF123 = Max(0, 25000 - dga_modulus) * BF65
BF124 = Max(0, Subgrade_modulus - 6000) * BF123
BF125 = Max(0, dga_modulus - 20000) * BF114

PCC_Thickness_IRI_model = 12 + 8 * BF1 - 2.40469 * BF2 - 0.00439067 * BF4
- 0.116775 * BF5 + 0.208497 * BF6 + 0.0000266714 * BF7 + 0.00145557 * BF8
- 0.000000157493 * BF10 + 0.0000683124 * BF11 - 0.000251866 * BF12
+ 0.0000000366777 * BF13 - 0.000000269348 * BF14 - 0.0000224896 * BF15
+ 0.759073 * BF17 - 1.37644 * BF19 + 0.0000000000511822 * BF21
+ 0.0000000000510271 * BF22 + 0.030521 * BF24 - 0.00000697739 * BF25
+ 0.00000657316 * BF26 + 0.734871 * BF27 - 0.00000948029 * BF29
+ 0.0000000084211 * BF31 - 0.0000000301595 * BF32 - 0.0000000000166428 * BF33
+ 0.0000000000152295 * BF34 - 0.0000000000275004 * BF35 + 0.000709413 * BF38
- 0.00000487643 * BF39 + 0.00000598955 * BF40 + 0.0000000183886 * BF41
- 0.0000000312566 * BF42 - 0.00000000304888 * BF43 + 0.0000000146612 * BF44
- 0.0000000035493 * BF45 - 0.00000000000213056 * BF47
- 0.0000000000018318 * BF48- 0.00000362812 * BF49 + 0.00000154333 * BF50
- 0.00000000280686 * BF51 + 0.000000000703195 * BF52 + 0.0585659 * BF53
- 0.04907 * BF54 - 0.000000247202 * BF57 + 0.0000000708143 * BF58
+ 0.0000203911 * BF59 + 0.00000000192606 * BF61 - 0.00000000031992 * BF62
- 0.00000000461991 * BF63 - 0.00000440599 * BF66 - 0.000000402643 * BF67
+ 0.0000000950378 * BF68 - 0.000000191137 * BF69 - 0.0000335145 * BF70
- 0.0000000000540143 * BF76 + 0.0000978433 * BF79 + 0.0000000000020334 * BF81
+ 0.00000000261049 * BF83 - 0.0000600196 * BF85 + 0.00000000000328632 * BF86
- 0.00000000152508 * BF88 + 0.0000000007801 * BF89
+ 0.00000000000103828 * BF90 + 0.0000000922468 * BF92
- 0.00000000412573 * BF93 - 0.00000000115396 * BF94 - 0.0788597 * BF95
+ 0.00000000000851431 * BF97 + 0.00000000024263 * BF98
+ 0.0000000000797173 * BF99 - 0.0000000000438361 * BF100
+ 0.00000943053 * BF102 - 0.000000000954044 * BF103 + 0.0000000121601 * BF104
+ 0.0000000063697 * BF105 - 0.00000000258842 * BF106 + 0.0000193924 * BF107
- 0.0000000495256 * BF112 + 0.0000000293391 * BF113 + 0.0000000698539 * BF114
- 0.0000000000289423 * BF115 - 0.00000000329574 * BF116

- 0.00000000230475 * BF118 - 0.00000611177 * BF120 + 0.0000105614 * BF121
+ 0.00000000347368 * BF123 + 0.00000000000943868 * BF124
– 0.0000000000210976 * BF125

MARS Model for PCC Slab Cracking

BF1 = Max(0, pcc_thickness_for_cracking - 8)
BF2 = Max(0, 8 - pcc_thickness_for_cracking)
BF3 = Max(0, Subgrade_modulus - 9000) * BF2
BF4 = Max(0, 9000 - Subgrade_modulus) * BF2
BF5 = Max(0, DOWEL_DIAMETER - 1.5) * BF1
BF6 = Max(0, 1.5 - DOWEL_DIAMETER) * BF1
BF7 = Max(0, dga_modulus - 20000) * BF2
BF8 = Max(0, DGA_Thickness - 8) * BF2
BF9 = Max(0, 8 - DGA_Thickness) * BF2
BF10 = Max(0, AADTT - 2500)
BF11 = Max(0, 2500 - AADTT)
BF13 = Max(0, 10 - pcc_thickness_for_cracking) * BF11
BF14 = Max(0, Subgrade_modulus - 12000) * BF9
BF15 = Max(0, 12000 - Subgrade_modulus) * BF9
BF16 = Max(0, dga_modulus - 30000) * BF9
BF17 = Max(0, 30000 - dga_modulus) * BF9
BF18 = Max(0, Subgrade_modulus - 6000) * BF17
BF19 = Max(0, Subgrade_modulus - 6000) * BF16
BF20 = Max(0, dga_modulus - 25000) * BF8
BF21 = Max(0, 25000 - dga_modulus) * BF8
BF22 = Max(0, Subgrade_modulus - 10500) * BF21
BF23 = Max(0, 10500 - Subgrade_modulus) * BF21
BF24 = Max(0, pcc_thickness_for_cracking - 12) * BF10
BF25 = Max(0, 12 - pcc_thickness_for_cracking) * BF10
BF26 = Max(0, dga_modulus - 25000) * BF4
BF27 = Max(0, 25000 - dga_modulus) * BF4
BF28 = Max(0, DGA_Thickness - 6) * BF27
BF29 = Max(0, dga_modulus - 35000) * BF9
BF30 = Max(0, 35000 - dga_modulus) * BF9
BF31 = Max(0, Subgrade_modulus - 6000) * BF30
BF32 = Max(0, DGA_Thickness - 14) * BF2
BF33 = Max(0, 14 - DGA_Thickness) * BF2
BF34 = Max(0, Subgrade_modulus - 9000) * BF32
BF35 = Max(0, 9000 - Subgrade_modulus) * BF32
BF36 = Max(0, dga_modulus - 25000) * BF33
BF37 = Max(0, 25000 - dga_modulus) * BF33
BF38 = Max(0, DGA_Thickness - 14) * BF26
BF39 = Max(0, 14 - DGA_Thickness) * BF26
BF40 = Max(0, dga_modulus - 25000) * BF2
BF41 = Max(0, 25000 - dga_modulus) * BF2
BF43 = Max(0, 10500 - Subgrade_modulus) * BF37
BF44 = Max(0, Subgrade_modulus - 7500) * BF8
BF45 = Max(0, 7500 - Subgrade_modulus) * BF8

BF46 = Max(0, dga_modulus - 25000) * BF44
BF47 = Max(0, 25000 - dga_modulus) * BF44
BF48 = Max(0, Subgrade_modulus - 10500) * BF41
BF49 = Max(0, 10500 - Subgrade_modulus) * BF41
BF50 = Max(0, DGA_Thickness - 6) * BF49
BF51 = Max(0, DGA_Thickness - 6) * BF48
BF52 = Max(0, dga_modulus - 20000)
BF54 = Max(0, 10 - pcc_thickness_for_cracking) * BF52
BF55 = Max(0, AADTT - 499.999) * BF54
BF57 = Max(0, 8 - DGA_Thickness) * BF55
BF59 = Max(0, 9000 - Subgrade_modulus) * BF55
BF60 = Max(0, Subgrade_modulus - 6000) * BF25
BF61 = Max(0, Subgrade_modulus - 12000) * BF40
BF62 = Max(0, 12000 - Subgrade_modulus) * BF40
BF63 = Max(0, DGA_Thickness - 14) * BF62
BF64 = Max(0, 14 - DGA_Thickness) * BF62
BF65 = Max(0, Subgrade_modulus - 9000) * BF33
BF66 = Max(0, 9000 - Subgrade_modulus) * BF33
BF67 = Max(0, dga_modulus - 30000) * BF66
BF68 = Max(0, 30000 - dga_modulus) * BF66
BF69 = Max(0, dga_modulus - 30000) * BF65
BF70 = Max(0, 30000 - dga_modulus) * BF65
BF71 = Max(0, DGA_Thickness - 14) * BF40
BF75 = Max(0, dga_modulus - 30000) * BF2
BF76 = Max(0, 30000 - dga_modulus) * BF2
BF77 = Max(0, Subgrade_modulus - 12000) * BF75
BF78 = Max(0, 12000 - Subgrade_modulus) * BF75
BF79 = Max(0, DGA_Thickness - 8) * BF78
BF80 = Max(0, 8 - DGA_Thickness) * BF78
BF81 = Max(0, Subgrade_modulus - 12000) * BF20
BF83 = Max(0, DGA_Thickness - 14) * BF76
BF84 = Max(0, 14 - DGA_Thickness) * BF76
BF85 = Max(0, Subgrade_modulus - 12000) * BF84
BF87 = Max(0, Subgrade_modulus - 6000) * BF83
BF88 = Max(0, dga_modulus - 20000) * BF45
BF89 = Max(0, Subgrade_modulus - 7500) * BF76
BF91 = Max(0, DGA_Thickness - 14) * BF89
BF93 = Max(0, DGA_Thickness - 8) * BF59
BF94 = Max(0, 8 - DGA_Thickness) * BF59
BF95 = Max(0, dga_modulus - 20000) * BF25
BF96 = Max(0, dga_modulus - 35000) * BF33
BF97 = Max(0, 35000 - dga_modulus) * BF33
BF98 = Max(0, Subgrade_modulus - 12000) * BF97
BF99 = Max(0, 12000 - Subgrade_modulus) * BF97

BF103 = Max(0, 8 - DGA_Thickness) * BF25
BF104 = Max(0, dga_modulus - 30000) * BF44
BF107 = Max(0, 12000 - Subgrade_modulus) * BF2
BF109 = Max(0, 14 - DGA_Thickness) * BF107
BF110 = Max(0, AADTT - 5000) * BF6
BF111 = Max(0, 5000 - AADTT) * BF6
BF113 = Max(0, 8 - DGA_Thickness)
BF115 = Max(0, 10 - pcc_thickness_for_cracking) * BF113
BF116 = Max(0, AADTT - 499.999) * BF115
BF117 = Max(0, Subgrade_modulus - 9000) * BF116
BF118 = Max(0, 9000 - Subgrade_modulus) * BF116
BF119 = Max(0, Subgrade_modulus - 6000) * BF10
BF120 = Max(0, Subgrade_modulus - 7500)
BF121 = Max(0, 7500 - Subgrade_modulus)
BF123 = Max(0, 10 - pcc_thickness_for_cracking) * BF121
BF124 = Max(0, AADTT - 499.999) * BF123
BF125 = Max(0, dga_modulus - 20000) * BF124

PCC_Cracked_Slabs = 14.6624 - 3.66713 * BF1 + 0.117253 * BF3 - 0.118028 * BF4
+ 4.90679 * BF5 - 14.1614 * BF6 + 0.0018901 * BF7 + 34.5886 * BF8 + 55.9501 * BF9
+ 0.00000799156 * BF10 - 0.00348731 * BF13 + 0.0125831 * BF14 - 0.0129853 * BF15
- 0.00915779 * BF16 - 0.00826792 * BF17 + 0.00000203817 * BF18
+ 0.000000938835 * BF19 - 0.00551828 * BF20 + 0.00622824 * BF21
+ 0.000000222653 * BF22 - 0.000000169427 * BF23 - 0.00000657782 * BF24
+ 0.000000109247 * BF26 - 0.0000312328 * BF27 + 0.00000397559 * BF28
+ 0.000659606 * BF29 - 0.000000319722 * BF31 - 4.47092 * BF32
+ 0.020403 * BF34 - 0.0190629 * BF35 + 0.00267538 * BF36 - 0.000145568 * BF37
- 0.00000012066 * BF38 + 0.00000387636 * BF39 - 0.0135572 * BF40
- 0.00000219076 * BF43 - 0.0197147 * BF44 + 0.0290133 * BF45
+ 0.00000163706 * BF46 - 0.00000194414 * BF47 - 0.00000465619 * BF48
+ 0.0000222393 * BF49- 0.00000412209 * BF50 + 0.00000187371 * BF51
- 0.00000715928 * BF54 - 0.0000000637394 * BF55 + 0.0000000080685 * BF57
+ 0.0000000000101627 * BF59 + 0.00000000854844 * BF60 + 0.000000733293 * BF61
+ 0.00000989803 * BF62 + 0.0000017075 * BF63 - 0.00000180984 * BF64
- 0.019286 * BF65 - 0.00000375343 * BF67 + 0.00000378087 * BF68
- 0.000000138311 * BF69 + 0.000000108384 * BF70 - 0.00237743 * BF71
- 0.00285822 * BF75 - 0.000000648289 * BF77 + 0.0000000892147 * BF79
+ 0.00000275656 * BF80 - 0.00000175746 * BF81 - 0.00101639 * BF83
+ 0.000441566 * BF84 + 0.000000296903 * BF85 + 0.000000694885 * BF87
- 0.00000174488 * BF88 - 0.000000831263 * BF91 - 0.000000000000849999 * BF93
- 0.0000000000253515 * BF94 - 0.00000000208855 * BF95 + 0.000168074 * BF96
- 0.00000024466 * BF98 - 0.0000000436689 * BF99 + 0.0000134748 * BF103
+ 0.000000109378 * BF104 + 0.00145558 * BF109 + 0.000335862 * BF110
 - 0.000101392 * BF111 + 0.0488656 * BF115 + 0.000362671 * BF116

- 0.000000029367 * BF117 + 0.0000000644746 * BF118 + 0.00000000137711 * BF119
- 0.00000794118 * BF120 + 0.0000555708 * BF123 + 0.000000441691 * BF124
- 0.0000000000235488 * BF125

MARS Model for PCC Faulting

BF1 = Max(0, AADTT - 5000)
BF2 = Max(0, 5000 - AADTT)
BF3 = Max(0, PCC_Thickness_for_Faulting - 10)
BF4 = Max(0, 10 - PCC_Thickness_for_Faulting)
BF5 = Max(0, PCC_Thickness_for_Faulting - 12) * BF2
BF6 = Max(0, 12 - PCC_Thickness_for_Faulting) * BF2
BF7 = Max(0, PCC_Thickness_for_Faulting - 12) * BF1
BF8 = Max(0, 12 - PCC_Thickness_for_Faulting) * BF1
BF9 = Max(0, DOWEL_DIAMETER - 1.25) * BF3
BF10 = Max(0, AADTT - 15000) * BF3
BF11 = Max(0, 15000 - AADTT) * BF3
BF12 = Max(0, AADTT - 15000) * BF9
BF14 = Max(0, DGA_Thickness - 6) * BF1
BF15 = Max(0, PCC_Thickness_for_Faulting - 12) * BF14
BF16 = Max(0, 12 - PCC_Thickness_for_Faulting) * BF14
BF17 = Max(0, Subgrade_modulus - 9000) * BF1
BF18 = Max(0, 9000 - Subgrade_modulus) * BF1
BF19 = Max(0, Subgrade_modulus - 6000) * BF4
BF20 = Max(0, AADTT - 2500)
BF21 = Max(0, 2500 - AADTT)
BF22 = Max(0, PCC_Thickness_for_Faulting - 12) * BF21
BF23 = Max(0, 12 - PCC_Thickness_for_Faulting) * BF21
BF24 = Max(0, DGA_Thickness - 6)
BF25 = Max(0, AADTT - 7500)
BF26 = Max(0, 7500 - AADTT)
BF27 = Max(0, PCC_Thickness_for_Faulting - 8) * BF26
BF28 = Max(0, 8 - PCC_Thickness_for_Faulting) * BF26
BF30 = Max(0, AADTT - 10000) * BF24
BF31 = Max(0, 10000 - AADTT) * BF24
BF32 = Max(0, Subgrade_modulus - 7500) * BF3
BF33 = Max(0, 7500 - Subgrade_modulus) * BF3
BF34 = Max(0, PCC_Thickness_for_Faulting - 8) * BF24
BF35 = Max(0, 8 - PCC_Thickness_for_Faulting) * BF24
BF36 = Max(0, AADTT - 15000) * BF34
BF38 = Max(0, dga_modulus - 20000) * BF24
BF39 = Max(0, AADTT - 5000) * BF32
BF40 = Max(0, 5000 - AADTT) * BF32
BF42 = Max(0, 20000 - AADTT) * BF24
BF43 = Max(0, Subgrade_modulus - 7500) * BF9
BF44 = Max(0, 7500 - Subgrade_modulus) * BF9
BF45 = Max(0, DGA_Thickness - 6) * BF23
BF48 = Max(0, Subgrade_modulus - 9000) * BF25

BF49 = Max(0, 9000 - Subgrade_modulus) * BF25
BF50 = Max(0, PCC_Thickness_for_Faulting - 10) * BF38
BF51 = Max(0, 10 - PCC_Thickness_for_Faulting) * BF38
BF52 = Max(0, Subgrade_modulus - 10500) * BF26
BF53 = Max(0, 10500 - Subgrade_modulus) * BF26
BF55 = Max(0, 12 - DGA_Thickness) * BF25
BF57 = Max(0, 1.5 - DOWEL_DIAMETER) * BF53
BF59 = Max(0, 10500 - Subgrade_modulus) * BF23
BF60 = Max(0, AADTT - 2500) * BF38
BF61 = Max(0, 2500 - AADTT) * BF38
BF62 = Max(0, AADTT - 2500) * BF44
BF63 = Max(0, 2500 - AADTT) * BF44
BF65 = Max(0, 5000 - AADTT) * BF43
BF66 = Max(0, DOWEL_DIAMETER - 1.5) * BF31
BF67 = Max(0, 1.5 - DOWEL_DIAMETER) * BF31
BF68 = Max(0, AADTT - 10000) * BF3
BF69 = Max(0, 10000 - AADTT) * BF3
BF70 = Max(0, DOWEL_DIAMETER - 1.25) * BF69
BF71 = Max(0, AADTT - 20000) * BF3
BF73 = Max(0, AADTT - 20000) * BF9
BF75 = Max(0, DGA_Thickness - 14) * BF8
BF77 = Max(0, PCC_Thickness_for_Faulting - 8) * BF61
BF78 = Max(0, 8 - PCC_Thickness_for_Faulting) * BF61
BF79 = Max(0, Subgrade_modulus - 12000) * BF38
BF81 = Max(0, Subgrade_modulus - 6000) * BF35
BF84 = Max(0, Subgrade_modulus - 7500) * BF6
BF85 = Max(0, 7500 - Subgrade_modulus) * BF6
BF86 = Max(0, PCC_Thickness_for_Faulting - 12) * BF25
BF88 = Max(0, AADTT - 5000) * BF33
BF89 = Max(0, 5000 - AADTT) * BF33
BF90 = Max(0, DOWEL_DIAMETER - 1.25) * BF88
BF91 = Max(0, Subgrade_modulus - 6000) * BF24
BF92 = Max(0, PCC_Thickness_for_Faulting - 12) * BF38
BF94 = Max(0, Subgrade_modulus - 10500) * BF12
BF95 = Max(0, 10500 - Subgrade_modulus) * BF12
BF97 = Max(0, 30000 - dga_modulus) * BF4
BF98 = Max(0, dga_modulus - 25000) * BF1
BF99 = Max(0, 25000 - dga_modulus) * BF1
BF100 = Max(0, DOWEL_DIAMETER - 1.5) * BF24
BF101 = Max(0, 1.5 - DOWEL_DIAMETER) * BF24
BF103 = Max(0, 7500 - Subgrade_modulus) * BF101
BF104 = Max(0, DGA_Thickness - 10) * BF8
BF105 = Max(0, 10 - DGA_Thickness) * BF8
BF106 = Max(0, dga_modulus - 20000) * BF25

BF107 = Max(0, DGA_Thickness - 12) * BF57
BF108 = Max(0, 12 - DGA_Thickness) * BF57
BF109 = Max(0, Subgrade_modulus - 7500) * BF24
BF112 = Max(0, 5000 - AADTT) * BF109
BF114 = Max(0, 8 - PCC_Thickness_for_Faulting) * BF57
BF115 = Max(0, Subgrade_modulus - 9000) * BF42
BF118 = Max(0, 2500 - AADTT) * BF91
BF119 = Max(0, DOWEL_DIAMETER - 1.5) * BF118
BF120 = Max(0, 1.5 - DOWEL_DIAMETER) * BF118
BF122 = Max(0, 7500 - Subgrade_modulus) * BF105
BF123 = Max(0, Subgrade_modulus - 10500) * BF2
BF125 = Max(0, AADTT - 499.999) * BF97

PCC_Faulting = 0.0983638 + 0.0000262045 * BF1 - 0.000028124 * BF2
- 0.110532 * BF3 - 0.00893544 * BF4 - 0.0000074887 * BF5 + 0.0000053497 * BF6
+ 0.0000080921 * BF7 - 0.00000719383 * BF8 + 0.0228004 * BF9
- 0.00000806521 * BF10 + 0.00000728087 * BF11 + 0.00000135794 * BF12
+ 0.0000000285137 * BF14 - 0.00000000177984 * BF15 + 0.0000000387202 * BF16
- 0.0000000000269618 * BF17 + 0.000000000123853 * BF18 - 0.000000381604 * BF19
- 0.00000220038 * BF20 + 0.000000969738 * BF22 - 0.00000461909 * BF23
- 0.0011575 * BF24 - 0.00000396673 * BF25 + 0.000000716851 * BF27
- 0.00000124292 * BF28 - 0.0000000423733 * BF30 + 0.0000000625647 * BF31
- 0.000000203818 * BF32 + 0.000000565497 * BF33 + 0.000123208 * BF34
- 0.0001214 * BF35 + 0.00000000158978 * BF36 - 0.0000000104651 * BF38
- 0.00000000000869474 * BF39 + 0.00000000013477 * BF40
+ 0.000000348852 * BF43 - 0.000000396989 * BF44 + 0.0000000492112 * BF45
+ 0.0000000000442031 * BF48 - 0.000000000139407 * BF49
+ 0.0000000030188 * BF50 - 0.00000000203447 * BF51 - 0.0000000000360348 * BF52
+ 0.000000000081403 * BF53 - 0.00000000360377 * BF55
+ 0.000000000190888 * BF57 - 0.0000000000434437 * BF59
- 0.00000000000137599 * BF60 + 0.00000000000536806 * BF61
- 0.000000000202033 * F62 + 0.000000000173662 * BF63
- 0.000000000189529 * BF65 - 0.0000000982528 * BF66 + 0.000000170595 * BF67
- 0.00000102789 * BF68 + 0.00000189733 * BF70 - 0.000000433917 * BF71
+ 0.000000735276 * BF73 - 0.0000000223251 * BF75 - 0.00000000000803453 * BF77
+ 0.00000000000149875 * BF78 + 0.000000000000635453 * BF79
+ 0.00000000851328 * BF81 + 0.0000000000627669 * BF84
- 0.0000000000529592 * BF85 - 0.000000349767 * BF86 - 0.000000000145754 * BF89
+ 0.000000000226749 * BF90 + 0.0000000214037 * BF91 - 0.00000000153384 * BF92
+ 0.0000000000112727 * BF94 - 0.0000000000456597 * BF95
+ 0.00000000927464 * BF97 - 0.0000000000441278 * BF98
+ 0.00000000000553462 * BF99 + 0.000173139 * BF100 - 0.00155742 * BF101
+ 0.000000175176 * BF103 - 0.000000014112 * BF104
+ 0.0000000000479305 * BF106 - 0.000000000025096 * BF107

+ 0.0000000000110042 * BF108 - 0.0000000195429 * BF109
- 0.00000000000406104 * BF112 + 0.000000000129163 * BF114
+ 0.000000000000408028 * BF115 + 0.00000000000794811 * BF118
- 0.0000000000211958 * BF119 - 0.0000000000311629 * F120
+ 0.0000000000514744 * BF122 - 0.0000000000801253 * BF123
+ 0.00000000000634202 * BF125

MARS Model for PCC IRI
BF1 = Max(0, DOWEL_DIAMETER - 1.5)
BF2 = Max(0, 1.5 - DOWEL_DIAMETER)
BF3 = Max(0, AADTT - 7500)
BF4 = Max(0, 7500 - AADTT)
BF5 = Max(0, pcc_thickness_for_IRI - 8) * BF4
BF6 = Max(0, 8 - pcc_thickness_for_IRI) * BF4
BF7 = Max(0, pcc_thickness_for_IRI - 6) * BF2
BF8 = Max(0, AADTT - 2500) * BF2
BF9 = Max(0, 2500 - AADTT) * BF2
BF10 = Max(0, Subgrade_modulus - 9000) * BF6
BF11 = Max(0, 9000 - Subgrade_modulus) * BF6
BF13 = Max(0, 12 - pcc_thickness_for_IRI) * BF3
BF14 = Max(0, dga_modulus - 20000) * BF6
BF15 = Max(0, DGA_Thickness - 8) * BF2
BF16 = Max(0, 8 - DGA_Thickness) * BF2
BF17 = Max(0, AADTT - 5000) * BF7
BF18 = Max(0, 5000 - AADTT) * BF7
BF19 = Max(0, DGA_Thickness - 8) * BF6
BF20 = Max(0, 8 - DGA_Thickness) * BF6
BF21 = Max(0, DGA_Thickness - 6) * BF3
BF22 = Max(0, Subgrade_modulus - 9000) * BF3
BF23 = Max(0, 9000 - Subgrade_modulus) * BF3
BF24 = Max(0, Subgrade_modulus - 12000) * BF20
BF25 = Max(0, 12000 - Subgrade_modulus) * BF20
BF26 = Max(0, dga_modulus - 30000) * BF20
BF27 = Max(0, 30000 - dga_modulus) * BF20
BF28 = Max(0, dga_modulus - 30000) * BF25
BF29 = Max(0, 30000 - dga_modulus) * BF25
BF31 = Max(0, AADTT - 15000) * BF1
BF33 = Max(0, Subgrade_modulus - 6000) * BF27
BF34 = Max(0, Subgrade_modulus - 6000) * BF26
BF35 = Max(0, Subgrade_modulus - 9000) * BF19
BF36 = Max(0, 9000 - Subgrade_modulus) * BF19
BF37 = Max(0, dga_modulus - 20000) * BF7
BF38 = Max(0, DGA_Thickness - 14) * BF9
BF39 = Max(0, 14 - DGA_Thickness) * BF9
BF40 = Max(0, Subgrade_modulus - 9000) * BF18
BF41 = Max(0, 9000 - Subgrade_modulus) * BF18
BF43 = Max(0, 25000 - dga_modulus) * BF19
BF44 = Max(0, Subgrade_modulus - 9000) * BF43
BF45 = Max(0, 9000 - Subgrade_modulus) * BF43
BF46 = Max(0, Subgrade_modulus - 10500) * BF43
BF48 = Max(0, Subgrade_modulus - 7500) * BF1

BF49 = Max(0, 7500 - Subgrade_modulus) * BF1
BF51 = Max(0, pcc_thickness_for_IRI - 6) * BF16
BF52 = Max(0, dga_modulus - 35000) * BF20
BF53 = Max(0, 35000 - dga_modulus) * BF20
BF54 = Max(0, Subgrade_modulus - 6000) * BF53
BF55 = Max(0, dga_modulus - 20000) * BF15
BF56 = Max(0, pcc_thickness_for_IRI - 6) * BF55
BF57 = Max(0, dga_modulus - 25000) * BF38
BF58 = Max(0, 25000 - dga_modulus) * BF38
BF60 = Max(0, pcc_thickness_for_IRI - 6) * BF58
BF62 = Max(0, 9000 - Subgrade_modulus) * BF9
BF63 = Max(0, pcc_thickness_for_IRI - 6) * BF62
BF64 = Max(0, dga_modulus - 20000) * BF9
BF65 = Max(0, Subgrade_modulus - 7500) * BF19
BF68 = Max(0, 25000 - dga_modulus) * BF65
BF69 = Max(0, Subgrade_modulus - 10500) * BF58
BF70 = Max(0, 10500 - Subgrade_modulus) * BF58
BF71 = Max(0, AADTT - 7500) * BF48
BF72 = Max(0, 7500 - AADTT) * BF48
BF74 = Max(0, 2500 - AADTT) * BF15
BF77 = Max(0, dga_modulus - 20000) * BF21
BF78 = Max(0, AADTT - 2500) * BF1
BF80 = Max(0, DGA_Thickness - 6) * BF1
BF81 = Max(0, AADTT - 7500) * BF80
BF82 = Max(0, 7500 - AADTT) * BF80
BF83 = Max(0, DGA_Thickness - 14) * BF7
BF84 = Max(0, 14 - DGA_Thickness) * BF7
BF86 = Max(0, 25000 - dga_modulus) * BF39
BF87 = Max(0, dga_modulus - 25000) * BF18
BF88 = Max(0, 25000 - dga_modulus) * BF18
BF90 = Max(0, 2500 - AADTT) * BF51
BF91 = Max(0, pcc_thickness_for_IRI - 8) * BF86
BF92 = Max(0, 8 - pcc_thickness_for_IRI) * BF86
BF93 = Max(0, Subgrade_modulus - 9000) * BF92
BF94 = Max(0, 9000 - Subgrade_modulus) * BF92
BF96 = Max(0, 8 - pcc_thickness_for_IRI) * BF57
BF97 = Max(0, Subgrade_modulus - 10500) * BF6
BF99 = Max(0, dga_modulus - 25000) * BF6
BF100 = Max(0, 25000 - dga_modulus) * BF6
BF101 = Max(0, Subgrade_modulus - 9000) * BF100
BF102 = Max(0, 9000 - Subgrade_modulus) * BF100
BF103 = Max(0, DGA_Thickness - 6) * BF101
BF104 = Max(0, DGA_Thickness - 6) * BF102
BF105 = Max(0, Subgrade_modulus - 10500) * BF53

BF108 = Max(0, 25000 - dga_modulus) * BF97
BF109 = Max(0, DGA_Thickness - 6) * BF108
BF110 = Max(0, AADTT - 2500) * BF56
BF111 = Max(0, 2500 - AADTT) * BF56
BF112 = Max(0, AADTT - 20000) * BF1
BF115 = Max(0, 12 - pcc_thickness_for_IRI) * BF22
BF116 = Max(0, Subgrade_modulus - 7500) * BF6
BF118 = Max(0, DGA_Thickness - 6) * BF116
BF120 = Max(0, AADTT - 5000) * BF55
BF121 = Max(0, 5000 - AADTT) * BF55
BF122 = Max(0, DGA_Thickness - 6) * BF5
BF123 = Max(0, DGA_Thickness - 14) * BF6
BF125 = Max(0, dga_modulus - 20000) * BF123

PCC_IRI = 98.7657 - 56.0196 * BF1 + 268.308 * BF2 + 0.00159417 * BF3 -
0.00684471 * BF4 + 0.000791239 * BF5 + 0.00410576 * BF6 - 57.6408 * BF7
+ 0.037209 * BF8 - 0.0272917 * BF9 - 0.000000309614 * BF10
+ 0.000000299905 * BF11 + 0.00128095 * BF13 - 0.000000264094 * BF14
+ 12.3761 * F16 - 0.0102506 * BF17 + 0.00745045 * BF18 + 0.00162737 * BF20
- 0.0000226431 * BF21 - 0.00000000930977 * BF22 + 0.0000000262083 * BF23
- 0.000000780545 * BF24 - 0.000000218695 * BF25 - 0.000000769585 * BF26
- 0.000000848214 * BF27 + 0.000000000123097 * BF28 + 0.000000000133666 * BF29
- 0.00102568 * BF31 + 0.000000000188719 * BF33 + 0.000000000104779 * BF34
+ 0.0000000240228 * BF35 - 0.0000000160594 * BF36 - 0.0000242873 * BF37
+ 0.00556472 * BF38 - 0.00535784 * BF39 - 0.0000000333755 * BF40
+ 0.000000304164 * BF41 + 0.0000000000962618 * BF44
+ 0.0000000000156609 * BF45 - 0.000000000168481 * BF46 - 0.000741002 * BF48
+ 0.00117042 * BF49 - 2.9934 * BF51 + 0.000000080461 * BF52
- 0.0000000000403722 * BF54 - 0.000628922 * BF55 + 0.0000946168 * BF56
+ 0.000000104017 * BF60 + 0.00000104098 * BF62 - 0.000000901846 * BF63
+ 0.000000165887 * BF64 - 0.0000000964453 * BF65 - 0.000000000036719 * BF68
- 0.000000000205288 * BF69 - 0.000000000127716 * BF70 + 0.0000000368438 * BF71
+ 0.000000112131 * BF72 - 0.00505372 * BF74 - 0.000000000266388 * BF77
- 0.00166077 * BF78 - 0.434641 * BF80 + 0.0000766845 * BF81
+ 0.000140826 * BF82 - 0.455159 * BF83 + 0.35239 * BF84 - 0.0000000250685 * BF87
+ 0.0000000459999 * BF88 + 0.00112296 * BF90 - 0.0000000333943 * BF91
- 0.000000390819 * BF92 + 0.00000000107705 * BF93 + 0.00000000152392 * BF94
- 0.000003087 * BF96 + 0.000000207465 * BF99 - 0.000000000629382 * BF101
- 0.000000000839356 * BF102 + 0.000000000053057 * BF103
+ 0.0000000000818918 * BF104 + 0.000000000010105 * BF105
- 0.000000000143423 * BF108 + 0.000000000118653 * BF109
+ 0.0000000226967 * BF110 - 0.000000028046 * BF111 - 0.000493513 * BF112
+ 0.0000000289579 * BF115 + 0.000000075535 * BF118 - 0.0000000934255 * BF120
+ 0.000000115346 * BF121 - 0.00000354646 * BF122 - 0.00113609 * BF123

+ 0.000000222569 * BF125

Appendix B – User Guide for Software

User's Guide

KYPDT[TM]
Pavement Design Tool

University of Kentucky
Copyright 2012

Introduction

A pavement is an engineered structure designed to transmit vehicle loads to the soil or rock subgrade below. Pavements are typically a multilayer system with the relatively weaker materials below and progressively stronger materials above. This type of structure leads to an economical use of available materials. Flexible pavements typically consist of several layers starting with an unbound base such as DGA (dense-graded-aggregate), one or more courses of asphalt bound base (Hot Mix Asphalt – HMA) following by an asphalt riding surface. Rigid pavements consist of two layers, the concrete slab and the bound or unbound base layer. An idealized pavement structure is given in Figure 57.

Bound Material (3" – 15" thick) Hot Mix Asphalt or Portland Cement Concrete
Unbound Material (4" – 20" thick) Crushed Aggregates
Subgrade Material Compacted Native Soil or Modified Materials
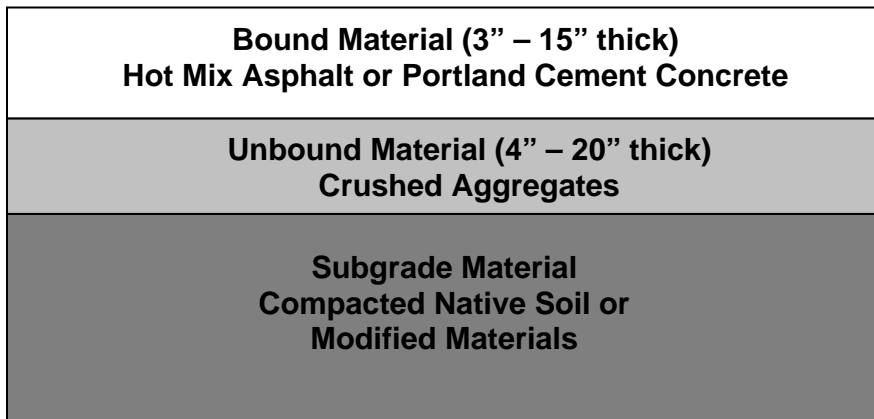
Figure 57. Idealized Pavement Structure

Each of these layers in a pavement structure has different properties which define its strength and it response to changes in the environment and the passage of vehicle loads along the roadway. For instance, Hot Mix Asphalt is very sensitive to changes in temperature. This change may reduce the strength of the asphalt by as much as 60 – 70 percent during the summer months. While the subgrade materials may be influenced by

the amount of moisture which may be present. Again fluctuations of more than 50

percent would not be uncommon as the rainfall changes throughout the year.

In its simplest form the design of a pavement deals with determining the thickness

of each of the pavement layers given in Figure 57, taking into consideration their

materials and their corresponding strength, along with the amount of traffic which the

roadway will carry. Design procedures typically fall into three categories:

- Mechanistic – analysis of the engineering response to the pavement based on the load applied, or essentially a theoretical analysis of the pavement.

- Empirical – an analysis based on experience or a detailed experiment

- Mechanistic/Empirical – a procedure which is based on theory, then has been calibrated based on observed conditions or experimental testing.

The AASHTO Joint Task Force on Pavements recommended in the mid 1990's that

the existing pavement design procedure needed to be revised. They recommended that

the design guide should be a mechanistic-empirical procedure which utilized pavement

design theory with real world pavement performance. The AASHTO Joint Task Force

initiated a research project through the National Cooperative Highway Research Program

(NCHRP) which functions under the Transportation Research Board (TRB) of the

National Academy of Sciences. This project, 1-37A was initiated in 2007 and completed

and released to the research community in July 2004. The goal of this research effort was

to utilize existing methodologies to address some of the shortcomings of the previous

pavement design guide.

The new mechanistic-empirical design procedure implements an integrated analysis procedure for predicting pavement performance over time, accounting for the interaction of traffic loadings, environmental factors and structural materials. The designer must first consider the site conditions such as; traffic, climate, subgrade, and existing pavement condition for rehabilitation and construction conditions.   An idealized flowchart of the process is given in Figure 58.
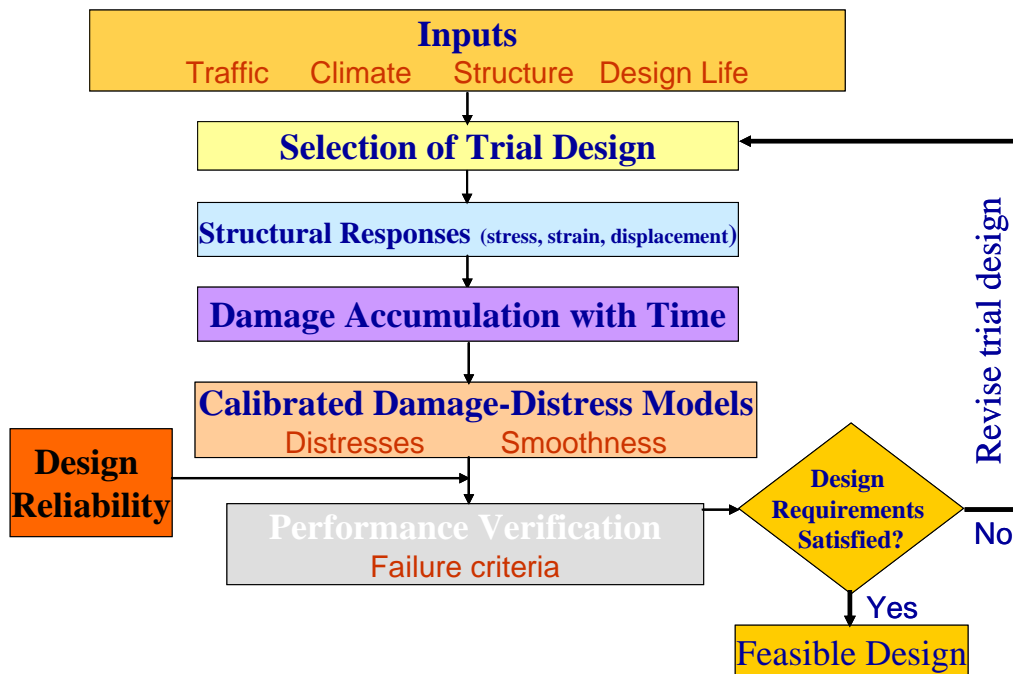

Figure 58 NCHRP MEPDG Design Process

The designer then proposes a trial design which is evaluated by the mechanistic-empirical process to determine key performance indicators such as cracking and smoothness. If the design does not meet the desired performance, it is revised and the process is repeated as necessary.

The NCHRP process has numerous input variables for each of the input categories illustrated above.   A summary of the number of input variables considered by the NCHRP MEPDG and by the KYPDT software is given in Table 23.

Table 23 Comparison of Design Inputs

Design Input	KYPDT	Number of Inputs Required NCHRP MEPDG
Climate	None	three
Hot-Mix Asphalt Materials	one per layer	more than 20 per layer
PCC Materials	one per layer 1	more than 10 per layer
Unbound Materials Granular and Subgrade	one per layer	eight per layer
Traffic	1	50
Thickness	Predicted by Design	one per layer
Performance	Selected by User (cracking, rutting, roughness, faulting, and etc.)	Predicted by Design/Analysis Procedure
Run Time for Single Design	Less than 1 min.	10 – 30 minutes

The NCHRP MEPDG procedure is an iterative process that the designer must utilized to determine an acceptable design.   This has the potential to take significant amounts of time based on the fact that a single design may take up to thirty minutes to complete.

The KYPDT process was developed to provide an estimation of a design thickness based on a desired level of performance. This estimated performance could then be used as an initial starting point for use of the NCHRP MEPDG procedure. This

streamlined procedure will allow a designer to very quickly determine a pavement

thickness and an estimate of the performance of that pavement design.

Development of Streamlined Model

The KYPDT model was developed by utilizing the full NCHRP MEPDG design

process over a range of typical input variables, which were selected based on sensitivity

studies of the NCHRP guide and the evaluation of the designers ability to have access to

the information or have some control over the information included in the design.   More

than 1,000 design runs were completed using the NCHRP process and then modeling

using the Multiple Adaptive Regression Spline (MARS) procedure.

The datasets used for the development of the streamlined model are based on the

MEPDG program that was developed during the NCHRP 1-37A project. These data sets

consist of multiple analysis runs over a range of values for selected design inputs.

Streamlined models have been developed for both flexible and rigid pavements.

A summary of the variables utilized in each of these designs is given in Table 24.

For the development of these models all required input values for climate, bound and

unbound materials, and traffic were held constant, information regarding these default

values may be found in previous research by the authors (Graves & Mahboub, 2006).

Table 24. Summary of Variables in the Streamlined Model

Flexible Pavement	Rigid Pavements
AADTT	AADTT
HMA Thickness	PCC Thickness
DGA Thickness	DGA Thickness
DGA Modulus	DGA Modulus
Subgrade Modulus	Subgrade Modulus
	Dowel Diameter

To develop the streamlined models, a series of designs were developed and processed through the NCHRP design software, these designs were randomly selected from the input parameter set of possible design combinations. A summary of the input variable combinations is given in Table 25and Table 26 for each type of pavement.   If a full factorial matrix were to be this would involve several thousands of different design runs. Each of these design runs takes in excess of 30 minutes to complete. Therefore, a random sampling was used to determine the final set of 1,500 different pavement designs for each of the pavement types; these designs were utilized to develop the streamlined models. With this large dataset of solutions, one could simply utilize some type of search routine to determine the design which most closely fits the required performance parameters for design. However, this may not provide the most efficient design since the thickness increments are at least one inch apart

Table 25. Flexible Pavement Input Variables

AADTT (Average Annual Daily Truck Traffic)	500, 2,500, 5,000, 7,500, 10,000, 15,000, 20,000, 25,000
HMA Thickness (in)	4, 6, 8, 10, 12, 14
DGA Thickness (in)	6, 8, 10, 12, 14, 16
DGA Modulus (psi)	20,000, 25,000, 30,000, 35,000, 40,000
Subgrade Modulus (psi)	6,000, 7,500, 9,000, 10,500, 12,000, 13,500

Table 26. Rigid Pavement Input Variables

AADTT (Average Annual Daily Truck Traffic)	500, 2,500, 5,000, 7,500, 10,000, 15,000, 20,000, 25,000
PCC Thickness (in)	6, 8, 10, 12, 14
DGA Thickness (in)	6, 8, 10, 12, 14, 16
DGA Modulus (psi)	20,000, 25,000, 30,000, 35,000, 40,000
Subgrade Modulus (psi)	6,000, 7,500, 9,000, 10,500, 12,000, 13,500
Dowel Bar Diameter (in)	1.25, 1.5, 1.70

The streamlined model provides a means to go from a discrete set of solutions so a continuous solution space which will allow the designer to determine the most efficient design.

Software Usage

Software Startup and Home Screen

      The software is a self-contained executable program which does not require

additional software or input files to run. Once the program is initiated, the splash screen

given in Figure 59 is displayed.

Figure 59. KYPDT opening screen

Once the user selects the "OK" button to proceed they are asked to agree with the license

agreement for the software as shown in Figure 60 before being permitted to proceed into

the program.

License Agreement

This software was developed to arrive at reasonable first design estimation for flexible and rigid pavements. The results obtained from this software are not to be viewed as the "optimum" design solution. It is not intended to be a replacement for the National Cooperative Highway Research Program (NCHRP) Mechanistic-Empirical Pavement Design Guide (MEPDG) which was used to generate input designs for this process.

This software was based on multiple runs of the 2008 version of the NCHRP-MEPDG software. The authors of this software and the University of Kentucky do not accept any responsibility for any results generated by the KYPDT software. The software user assumes all responsibility and liability for any and all designs which may be developed based on this software.

All rights reserved. Federal copyright law prohibits unauthorized reproduction by any means.
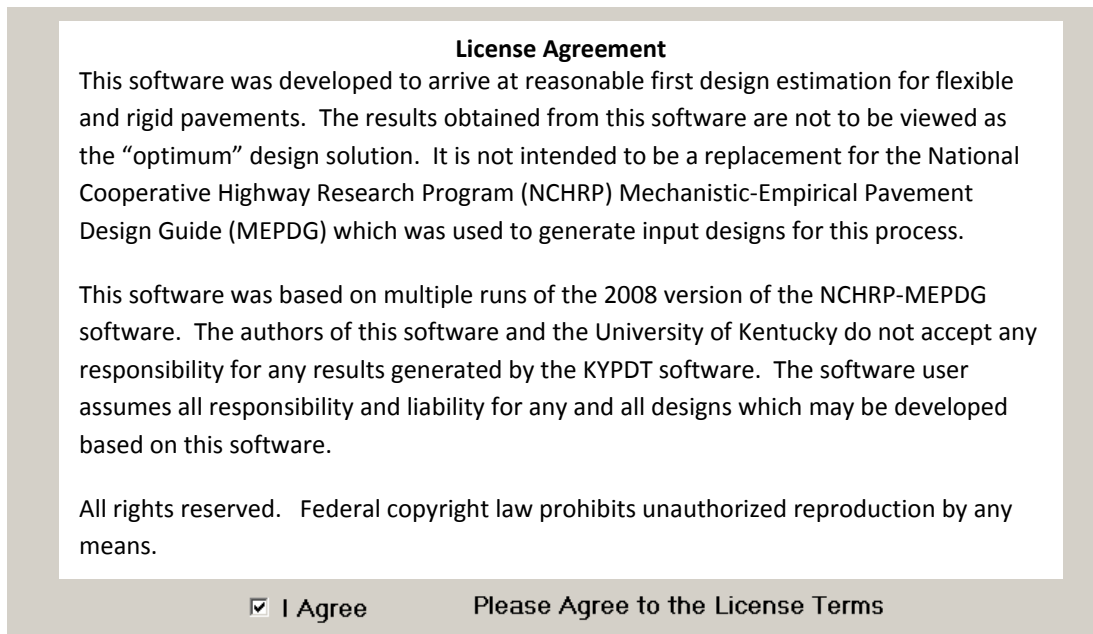
☑ I Agree   Please Agree to the License Terms

Figure 60. KYPDT license agreement

The KYPDT software is designed to work with both U.S. Customary Units (US) and System International (SI) units, this is selected by the user prior to selecting the type of design be conducted. Once the type of units is selected, it must be used throughout the remainder of the session, if the user would like to change the type of design they must return to the initial "Home" screen and select the other type of design.

From the home screen, the user not only selects the units to be used for design, but also the type of design to be completed. The user has three types of design to select from; New Construction which includes both Flexible (Hot-Mix Asphalt) and Rigid (Portland Cement Concrete) Pavements, Hot-Mix Asphalt Rehabilitation, and PCC Rehabilitation. The options which are available on the home screen are given in Figure 61.
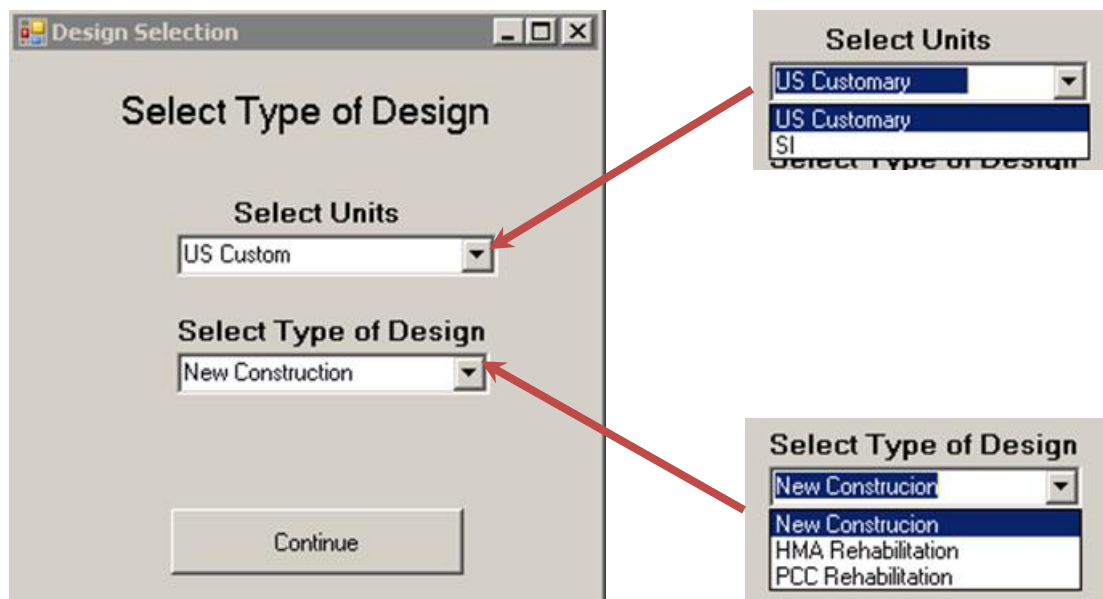
Figure 61. KYPDT home screen options

Design for New Construction

The new construction section contains two input screens which must be completed consecutively. The first "Design Input". The first of these two screens outline the basic pavement design inputs and the information used to calculate the cost estimate for each design.   The basic pavement design inputs are the same regardless of the type of design (flexible or rigid) that is being completed.   The required input variables and acceptable ranges are given in Table 27.

Table 27. Range of Allowable Pavement Design Inputs

Input Parameter	Maximum	Minimum
AADTT	500	25,000
Subgrade Modulus (psi)	6,000	20,000
DGA Modulus (psi)	20,000	50,000
DGA Thickness (in)	6	14
Stabilized Subgrade	Yes/No	

The screen may be broken down into two sections, the first deals with the design inputs which were given in Table 27, the second deals with basic cost information for the project.   The cost information is provided by the designer in the form of dollars per ton for hot-mix asphalt and granular base. For the Portland cement concrete layers, the designer has two options, one being to input the cost in terms of dollars per cubic yard, the other in terms of dollars per square yard per inch of thickness. This method is included to assist different agencies who may calculate unit cost differently. An example of a typical "Design Input screen is given in Figure 61.

Figure 62. KYPDT, design input screen

It may also be seen that the designer has the option to select a stabilized pavement layer. The NCHRP MEPDG software includes the analysis of stabilized materials. However this part of the design guide was never calibrated. Therefore an alternative methodology was incorporated into the KYPDT software.

In the KYPDT software a thicker granular layer with a high modulus was utilized to simulate the presence of the stabilized layer. This simulated stabilized layer consisted of eight inches of granular base with a modulus of 50,000 psi. Based on research conducted by Hopkins (Hopkins, Bechkham, & Sun, 2002) this estimate would be somewhat conservative, this study determined that the long-term strength of stabilized subgrades would range from 40,000 psi to more than 150,000 psi.

In the KYPDT software, when the stabilized layer is selected, the "simulated" stabilized layer is added to the structure, any granular base thickness specified would be in addition to the eight inch simulated stabilized layer. It is anticipated that once the MEPDG's stabilized models have been calibrated, new MARS models could be developed and incorporated into the KYPDT software, to potentially provide better analysis of pavement structures containing stabilized layers.

The second screen in the calculation of new construction pavements allows the designer to establish the pavement performance thresholds for each pavement distress and then determine the material thickness (hot-mix asphalt or Portland cement concrete) necessary. There are four distinct areas (Design Inputs, HMA Thresholds, PCC Thresholds, and Design Calculations and Cost) contained on the Design Thresholds as

identified in Figure 63. Each of these areas will be briefly discussed and highlighted in subsequent figures.
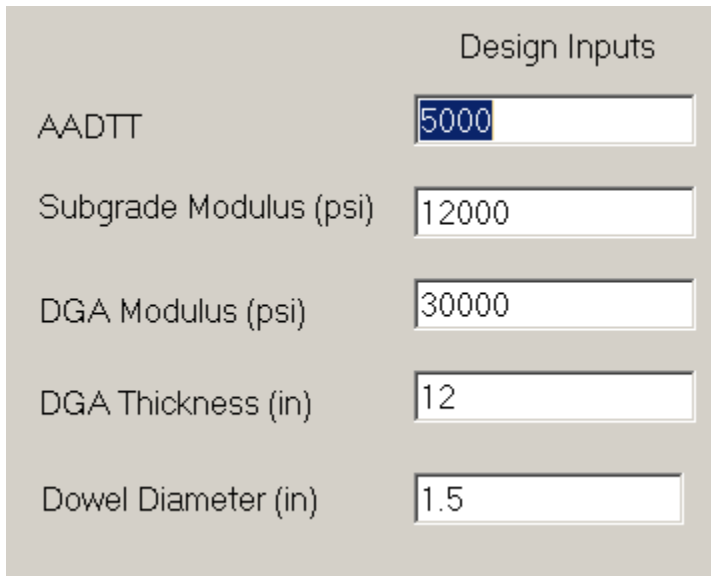

Figure 63. KYPDT design thresholds screen

The Design Input area, Figure 64, provide the user with the option to modify any of the basic design inputs, which are common to both pavement types, along with adding information relating to the Dowel Bar diameter for rigid pavements. It should be noted that the AADTT values utilized is the current year AADT. The models used in the KYPDT software are based on a 20-year projection of this value.   In each of these input

178

boxes there are limits established to keep the user from using values which are outside

the bounds of the model.   In the event the user inputs a value outside this range a dialog

box will be displayed, Figure 65.   The user is required to input values within the range to

continue further.

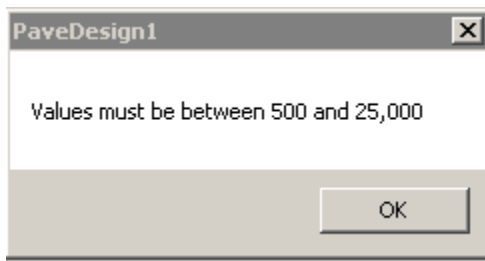

Figure 64. KYPDT, design inputs

Figure 65. Dialog box showing bounds of user input of AADT

The HMA thresholds section Figure 66 provides the designer the option of selecting the desired level of performance for three different pavement distresses, Fatigue Cracking, Rutting, and IRI. These should be the desired distress level which would be anticipated at a 20 year design life. A required thickness for each of these distress levels will be determined by the software.   This would be the required thickness to carry the current year AADTT for 20 years assuming a two percent traffic growth rate. The PCC thresholds are illustrated in Figure 67.

Figure 66. HMA distress thresholds

Figure 67. PCC distress thresholds

Once all of the distress thresholds have been included the user will click the "Calculate" button, which will initially be highlighted in red, once the design is completed, the button will turn green and indicate "Finished". If any of the input values, or distress thresholds are changed, the button will return to red and indicate that recalculation is necessary.

The results for the design are contained in the "Design Calculations and Cost" section identified in Figure 63. This section contains the predicted pavement thicknesses based on the various distress models for each pavement type, these results are displayed in the area highlighted in red in Figure 68. These predicted thicknesses are then used to with the original design information (AADTT, subgrade modulus, and etc.) to calculate estimates of distress for each proposed design; this area is highlighted in yellow in Figure 68.   The cost per lane mile for each of the proposed design thickness is also provided in this section, this information is highlighted in green in Figure 68. It should be noted that the construction cost calculated is based on the information provided on the cost of in-place materials and does not include any cost for preparation of the subgrade materials, excavation, or embankment.

Figure 68. Design results and cost estimates

Rehabilitation Design

The rehabilitation design has been separated by pavement type. The rehabilitation of flexible pavements is fundamentally different than that for rigid pavements. Incremental asphalt layers as thin as one inch can be added to flexible pavements to increase their performance. This type of procedure is not available for rigid pavements. Therefore, for flexible pavements, an "Effective Thickness" of existing pavement conditions will be determined along with an overlay thickness of HMA necessary to achieve a desired level of future performance. For rigid pavements, an effective thickness of existing pavement conditions and a future total pavement thickness for a desired level of future performance will be determined. The means to achieve this future performance will be determined by the designer based on typical construction practices available.

182

To establish the effective thickness for both flexible and rigid pavements an estimate of the initial traffic level when the pavement was first constructed was needed. This traffic level is determined based on the current traffic level and the assumption that this traffic has grown at two percent for 20 years. Therefore, the initial traffic level can be backcalcualted. Another fundamental assumption to this process is that the majority of the distress occurs based on the accumulation of traffic and not the amount of time that has elapsed since the pavement was constructed.

This initial traffic in conjunction with the existing pavement conditions (cracking, rutting, faulting, etc.) was used to calculate the "Effective Thickness" using the MARS model's previously discussed. This "Effective Thickness" represents the thickness that would have been designed using the initial traffic calculated, material properties (subgrade modulus, DGA modulus, DGA thickness), and had the existing pavement conditions been used as target thresholds. This thickness can then be compared to the design using the current year traffic, material properties (subgrade modulus, DGA modulus, DGA thickness), and the desired future pavement conditions (overlay thresholds).

The input screen for the HMA rehabilitation is given in Figure 69. The area highlighted in red contains the current year AADTT, along with the calculated initial AADT. In addition, it contains the basis material properties of subgrade modulus, DGA modulus and DGA thickness. As was previously discussed the material information is used in both the determination of the "Effective Thickness" and the required future thickness. The area highlighted in green provides the information relating to the existing

pavement distress conditions, which are used to calculate the "Effective Thickness" of the structure. The desired or "Overlay Thresholds" are highlighted in the yellow box. These are the desired conditions that the designer would like the pavement to achieve with an overlay. The summary of the existing conditions, and calculated overlay thicknesses are given in the area highlighted in blue. The overlay thickness is calculated by subtracting the "Effective Thickness" from the total new pavement thickness calculated from the desired levels of distress. It may be seen that three overlay thicknesses are determined, one each for the different thickness calculation models. The predicted performance for each of the future thickness determined is also given. This would be the anticipated performance that could be achieved by adding the calculated overlay.

Figure 69. HMA overlay design

The input screen for the PCC rehabilitation is given in Figure 70. The rigid pavement process follows the same general procedures as the flexible pavement process with the exception that no overlay thickness is determined. One other assumption that is made is that the dowel bar diameter will be the same in the new pavement structure as it was in the existing pavement structure.   Only the future thickness required is provided. As was previously mentioned, the method used to achieve this future thickness is based on the construction techniques available.

Figure 70. PCC rehabilitation

References

AASHO. (1961). *The AASHO Road Test, Highway Research Board Special Report 61A.* Washington, DC: Highway Research Board, National Academy of Sciences.

AASHTO. (1993). *Pavement Design Guide.* Washington, DC: American Association of State Highway and Transportation Officals.

AASHTO. (2010). *Guide for the Local Calibration of the Mechanistic-Emperical pavemetn Design Guide.* Washington, DC: American Association of State Highway and Transportation Officals.

AASHTO. (2011). *DARWinME Mechanistic Empirical Pavemnet Desiogn.* Washington, DC: Ameriacan Association of State Highway and Transportation Officials.

Abraham, A., & Steinberg, D. (2004). Is Neural Network a Reliable Forecaster on Earth? A MARS Query! *Bio-Inspired Applications of Connectioinism, Lecure Notes in Computer Science, 2085*, pp. 679 - 686.

Automation Anywhere. (2006). Automation Anywhere Standard -- Version 4.0. San Jose, CA.

Baker, R. F., & Drake, W. B. (1949). *Investigation of Field and Laboratory Methods for Evaluating Subgrade Support in the Design of Highway Flexible Pavements, Bulletiin No. 1, Vol 4 .* Lexington, Ky: Engineering Experiment Station, University of Kentucky.

Bracher, M. T., & Papagiannakis, T. (2004, December). Sensitivity of the 2002 Pavement Design Guide to Traffic Data Inpu. *Thesis*. Washington State University.

Cogger, K. (2001). *Modern Regression Methods: A Comparative Discussion.* Conifer, CO: Peak Consulting Inc.

Darter, M. (2007). Reliability Analysis of Cracking an Faulting Prediction Included in the New Mehanistic-Emperical Pavement Design Guide. *Presentation to AASHTO*. Retrieved October 4, 2012, from http://design.transportation.org/Documents/Reliabilityinrigidpavementanalysis(Darter)(1-2007).pdf

Darter, M., Khazanovich, L., Yu, T., & Mallela, J. (2005). Reliability Analysis of Cracking an Faulting Prediction Included in the New Mehanistic-Emperical Pavement Design Guide. *Transportation Research Record*, pp. 150 - 160.

De Veauz, R. D., Pischogios, D. C., & Ungar, L. H. (1993). A Comparison of Two Nonparametric Estimation Schemes: MARS and Neural Networks. *An International Journal of Computer Applications in Chemical Engineering, 17*(8), 819-837.

El_Basyouny, M., & Witczak, M. (2004, May). Calibration of the Fatigue Cracking Model for the 2002 Design Guide. *Dissertation*. University of Arizona.

FHWA. (1999). *Product Brief: LTPPBind: A New Tool for Selecting Cost-Effective Superpave Asphatl Binder Performance.* Federal Highway Administration, United States Department of Transportation.

Francis, L. (2003). Martian Chronicles: Is MARS Better than Neural Networks? *Paper Presentation, Ratemaking Seminar.* San Antonio, TX: Casualty Actuary Society.

187

Friedman, J. H. (1991). Multivariate Adaptive Regression Splines. *Annals of Statistics, 19*, 1-141.

GAO. (1997). *Transportation Infrastructure Highway Pavement Design Guide is Outdated (GA0/RCED-98-9).* Washington, DC: United States General Accounting Office.

Graves, R. C., & Mahboub, K. C. (2006). Flexible Pavement Design: Sensitivity of the NCHRP 1-37A Pavement Design Guide, a Global Approach. *Airfield and Highway Pavement: Meeting Today's Challenges with Emerging Technologies* (pp. 224-235). American Society of Civil Engineers.

Graves, R. C., & Mahboub, K. C. (2006). Flexible Pavements: Pilot Study in Sampling Analysis of NCHRP Design Guide for Flexible Pavements. *Transportation Research Record*, 123-135.

Graves, R. C., & Mahboub, K. C. (2011). Sampling-Based Flexible Pavement Design Reliability: An Evaluation of. *8th International Conference on Managing Pavement Assets.* Santiago, Chili.

Graves, R. C., & Mahboub, K. C. (2012). Streamlining the use of the NCHRP Mechanistic Empirical Pavement Design Guide (MEPDG). *Transportation Research Record (publication Pending)*.

Haleem, K., Abdel-Aty, M., & Santos, J. (2010). Multiple Applications of Multivariate Adaptive Regression Splines Technique to Predict Rear-End Crashes at Unsignalized Intersections. *Transportation Research Record*, 33-41.

Hastie, Tibshirani, & Friedman. (2001). *The Elements of Statistical Learning, Data Mmining, Inference, and Prediction.* Springer.

Havens, J. H., Deen, R. C., & Southgate, H. F. (1981). *Design Guide for Bituminous Concrete Pavement Structures.* Kentucky Transportation Research Program, University of Kentucky.

Helton, J. C. (2004). Sampling-Based Methods for Uncertainty and Sensitivity Analysis. *Fourth International Conference on Sensitivity Analysis of Modeling Output (SAMO 2004).* Santa Fe, NM: Las Alamos National Laboratory.

Helton, J. C., & Davis, F. J. (2000). *Sampling-Based Methods for Unvertainty and Sensitivity Analysis (SAND99-2240).* Sandia National Laboratories.

Hopkins, Bechkham, & Sun. (2002). *Long-Term Benefits of Stabilizingsoil Subgrades.* Lexington, KY: Kentucky Transportation Center, University of Kentucky .

Huang, Y. H. (2004). *Pavement Design and Analysis.* Upper Saddle River, NJ: Pearson.

Iman, R. L., & Helton, J. C. (1995). *A Comparison of Uncertainty and Sensitivity Analysis Techniques for Computer Models (NUREG CR-3904, SAND84-1461).* Washington, DC: U.S. Nuclear Regulartory Commission.

KYTC. (2008). Kentucky Transportation Cabinet, Standard Specifications for Road and Bridge Construction .

KYTC. (2009). Kentucky Department of Highways Warrants for Selecting Asphatl Mixtures and Compaction Options. Department of Highways, Kentucky Transportation Cabinet.

Lee, M. C., & Hall, K. (2004, December). Mechanistic-Empeirical Pavement Design Guide: Devlation of Flexible Pavement Inputs. *Thesis*. University of Arkansas.

Masad, S. A., & Little, D. N. (2004). *Sensitivity Analysis of Flexible Pavement Response and AASHTO 2002 Design Guide to.* Austin, TX: International Center for Aggregates Research.

Mrawira, M. D. (1996). Streamlining the World Bank's Highway Design and Maintenance Standars Model (HDM-III) for Network Level Application. *Thesis.* Univeristy of Waterloo.

NCHRP. (2003). *Guide for Mechanistic-Empirical Design of New and Rehabilited Pavement Structures -- Appendix BB: Design Reliability.* Washington, DC: National cooperative Highway Research Program, Transportation Research Board, National Research Council.

NCHRP. (2004). *Guide for Mechanistic-Empirical Design of New and Rehabilitated Pavement Structures -- Part 1 Introduction.* Washington, DC: National cooperative Highway Research Program, Transportation Research Board, National Research Council.

NCHRP. (2006). *Research Results Digest 308 -- Changes to the Mechanistic-Empirical Pavement Design Guide Software Through Version 9.0.* National cooperative Highway Research Program, Transportation Research Board, National Research Council.

NCHRP. (2011). *A performance-Related Specification for Hot-Mix Asphalt NCHRP Report 204.* Washington, DC: National Cooperative Highway Research Program.

NCHRP. (March 2004). *Guide for Mechanistic-Empirical Design of New and Rehabilitated Pavement Structures --Part 3 Design Analysis.* Washington, DC: National cooperative Highway Research Program, Transportation Research Board, National Research Council.

Ovik, J. M., Birgisson, B., & Newcomb, D. E. (2000). *Characterizing Seasonal Variations in Pavement Material Properties for use in a Mechanistici-Empericial Design Procedure.* Minneapolis, MN: University of Minnesota -- Dept. of Civil Engineering.

Park, H. M. (2012). Testing the Normality in SAS, STATA, and SPSS. Retrieved October 1, 2012, from www.indiana.edu/~statmath/stat/all/normality/normality.pdf

Pierce, L. (2007). Reliability in the MEPDG -- One States Perspective. *Workshop Presentation 86th Transportation Research Board Annual Meeting.* Washington, DC: Transportation Research Board of the National Academies.

Salford Systems. (2009). Salford Predictive Modeler Software Suite -- MARS . San Diego, CA.

Saltelli, A., Chan, K., & Scott, E. M. (2000). *Sensitivity Analysis.* West Sussex, England: John Wiley & Sons.

Saltelli, A., Tarantola, S., & Ratto, M. (2004). *Sensitivity Analysis in Practice A guide to Assessing Scientific Models.* West Sussex, England: John Wiley & Sons.

SAS. (2006). SAS Annotated Output Proc Univariate. Retrieved July 31, 2006, from http://www.ats.ucla.edu/stat/sas/output/univ.htm

Smith, K. L. (1993). *Volume3: Treatment of Cracks in Asphalt Concrete-Surfaced Pavements (SHRP-H-354).* Washington, DC: Strategic Highway Research Program.

Southgate, H. F., Deen, R. C., & Havens, J. H. (1968). *Rational Analysis of Kentucky Flexible Pavement Design Criterian, Research Report 270.* Lexington, Ky: Division of Research, Kentucky Department of Highways.

Stubstad, R., Tayabji, S., & Lukanen, E. (2002). *LTPP Data Analysis: Variations in Pavement Design Inuts NCHRP Web Document 48.* Washington, DC: National cooperative Highway Research Program, Transportation Research Board, National Research Council.

Vita

R. Clark Graves II, P.E., P.G.

Born in Ashland, KY May 24, 1965

CURRENT POSITION: Program Manager for Pavements, Materials and Geotech
                     Kentucky Transportation Center

PROFESSIONAL REGISTRATION:
Professional Engineer, Kentucky: 17179
Professional Geologist, Kentucky: 2113

EDUCATION:

B.S. in Civil Engineering, University of Kentucky, December, 1987
M.S. in Civil Engineering, University of Kentucky, August, 1989

PROFESSIONAL EMPLOYMENT:

4/07 – Present Program Manager for Pavements, Materials, and Geotech Kentucky
Transportation Center, University of Kentucky,
Lexington, KY

8/03 – 04/07   Associate Program Manager for Pavements and Materials, Kentucky
Transportation Center, University of Kentucky,
Lexington, KY

8/89 – 8/03 Transportation Research Engineer Kentucky Transportation Center,
University of Kentucky, Lexington, KY

5/89 - 8/89 Research Engineer (temporary), Kentucky Transportation Center, University
of Kentucky, Lexington, KY

8/87 - 5/89 Research Assistant, Kentucky Transportation Center, University of Kentucky,
Lexington, KY

8/96 - Present: Assistant Instructor, Department of Civil Engineering, University of
Kentucky, Lexington, KY

AREAS OF RESEARCH SPECIALIZATION

Nondestructive Evaluation of Pavement Structures using Falling Weight Deflectometer and Ground Penetrating Radar

Pavement Management Systems

Pavement Structural Design and Rehabilitation Design

Life-Cycle-Cost Analysis of Pavement Rehabilitation Alternatives

Pavement Materials Characterization and Evaluation of Pavement Construction Techniques

Evaluation of Pavement Maintenance Treatments

Analysis of Traffic Characteristics, Traffic Growth Trends, Truck Weight Distributions, Pavement Damage Analysis, Construction Delay Analysis, and user Cost Analysis

Evaluation of Highway Drainage Systems, Including Culvert Systems and Subsurface Drainage Systems.

Field Instrumentation of In-Situ Pavements and Bridges

Pavement Type Selection Policy

Evaluation of Alternate Bidding Procedures, A+B+C

CURRENT RESEARCH ACTIVITIES

Development of a Strategic Plan for Implementation of the Mechanistic Empirical Pavement Design Guide (MEPDG) for Kentucky

Forensic Evaluation of PCC Distress

Cost Effectiveness of Pavement Treatments

Evaluation of Automated Pavement Distress Identification

Evaluation of Subgrade Stabilization

Evaluation of Non-Nuclear Methods for Compaction Quality Control

Evaluation of the Effectiveness of Internal Drainage Layers Used in Pavement Structures

192

Identification of Factors that Influence Pavement Performance

Improved Asphalt Longitudinal Joint Construction

Evaluation of Warm-Mix Asphalt
TEACHING AND TECHNOLOGY EXCHANGE

Assistant Instructor of CE 381: Fall 1996, spring 1997, Fall 1997, Spring 1998
Assistant Instructor of CE 471G: Fall 2001, Spring 2002
Instructor of CE 381, Spring 2009 – present
Workshop Instructor, Kentucky Transportation Center Technology Exchange
1990 – present

Provide technical assistant to numerous State, County, and Local government agencies along with many consulting engineering companies regarding pavement and highway construction related issues.

SELECTED PROFESSIONAL ACTIVITIES

Current Member of the Board of Directors for the American Road and Transportation Builders Association (ARTBA) – Research and Education Division
Current Vice President of the ARTBA Research and Education Division

Transportation Research Board
    Member of ASF60 – Subsurface Drainage Committee
    Friend of AFD60 – Flexible Pavement Design Committee
    Friend of AFD50 – Rigid Pavement Design Committee

Member of the FHWA Lead States Group for Implementation of the MEPDG

Member of the Southeastern States MEPDG Technical Working Group

Member of FHWA Pooled Fund Study Advisory Group for PrepME Software (software to prepare input for MEPDG design guide)

Graduate of the ARTBA Young Executive Development Program

Past Member of NCHRP Panel 20-50 LTPP Data Analysis: Feasibility of Using FWD Deflection Data to Characterize Pavement Construction Quality

Participant in National Workshops for Life-Cycle-Cost Analysis of Pavements, Demonstration Project 115.

Past Member of the SHRP National Technical Working Group (TWG) for SHRP Falling Weight Deflectometer Quality Assurance Software.

Past Member of the Technical Advisor Group (TAG) for FHWA Project Entitled "Well and Poor Performing Pavements."

Past Member of the Policy Oversight Group of the National Governors Council, which monitored the progress of the FHWA Comprehensive Truck Size and Weight Study?

SELECTED REPORTS/PUBLICATIONS/PRESENTATIONS

Graves, R. C., "Evaluation of US 31W, Hardin KY Project F-31-1(3)," Kentucky Transportation Center, KTC-89-34, April 1989.

Graves, R. C., "Pavement Failures: I-71 Oldham-Henry Counties, EACIR 71-1(64)22," Kentucky Transportation Center, KTC-89-35, April 1989

Sharpe, G. W. and Graves, R. C., "Pavement Evaluation Elkhorn Drive," Kentucky Transportation Center, KTC-89-37, June 1989.

Graves, R. C., "Pavement Deflection Determination Using Velocity Transducers," Master of Science Thesis, University of Kentucky, August 1989.

Allen, D.L. and Graves, R. C., "Pavement Inspection -- Derbyshire Estates," Kentucky Transportation Center, KTC-89-44, September, 1989.

Graves, R. C., "Pavement Base Evaluation -- KY 55 Taylor County," Kentucky Transportation Center, KTC-89-48, October 1989.

Hunsucker, D. Q. and Graves, R. C., "Preliminary Engineering, Monitoring of Construction, and Initial Performance Evaluation; Use of Ponded Fly Ash in Highway Road Base," Kentucky Transportation Center, November, 1989.

Fleckenstein, J. L., Allen, D. L, and Graves, R. C., "Investigation of Premature Cracking on the National Turnpike, Jefferson County," Kentucky Transportation Center, KTC-90-5, March 1990.

Drnevich, V .P., Hossain, M. M., Wang, J., and Graves, R. C., "Determination of Layer Moduli in Pavement systems by Non-Destructive Testing,", Transportation Research Record 1278, 1990.

Graves, R. C. and Allen, D. L. "Road Rater Correlation," Kentucky Transportation Center, KTC-90-22, September 1990.

Hunsucker, D. Q. and Graves, R. C. "Performance Evaluations of Crushed Sandstone Aggregates in Bituminous Bases", Kentucky Transportation Center, KTC 90-26, December 1990.

Graves, R. C., and Drnevich, V.P., "Calculating Pavement Deflections with Velocity Transducers", Transportation Research Board Annual Meeting, January, 1991.

Graves, R. C., and Allen, D. L., "Pavement Deflection Evaluations," Kentucky Transportation Center, KTC-92-1, January 1992.

Allen, D.L., Graves, R. C., and Fleckenstein, L. J., "Laboratory and Field Evaluations and Correlations of Properties of Pavement Components," Kentucky Transportation Center, KTC-92-10, July 1992.

Graves, R. C. and Hunsucker, D. Q., "Atmospheric Fluidized Bed Combustion Residue in Highway Base and Subbase Construction," Kentucky Transportation Center, KTC-92-17, October 1992

Graves, R. C., Allen, D.L., and Sharpe, G. W., "Breaking and Seating of Concrete Pavements Kentucky's Experience," Transportation Research Board Annual Meeting, January 1993.

Graves, R. C., Hopkins, T. C., and Hunsucker, D. Q., "Construction and Performance of Highway Soil Subgrades Modified with Atmospheric Fluidized Bed Combustion and Multicone Kiln Dust," Kentucky Transportation Center, KTC-93-4, January 1993.

Allen, D. A., Fleckenstein, L. J., and Graves, R. C., "Field Performance Evaluation of Precast Concrete Box Culverts, Aluminum Culverts, and Galvanized Metal Arches and Pipe Arches," Kentucky Transportation Center, KTC-93-9, March 1993

Allen, D. L, Gary, M. J., Graves, R. C., Guo, M., Harik, I. E., Harrison, J., Street, R. L., "Seismic Analysis of the Brent-Spence Bridge," Kentucky Transportation Center, KTC-93-15, June 1993

Graves, R. C., and Hunsucker, D. Q., "Performance of Experimental Highway Base and Subbase Layers Containing By-Product Materials, From Coal-Fired Power Plants: KT Route 3074 and Bleich Road," Kentucky Transportation Center, KTC-93-16, June 1993

Graves, R. C., and Allen, D. A., "FHWA Special Project 202, Break and Seat of Jointed Reinforced Concrete Pavement," Kentucky Transportation Center, KTC-93-19, July 1993.

Harik. I. E., Allen, D.L., Street, R. L., Graves, R. C., and et. al. "Seismic Analysis of the Brent-Spence Bridge," Kentucky Transportation Center, KTC-93-15, August 1993.

Deacon, J. A., Allen, D. A., Crabtree, J. D., Agent, K. R., Pigman, J. G., and Graves, R.. C., "Proposal for Development of a Resource and Commodity Highway System," Kentucky Transportation Center, KTC-94-5, January 1994 .

Allen, D. A., Graves, R. C., "Variability In Measurement of In-Situ Material Properties", Fourth International Conference on the Bearing Capacity of Roads and Airfields, Minneapolis, MN, July 1994.

Allen, D.A., Graves, R. C., Southgate, Yokota, H.,A Dynamic Analysis of Pavement Evaluation by Road Rater and FWD", Fourth International Conference on the Bearing Capacity of Roads and Airfields, Minneapolis, MN, July 1994.

Allen, D.A., Graves, R. C. "Pavement Evaluation Nandino Boulevard", July 1995.

Allen, D.A., Graves, R. C. "Pavement Evaluation, Oldham County", July 1995.

Graves, R. C., Stamatiadis, N., Schmidt, J.,"Best Practices for Commercial Vehicle Monitoring Facilities Design", FHWA Report FHWA-SA-96-001, September 1995

Agent, K., Crabtree, J., Deacon, J. A., Graves, R. C., and Pigman, J. G., "Impacts of Extended Weight Coal Haul Road System," Kentucky Transportation Center, KTC-95-25, December 1995

Graves, R. C., Stamatiadis, N., Schmidt, J.,"Considerations for Designing Commercial Vehicle Monitoring Facilities", 1996 Transportation Research Board Annual Meeting, Washington, DC, January 1996.

Allen, D. A., Graves, R. C. "Pavement Evaluation Kroger, Nicholasville, Kentucky", March 1996.

Allen, D. A., Graves, R. C. "Pavement Evaluation, Commonwealth Stadium, University of Kentucky, May 1996.

Allen, D. A., Graves, R. C. "Pavement Evaluation, Canebrake Drive", October 1996.

Allen, D. A., Fleckenstein, L. J., Graves, R. C., and Shull, M., "Performance Evaluation of Recycled PCC Pavement Used as a Dense Graded Aggregate," Kentucky Transportation Center, KTC-97-3, February 1997.

Allen, D. A., Graves, R. C. "Pavement Evaluation, Timber Creek Subdivision", June 1997

Allen, D.A., Graves, R. C. "Pavement Evaluation, Man O' War Boulevard", July 1997.

Graves, R. C., and Stamatiadis, N., "Considerations for Designing Commercial Vehicle Monitoring Facilities," International Large Truck Safety Symposium, Knoxville, TN, October 1997.

Graves, R. C., Pigman, J. G., and Weber, J., "Evaluation of Road Weather Information System: Interim Report," Kentucky Transportation Center, KTC-97-26, December 1997.

Graves, R. C., Allen, D. A. "Probabilistic Life Cycle Cost Analysis, FHWA Demonstration Project DP 115," Kentucky Transportation Center, KTC-98-24, December 1998

Graves, R. C., Allen, D. A. "Pavement Design Guide A Short Course," Kentucky Transportation Center, KTC-99-6, April 1999.

Graves, R.C., Allen, D.A., "Pavement Design Evaluations I-275 Boone and Kenton Counties MP 1.05 - 7.15", Kentucky Transportation Center, KTC-00-2, January 2000.

Graves, R.C., Allen, D.A., "I-275 Warranted Pavement, Boone and Kenton Counties, Kentucky", Kentucky Transportation Center, KTC-00-6, May 2001.

Scully, T.C., Graves, R.C., and Allen, D.A. "Construction Monitoring and Procedures for I-275 Warranty Project Kenton/Boone Counties", Kentucky Transportation Center, KTC-01-29/FR107-01-11, December 2001

Rister, B., and Graves, R.C. "The Cost of Construction Delays and Traffic Control for Life-Cycle Cost Analysis of Pavements", Kentucky Transportation Center, KTC-02-07/SPR 197-99&218-00-1F, January 2002

Barrett, M., Graves, R.C., and et. al "Analysis of Traffic Growth Rates", Kentucky Transportation Center, KTC-01-15/SPR213-00-1F, August 2002

Graves, R.C. and Allen, D. L. "Pavement Evaluation, I-64 Franklin Country", Kentucky Transportation Center, Publication Pending.

Graves, R. C., and Rister, B. W. "Pavement Evaluation, I-265 Jefferson Country", Kentucky Transportation Center, KTC-03-22/FR-122-03-1f November 2003.

Graves, R. C., "Development of Interstate Traffic Volume Index Stations", Kentucky Transportation Center, Publication Pending.

Graves, R. C., and Hunsucker, D., "Assessment of Data Collection for ESAL Determinations for the Kentucky Transportation Cabinet, Division of Planning", Kentucky Transportation Center, August 2004

Scully, T.S, Graves, R.C., and Allen, D.A. "Identification of Pavement Distress in Kentucky", Kentucky Transportation Center KTC-05-29/SPR267-02-1F, September 2005

Graves, R. C. and Allen, D.A. "Evaluation of the Current State-of-the-Art in Pavement Profiling for Use in Roadway Design", Kentucky Transportation Center, KTC-05-30/SPR-266-02-1F, September 2005

Graves, R.C. and Pigman, J.P. "Utilization of Index Stations for Prediction of Interstate Traffic Volumes", Kentucky Transportation Center, KTC-05-31/SPR/232-01-1F, September 2005

Graves, R.C., and Rister, B. "Pavement/Sub-grade Condition Assessment I-65, Approximate Milepost 97.5 to 102.5, (Transition from Asphalt to Concrete) To (KY 313 Overpass)", KTC-05-13/FRT 141-04-1F July 2005

Graves, R.C., and Rister, B. "Cumberland Gap Tunnel Evaluation" ", KTC-05-35 /KH50-05-1F, September 2005

Graves, R.C., and K.C. Mahboub. "Part 2: Flexible Pavements: Pilot Study in Sampling-Based Sensitivity Analysis of NCHRP Design Guide for Flexible Pavements," Transportation Research Record 1947, Transportation Research Board, National Research Council, Washington, DC, 2006; pp. 123—135.

Graves, R.C., and K.C. Mahboub. "Flexible Pavement Design: Sensitivity of the NCHRP 1-37A Pavement Design Guide, a Global Approach" ASCE Conference Proceedings -- *Airfield and Highway Pavement: Meeting Today's Challenges with Emerging Technologies* pp. 224-235 2006

Rister, B. and Graves, R.C. "Rideability Issues for Asphalt and Concrete Specification Modifications", KTC-07-30/SPR 304-05-1F, December 2007

Rister, B., Graves. R.C. and Creech, J "Investigation of the Extended Use of Ground Penetrating Radar (GPR) for Measuring In-situ Material Quality Characteristics", KTC-08-31/SPR 307-05-1F, June 2008

Graves, R.C, Pigman, J.G., Rister, B., Cain, D.H., and Tollner, N.
"Annual Update of Data for Estimating ESALS", KTC_08-32/PL13-08-1F
December 2008

Graves, R.C. and Fisher, J. "Durability Issues of Asphalt Pavement (Polymer Modifiers)
KTC-10-04/SPR298-05-1F, April 2010

Rister, B. and Graves, R.C. "Pavement Settlement Issues and Hydro-Geochemical Water
Testing Results for the Cumberland Gap Tunnel" KTC-10-03/KH58-07-1F, March 2010

Graves, R.C. and Allen, D.A. "Maintenance Customer Survey" KTC-11-03/UI56-09-1F,
December 2010

Graves, R. C. and Mahboub, K.C. "Sampling Based Flexible Pavement Design
Reliability Evaluation of the NCHRP Mechanistic Empirical Pavement Design Guide
(MEPDG)" 9th International Conference on Managing Pavement Assets, Santiago, Chili,
November 15 – 19, 2011

Graves, R. C. and Maboub, K.C. "Streamlining the use of the NCHRP Mechanistic
Empirical Pavement Design Guide (MEPDG)", Transportation Research Board Annual
Meeting, Washington, DC, January 22 – 26, 2012, Publication Pending.

Graves, R.C., Cohn, L. "Evaluation of Quiet Pavement Alternatives for the Louisville
Southern Indiana Bridges Project", Kentucky Transportation Center publication pending.